Hybridization signals in *Fucus* diversification

Susana Cerveira Campar Almeida

Mestrado em Biodiversidade, Genética e Evolução

Faculdade de Ciências

2016

Orientador

Gareth Pearson, Investigador Auxiliar, CCMAR,
Universidade do Algarve

Coorientador

José Melo-Ferreira, Investigador Auxiliar, CIBIO-InBIO,
Universidade do Porto

Acknowledgements

I would like to appreciate all the help I had from my supervisors, Gareth Pearson and José Melo-Ferreira. Additionally, I would like to acknowledge Ester Serrão, Cymon Cox, Filipe de Portugal. Finally, to my parents, for their invaluable support. This work was funded by FCT (Fundacão para a Ciência e a Tecnologia) through UID/Multi/04326/2013 and projects EXTANT (EXCL/AAG-GLO/0661/2012) and EVOSEXUAL (EXPL/BIA-EVF/2263/2013).

Sumário

A hibridação e consequente troca de material genético entre espécies distintas é uma das maiores forças evolutivas dos sistemas biológicos, cujo estudo continua a fascinar os investigadores. Os padrões criados por este fenómeno na composição genética dos organismos têm sido vastamente estudados, mas apenas com o aparecimento das técnicas de sequenciação massiva neste século é possível perceber o seu impacto genómico. A descrição dos padrões de introgressão, e a compreensão das causas e consequências deste processo, constitui um parâmetro fundamental para entender os processos evolutivos que levaram à diversidade biológica atualmente conhecida. O género *Fucus* (Fucales, Phaeophyceae) inclui algumas das espécies marinhas mais importantes nos ecossistemas intermareais do Norte Atlântico. A espécie *Fucus guiryi*, recentemente descrita, revela sinais de discordância filogenética nas populações do norte da sua distribuição, sugerindo a possível ocorrência de hibridação com duas espécies pertencentes ao mesmo grupo, *F. vesiculosus* e *F. spiralis*, onde estas ocorrem em simpatria. No entanto, a extensão da introgressão nuclear, bem como a sua contribuição para os processos de divergência e evolução adaptativa neste sistema não são ainda conhecidos e o seu estudo representa por isso um grande desafio. O principal objetivo deste trabalho consiste em analisar a extensão da introgressão nuclear entre estas espécies, e perceber se esta suporta um ou vários eventos de hibridação na origem do *F. guiryi*. Para responder a esta questão utilizámos dados de transcriptómica (sequenciação de RNA) para reconstruir a filogenia do grupo, analisar incongruências entre a árvore filogenética global e as reconstruídas para cada gene, inferindo a contribuição da retenção de polimorfismo ancestral e introgressão para estes padrões. Para tal combinámos métodos baseados em coalescência e métodos Bayesianos na análise de genealogias de múltiplos genes para revelar as relações filogenéticas entre estas espécies. Adicionalmente, testámos a ocorrência de introgressão entre populações ao longo das distribuições alopátrica e simpátrica das populações parentais e as potenciais populações híbridas. Este trabalho reporta a primeira análise genómica de larga escala efetuado para o género *Fucus*. Os resultados mostram padrões discordantes inferidos entre filogenias locais e globais, e que este padrão resulta de eventos de hibridação entre estas espécies, detetados nas populações simpátricas.

Palavras-chave

hibridação, transcriptómica, algas castanhas, evolução, filogenómica, biogeografia

Abstract

Hybridization is one of the major evolutionary forces driving speciation. Understanding the role of hybridization in diversification processes and the generation of evolutionary novelty is a fundamental goal in evolutionary biology. Hybridization is a ubiquitous process resulting in hybrid lineages with admixed genomes. Patterns of genome admixture may reflect different pathways of the evolutionary history of species that can be related to biogeographic processes. The marine genus *Fucus* (Fucales, Phaeophyceae) includes key foundational species that structure intertidal ecosystems on North Atlantic shores. A recently described species, *Fucus guiryi* revealed discordant phylogenetic signals in the northern part of its range and possible introgressive hybridization involving the sister group *F. vesiculosus*/*F. spiralis* where these occur in sympatry. However, to understand the extent of nuclear introgression and its contribution to divergence and adaptive evolution in this system remains a great challenge. The main objective of this project was to analyse the extent of nuclear introgression among *Fucus* species and to understand if hybridization signals support a single or multiple hybrid origin of *F. guiryi*, by undertaking comparative analyses across the extant species ranges. To answer these questions we used extensive transcriptome sequence data to assess incongruence between gene and species trees on a genome-wide scale, while accounting for ancestral shared polymorphism (incomplete lineage sorting, ILS). We combined phylogenomic tools based on coalescence and Bayesian analysis of multigene genealogies to untangle the relationships between these three lineages. Moreover, we tested for the occurrence of introgression between populations throughout the allopatric and sympatric distributional ranges of both parental and putative hybrid lineages. This work reports the first large-scale phylogenomic analysis of divergence in the genus *Fucus*. We found agreement between the different approaches applied to species tree reconstruction. Most importantly, we concluded that the conflicting patterns observed between gene phylogenies could be attributed to introgressive hybridization between these species.

Keywords

hybridization, transcriptomics, brown algae, evolution, phylogenomics, biogeography

Index

List of tables and figures

List of abbreviations

AIC: Akaike Information Criterion

BFGS: Broyden-Fletcher-Goldfarh-Shanno

BWA: Burrows-Wheeler Algorithm

CF: Concordance Factor

CI: Confidence Interval

FPKM: Fragments Per Kilobase per Million

GTR: General Time Reversible

HPD: High Posterior Density

ILS: Incomplete Lineage Sorting

MCC: Maximum Clade Credibility

MCMC: Markov Chain Monte Carlo

ML: Maximum Likelihood

Mya: Million years ago

NW: Northwest

PCT: Primary Concordance Tree

PP: Posterior Probability

revPoMo: reversible Polymorphism-aware Phylogenetic Model

SD: Standard Deviation

SE: Standard Error

SNP: Single Nucleotide Polymorphism

UK: United Kingdom

1. Introduction

Hybridization is an important evolutionary phenomenon that has been intriguing evolutionary biologists for more than 150 years, since Darwin first described hybrid formation (Darwin, 1859). Stemming from the foundation of the first species concepts (e.g., the biological species concept; Mayr, 1963), doubts first arose about the importance and frequency of hybridization, which led to it being considered relatively unimportant, particularly in animals (Mayr, 1963). In the early 90's, technological advances, and particularly the development of the PCR, fueled the continuously growing number of studies in this field and, in the last two decades, a tremendous increase of examples has allowed for a broader perspective on this phenomenon (reviewed in Schwenk *et al.*, 2008; Payser and Rieseberg, 2016). Currently it is recognized as a pervasive process across all groups of taxa (Mallet, 2005; Schwenk *et al.*, 2008) and it has been extensively reported (e.g., plants, Rieseberg *et al.*, 2003; insects, Mallet, 2009; mammals, Melo-Ferreira *et al.*, 2007; birds, Grant and Grant, 2010; amphibians, Ryan *et al.*, 2009; fishes, Keller *et al.*, 2013; bivalves, Pfenninger *et al.*, 2002). Being such a widespread phenomenon suggests that introgressive hybridization is an important factor for the evolution of species and the growing number of examples confirms that it is a frequent process that, along with new mutations and standing genetic variation, provides an important mechanism generating adaptive genetic variation (Hedrick, 2013).

1.1 Importance of natural hybridization in evolution

The great importance of interspecific hybridization derives from the fact that it is a prominent factor during speciation processes, on which it can have great impacts. In fact, even if rare, instances of hybridization can have enduring effects on gene pools (Schwenk *et al.*, 2008).

Natural hybridization occurs when reproductive barriers between species are somehow incomplete, allowing for gene exchange to occur between different species when in contact (Arnold, 1997). However, whether or not interspecific gene flow will lead to introgression depends on several factors. In closely related species undergoing secondary contact, hybridization may occur and allow gene flow, giving rise to genetically admixed individuals and populations and thus blurring species boundaries (Arnold, 1997; Petit and Excoffier, 2009). On the other hand, if selectively disadvantageous, it will likely accelerate species divergence by enhancing the establishment of reproductive isolation, for example by the origin of sterile hybrids or

hybrids with lower fitness compared to their parental species (Miller *et al.*, 2004), leading to subsequent reinforcement and eventually speciation (e. g., via adaptive introgression) (Hoskin *et al.*, 2005; Mallet, 2007; Hedrick, 2013).

Yet, opportunities for hybridization often vary over time due to, for example, accumulating reproductive isolation or fluctuations on the geographic ranges of species (Hewitt, 2011; Payseur and Rieseberg, 2016). Intrinsic features of species, such as the mating system, dispersal potential and preferences in mate choice may have a decisive role on the magnitude and timing of hybridization (Abbot *et al.*, 2013; Schumer *et al.*, 2014). In addition, whether gene flow occurs in sympatry or is triggered by secondary contact will result in different signatures on the genomic architecture of species (Payseur and Rieseberg, 2016). Hence, the interplay between reproductive barriers and geography has an important role in determining the nature and strength of gene flow, and remains controversial regarding the implications and the definition of speciation processes (Crispo *et al.*, 2006).

Likewise, introgression is unlikely to occur at the same rate and scale across the genome. While some variants may be strongly affected by selection, neutral variants may flow more freely between species and will eventually pervade into a foreign pool (Martinsen *et al.*, 2001; Neiva *et al.*, 2010). Alternatively, variants cross species boundaries because of drift. Particularly, at the wave front during range expansions, if reproductive barriers are still incomplete, asymmetric introgression will likely occur between the local and the colonizing species (Petit and Excoffier, 2009). In this case, intraspecific gene flow may have a major importance in facilitating or preventing introgression of variants from the local to the colonizing species (Petit and Excoffier, 2009). Moreover, factors such as the recombination rate (e.g., centromeric regions; Kliman *et al.*, 1993) and the inheritance mode of different parts of the genome (e.g. sex chromosomes or autosomes; Macholán *et al.*, 2008), may further contribute to asymmetric rates of genomic introgression. For example, mitochondrial DNA genes have been reported to display greater introgression rates than nuclear encoded genes (Rieseberg *et al.*, 1991; Martinsen *et al.*, 2001; Neiva *et al.*, 2010), which may be related to the fact that they are inherited as a single independent unit and hence not linked to other alleles with possible deleterious effects that would lead to a selective disadvantage (Martinsen *et al.*, 2001; Ballard *et al.*, 2004). Thus, mitochondrial introgression may be facilitated by selective sweeps resulting from positive selection (Gompert *et al.*, 2008; Galtier *et al.*, 2009) and this will likely contribute to the mosaic architecture of the resulting gene pools.

The preceding discussion therefore shows that genome mosaicism is a major feature with important implications for the dynamics of gene flow and, ultimately, for

speciation. Hence, genome-wide patterns of differentiation and admixture are shaped by a number of evolutionary processes that can complicate interpretations (reviewed in Twyford and Ennos, 2012; Stölting et al, 2013). Furthermore, understanding the role of selection on hybridization processes remains an open question that can potentially lead to different outcomes from hybridization (Payseur and Rieseberg, 2016).

Given the ubiquitous nature of interspecific hybridization, the impacts of genome admixture on speciation and consequences for the gene pool of species and populations have been highly debated (Arnold, 1997; Mallet, 2005). On the one hand, it is considered to be a process creating new variants on which selection can act, and thus contribute with evolutionary novelty that may lead to adaptive introgression (Pardo-Diaz *et al.*, 2012; Hedrick 2013), or even hybrid speciation (Rieseberg *et al.*, 1995; Arnold *et al.*, 1991). On the other hand, it may contribute to the extinction of indigenous or endemic species by threatening the genetic integrity and/or diversity of native species (e.g., Iberian waterfrog, Arano *et al.*, 1995; rainbow trout, Dowling *et al.*, 1992). This is particularly problematic for rare species when in contact with more abundant species, or for locally adapted species, since local adaptations may be lost (Reisenbichler and Rubin, 1999; Riley *et al.*, 2003), and has been accelerated by Human activities (Allendorf *et al.*, 2001; Rhymer and Simberloff, 1996). Thus, it is essential to have a detailed understanding focused on taxa vs. ecosystem scale, to enable a broader and rigorous framework. Particularly under current climate change scenarios, an understanding of the implications and possible impacts of hybridization (both positive and negative) in new environments is required. Several taxa are known to have undergone changes in distribution, with a number of populations becoming threatened or extinct (e.g., Nicastro *et al.*, 2013), hence, adaptive responses are essential for continued persistence. The potential contribution of adaptive introgression of new variants may have a determinant role in the survival of species (Rieseberg *et al.*, 2003; Hamilton and Miller, 2016).

Studies on patterns of introgression may give clues about the adaptive potential of hybridization (i.e. if gene flow is a creative force in adaptation) as well as for identifying the genetic basis of species differences (Baack and Rieseberg, 2007; Zhang *et al.*, 2016; Pease *et al.*, 2016). Genomic studies allowing for the robust detection of interspecific exchange and genome-wide patterns of introgression left on gene pools may help to unravel processes involved in speciation, such as the maintenance of reproductive barriers (e.g., pre- and post-zygotic isolation mechanisms, genes involved in the reproductive isolation), and hybrid formation (Rolán-Alvarez *et al.*, 1997; Arnold and Martin, 2010; Grant and Grant, 2010).

Genomic patterns of differentiation resulting from hybridization may result in phylogenetic incongruence, which provide the first insights into the occurrence of hybridization across taxa. Genome admixture may cause incongruence among gene trees, as well as between gene and species trees, which derives from the fact that each gene has its own evolutionary history, which may or may not be congruent with the evolutionary history of the species as a whole (Meng and Kubatko, 2009; Cui *et al.*, 2013). This leads to reticulate evolutionary histories that are inadequately explained by tree-like relationships (Huson and Bryant, 2006; Yu *et al.*, 2013). However, to unambiguously detect interspecific hybridization is not a straightforward process, being particularly challenging for recently-diverged species or populations, where similar patterns in the genomic background may be caused by incomplete lineage sorting (ILS) (Maddison and Knowles, 2006; Choleva *et al.*, 2014). Hence, by identifying phylogenetic incongruence we can hypothesize introgression, which we can then differentiate from ILS (Degnan and Rosenberg, 2009). ILS can be modelled, e.g. by multispecies coalescent approaches, which consider discordance between gene and species trees to be due solely to ILS, not taking into account other sources of discordance (Degnan and Rosenberg, 2009; Liu *et al.*, 2009). Thus, to properly model evolutionary histories derived from introgressive hybridization events, complementary approaches must be considered (Green *et al.*, 2010; Cui *et al.*, 2013; Wielstra *et al.*, 2014). Meanwhile, in attempting to distinguish hybridization from ILS (deep coalescence), several methods have been proposed for inferring evolutionary relationships (Ané *et al.*, 2007; Meng and Kubatko, 2009; Yu *et al.*, 2013).

While initial studies based on a few mitochondrial and nuclear markers allowed the first evidence of hybridization, using a few molecular markers may lead to inaccurate estimates of introgression. Since most alleles are expected to be quasi-independently transmitted within and among loci, different genomics regions might have different genealogical histories (Avise and Wollenberg, 1997; Bull *et al.*, 2006). Thus, a small set of markers will likely provide a limited or even biased perspective on the process. In this context, the development of high-throughput sequencing techniques over the last decade provide an unprecedented capacity to uncover genomic patterns of variation which allow to characterize footprints of genome admixture (Twiford and Ennos, 2012; Payser and Rieseberg, 2016). Moreover, the continuous development of evolutionary models and statistical methods raise the prospect for accurately detecting and understanding processes involving interspecific gene flow (Than *et al.*, 2008; Green *et al.*, 2010; Schrempf *et al.*, 2016).

In marine systems, hybridization has received much less attention and research has lagged behind terrestrial and freshwater systems. Although traditionally considered

much less common in the marine environment, over the last two decades there has been a surge in reports of hybridization in marine environments, particularly among corals and fishes (Richards and Hobbs, 2015; Montanari *et al.*, 2016). These studies have confirmed the relevance of this process in generating diversity in marine taxa (Richards and Hobbs, 2015), including in brown algal systems (Lewis and Neushul, 1995; Coyer *et al.*, 2002). Particularly, intertidal ecosystems are very compelling environments, comprising heterogeneous habitats over small spatial and temporal scales, where sharp gradients of physical (e.g., desiccation, temperature, wave exposure) and biotic (e.g., competition) selective pressures strongly shape species distribution (Harley and Helmuth, 2003). These systems have provided some classical examples of habitat-driven divergence with gene flow (e.g., *Littorina saxatilis*, Johannesson *et al.*, 1995) and are thus exceptional environments for exploring questions regarding adaptive divergence and maintenance of species in the face of gene flow.

1.2 *Fucus* as a model species to understand hybridization

The marine genus *Fucus* (Fucales, Phaeophyceae) includes key foundational and ecosystem-structuring species with wide geographic ranges along intertidal North Atlantic shorelines (Neiva *et al.*, 2016). The evolutionary history of *Fucus* features a recent radiation over the last ca. 3.8 Ma in the North Atlantic, where most of the species occur (Cánovas *et al.*, 2011). The complex history of the group was shaped by glacial-interglacial cycles that induced multiple range shifts and secondary contact zones with subsequent alterations in the genetic pool of several species, in some of which hybridization has been reported (Coyer *et al.*, 2002; Neiva *et al.*, 2010). Divided into two major groups (Serrão *et al.*, 1999; Coyer *et al.*, 2006), new species have been recently described within this genus for Lineage 2 (*sensu* Coyer *et al.*, 2006) (Pereyra *et al.*, 2009; Zardi *et al.*, 2011). In this clade, several species occur in sympatry across much of their distribution ranges and mosaic genomes have been reported (Engel *et al.*, 2005; Coyer *et al.*, 2011; Moalic *et al.,* 2011; Neiva *et al.*, 2012).

Fucus guiryi G.I.Zardi, K.R.Nicastro, E.A.Serrão & G.A.Pearson, a recently described species (Zardi *et al.*, 2011), was identified as showing signals of hybridization and introgression involving the sister group *Fucus spiralis* Linnaeus / *Fucus vesiculosus* Linnaeus (Fig. 1). Where they occur in sympatry, intermediate genotypes may have resulted from admixture following secondary contact during range expansions (Coyer *et al.*, 2011; Zardi *et al.*, 2011). These species have extensive sympatric distributions along northwest Iberia and northern Europe, while in southwest

Iberia they occur in allopatry and, of the three, only *F. guiryi* extends its distribution throughout Morocco (Fig. 2) (Zardi *et al.*, 2015). When in sympatry, they are vertically zonated intertidally, occupying distinct but overlapping vertical limits on exposed shores with respect to tidal level and emersion stress intensity (Billard *et al.*, 2010; Zardi *et al.*, 2011). Moreover, these species have different mating systems and morphological features (Billard *et al.*, 2010; Zardi *et al.*, 2011). *F. spiralis* is found on the upper shore, somewhat above *F. guiryi*, both hermaphroditic and mainly self-fertilizing, whereas the dioecious and outcrossing *F. vesiculosus* is located in the mid-intertidal, below the other sister species (Zardi *et al.*, 2011).

Figure 1. *Fucus* species considered in this study. A. *F. vesiculosus* (Tejo, Portugal); B. *F.spiralis* (Cornwall, UK); C. *F. guiryi* (Cornwall, UK).

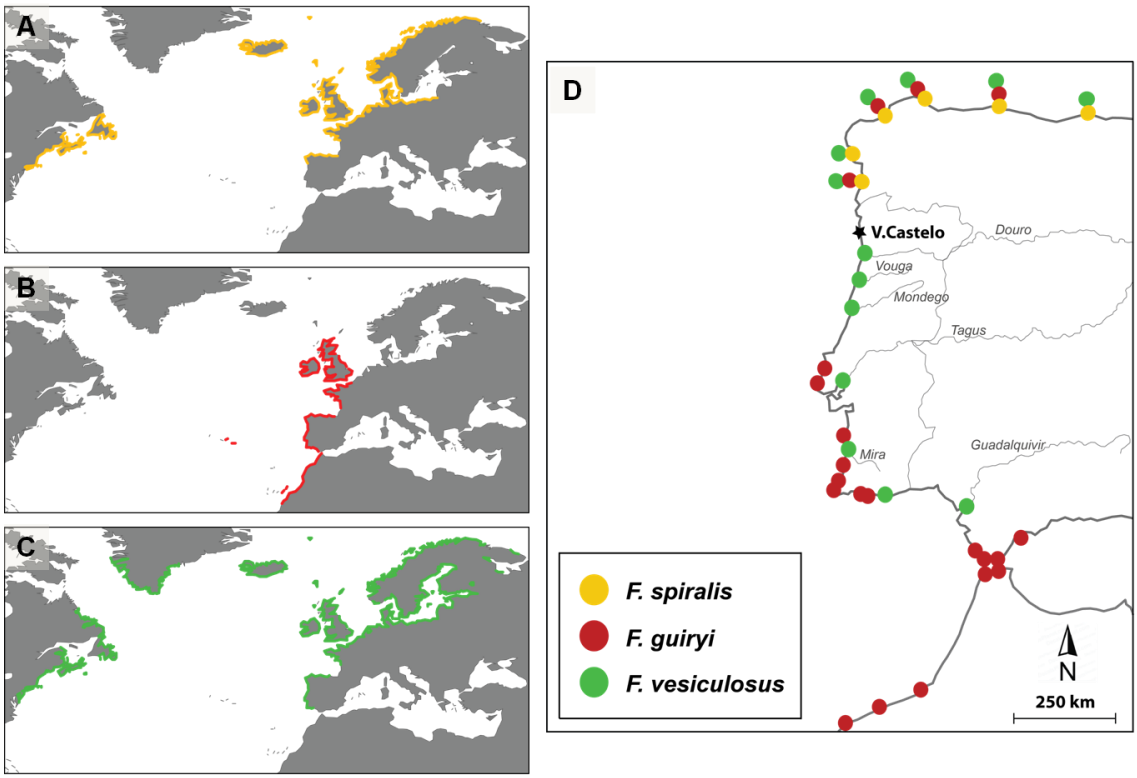

Figure 2. Distribution of the three *Fucus* species. A. *F. spiralis*; B. *F.guiryi*; C. *F. vesiculosus;* D. Occurrence of the species in the Iberian Peninsula. Dots in north Spain are for the representative distribution and not for the exhaustive coverage.

Traditionally, two species were recognized for these lineages, *F. vesiculosus* and *F. spiralis* (Serrão *et al.*, 1999; Coyer *et al.*, 2006). Hence, hermaphroditic *Fucus* belonging to Lineage 2 in the Atlantic were grouped together as *F. spiralis*. Billard *et al.* (2010), based on genetic (microsatellite markers) and ecological (vertical distribution on the shore and emersion time) evidence, was the first to challenge this view by describing a second hermaphroditic genetic entity corresponding to the morphotype *F. spiralis* var. *platycarpus* (Thuret) Batters and occurring in sympatry in Viana do Castelo (north Portugal) and in Santec (Brittany, France), with ecological niche divergence (mid-upper shore) suggested to be related to resilience to emersion stress.

Furthermore, based in both mitochondrial and nuclear (microsatellite) markers, a third hermaphroditic entity (*F. spiralis* South) was reported in Coyer *et al.* (2011), occurring on the open coast, mainly in allopatric southern locations of the *Fucus* distributional range, but with isolated occurrences also reported from Brittany, France. In this study, the hermaphroditic distinct entities *F. spiralis* High (= *F. spiralis* var. *typicus*) and *F. spiralis* South (south clade) were suggested to have originated following divergence from a common ancestor into geographically segregated northern- and southern-adapted entities. Occasional northward migration of individuals of the south clade and subsequent hybridization with *F. vesiculosus* in sympatry, could have originated the other North clade entity, *F. spiralis* Low (= *F. spiralis* var. *platycarpus*). Interestingly, *F. spiralis* South showed clearly distinct mithocondrial haplotypes, while both *F. spiralis* var. *typicus* and *F. spiralis* var. *platycarpus* shared haplotypes with *F. vesiculosus* (Coyer *et al.*, 2011).

Further genetic (diagnostic microsatellites and SNPs in protein-coding regions), morphological and physiological analyses found two distinct morphological entities, *F. spiralis* var. *typicus* and *F. spiralis* var. *platycarpus*, coherently assigned to distinct genetic groups (Zardi *et al.*, 2011). In this study, the lower-shore, hermaphrodite entity *F. spiralis* var. *platycarpus* was raised to a new species, *F. guiryi*. Even though, this genetic entity could not be consistently resolved with a multigene phylogeny, since sympatric morphotypes were polyphyletic (Zardi *et al.*, 2011). Other multigene phylogenetic analysis also supported the monophyly of two distinct hermaphrodite lineages, *F. spiralis* and *F. guiryi*, with *F. vesiculosus* as a sister species (Cánovas *et al.,* 2011). Despite this, monophyly was dependent on the exclusion of sympatric individuals of *F. guiryi*.

Hence, analyses from previous studies support the hypothesis for mitochondrial introgression between *F. vesiculosus*, *F. spiralis* and *F. guiryi* when in sympatry throughout the northern range, suggesting that species boundaries are permeable to gene flow (Coyer *et al.*, 2011). However, they do not support nuclear introgression as

given by the clear monophyly for both *F. guiryi* allopatric populations and *F. spiralis* (Zardi *et al.*, 2011; Cánovas *et al.*, 2011). Nevertheless, the fact that: i) relationships within *F. guiryi* when sympatric individuals were included could not be resolved with nuclear markers; and ii) *F. guiryi* sympatric individuals have shared haplotypes with *F. vesiculosus* and *F. spiralis*, helps strengthen the argument for hybridization with these lineages for populations in sympatry, particularly in the contact zone in northwestern Iberia (Zardi *et al.*, 2011; Cánovas *et al.*, 2011).

Hypotheses to explain incongruent phylogenetic signals have been mostly attributed to differences in mating system, since high levels of selfing in both *F. spiralis* and *F. guiryi* would prevent gene flow between these two lineages, while genetic exchanges with outcrossing *F. vesiculosus* appear more likely. An expansion northwards of the allopatric lineage of *F. guiryi* and hybridization with *F. vesiculosus* to form *F. guiryi* sympatric lineage has been suggested but not demonstrated (Coyer *et al.*, 2011). Then, different levels of habitat segregation: i) northern vs. southern range, for allopatric and sympatric *F. guiry*; ii) open coast versus sheltered habitats, for *F. vesiculosus* and allopatric *F. guiry*; and iii) distinct vertical distribution limits and resilience to emersion stress for the three entities when in sympatry, would explain the maintenance of the distinct lineages (Coyer *et al.*, 2011; Cánovas *et al.*, 2011; Zardi *et al.*, 2011).

The complex nature of *Fucus* relationships provides a fascinating challenge in trying to understand what processes underlie diversification. *Fucus* are broadcast spawners and evolutionary divergence between populations and species can take place rapidly in response to physical stress (e.g., emersion or thermal stress, Pearson *et al.*, 2000; 2009). Moreover, variation in the mating system between species is also a key feature in this clade, which can potentially influence reproductive isolation and the evolutionary responses to habitat differences (Cánova *et al.*, 2011; Monteiro *et al.*, 2012; 2016). Hence, this genus provides an excellent model to study hybridization patterns and evolutionary processes involved in speciation. However, so far, studies based on few molecular markers have not been able to fully resolve relationships at the species level, demanding a broader genome-scale approach to accurately untangle pathways involved in the creation of the cryptic diversity and complex relationships occurring within these key structural species.

1.3 Objectives

Making use of high-throughput technologies that allow for a genome-scale perspective, we aim to understand the role of hybridization in species diversification and how best

we can detect it in three lineages of the marine group of brown alga *Fucus*. The major question of this work is to detect the extent to which hybridization occurs and if hybridization signals support a single or multiple hybrid origin. For this we will:

i) use both supermatrix and supertree approaches to estimate the species tree;

ii) test for introgression and try to understand whether any incongruence detected results from introgressive hybridization between lineages or it is rather due to ILS.

2. Material and Methods

2.1 Sampling

This study was based on short read transcriptomic sequence data from a total of 61 individuals (approximately 3 individuals per population) from populations covering the five lineages (*Fucus serratus*, *F. ceranoides*, *F. guiryi*, *F. spiralis* and *F. vesiculosus*). Individuals were haphazardly sampled along 100m horizontal transects on intertidal shores under similar conditions during receding midday low tides (Fig. 3, Table 1). Apical tissue was conserved at low temperature in a liquid nitrogen cryoshipper in the field for transport to the laboratory, where it was stored at -80° C until extraction.

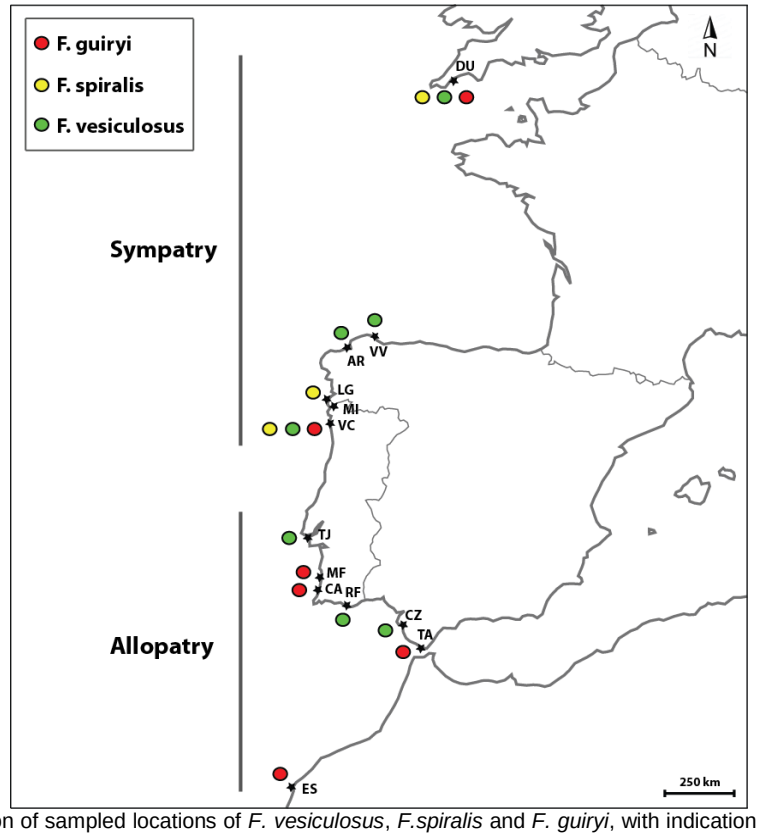

Figure 3. Distribution of sampled locations of *F. vesiculosus*, *F.spiralis* and *F. guiryi*, with indication of the distributional range where *F. vesiculosus* occurs in allopatry and sympatry with the hermaphroditic lineages (*F. spiralis/F. guiryi*). Circles indicate sampled locations. Codes correspond to locations in Table 1.

Table 1. Sampling locations for the five lineages of *Fucus.* Location: sampling locations; Code: code for locations; Latitude, Longitude: coordinates for locations in decimal degrees; Nb individuals: number of individuals sampled for each species.

Species	Location	Code	Latitude	Longitude	Nb individuals
F. serratus	Viana do Castelo, North Portugal	VC	41.696082°	-8.851550°	2
F. ceranoides	Ria de Viveiro, Galicia, Spain	VV	43.662160°	-7.597099°	2
	Ria de Ares, Galicia, Spain	AR	43.404495°	-8.161057°	3
	Rio Minho, North Portugal	MI	41.894742°	-8.821819°	2
	Viana do Castelo, North Portugal	VC	41.696082°	-8.851550°	1
F. guiryi	Durgan, Cornwall, UK	DU	50.103426°	-5.115086°	3
	Viana do Castelo, North Portugal	VC	41.696082°	-8.851550°	3
	Vila Nova de Milfontes, SW Portugal	MF	37.711074°	-8.791811°	1
	Carreagem, SW Portugal	CA	37.366916°	-8.836784°	3
	Tarifa, SW Spain	TA	36.015794°	-5.573238°	3
	Essaouira, Morocco	ES	31.514486°	-9.772983°	3
F. spiralis	Durgan, Cornwall, UK	DU	50.103426°	-5.115086°	2
	La Guardia, Galicia, Spain	LG	41.908636°	-8.877236°	3
	Viana do Castelo, North Portugal	VC	41.696082°	-8.851550°	3
F. vesiculosus	Durgan, Cornwall, UK	DU	50.103426°	-5.115086°	3
	Ria de Viveiro, Galicia, Spain	VV	43.674492°	-7.609900°	3
	Ria de Ares, Galicia, Spain	AR	43.426372°	-8.198205°	3
	Viana do Castelo, North Portugal	VC	41.696082°	-8.851550°	6
	Rio Tejo, West Portugal	TJ	38.761456°	-9.090567°	2
	Ria Formosa, South Portugal	RF	37.005743°	-7.965351°	3
	Cadiz, SW Spain	CZn	36.467177°	-6.251307°	3
	Cadiz, SW Spain	CZv	36.457197°	-6.229402°	3

2.2 Transcriptome sequence dataset

Total RNA was extracted as described previously by Pearson *et al.* (2006), cDNA libraries were prepared and 100 bp paired-end sequencing was performed on the Illumina platform by the sequence provider (Beijing Genomics Institute, BGI, Hong Kong, China). Data for *F. ceranoides* MI, *F. vesiculosus*, *F. serratus*, *F. spiralis* and *F. guiryi* from VC (Fig. 3, Table 1) were sequenced on the illumina HiSeq 2000 platform (6 x samples per lane), while the remaining samples were sequenced on a HiSeq 4000 machine (24 x samples per lane). Quality filtering was performed by the sequence provider using Filter_fq (GitHub), this included removing adapter sequences, contamination and low-quality reads (reads that failed a minimum threshold of Q = 20) from raw reads. Reports sent from BGI, with information on the distribution of base percentage and quality along reads after filtering, were verified to assure quality of the data using FastQC v0.10.1 tool (Andrews, 2011).

Read mapping was performed against a reference transcriptome for *F. ceranoides* (EMBL-EBI ENA Accession PRJEB11969) that was first filtered for putative single-copy genes. Single copy genes were identified by comparison with a second reference transcriptome for *F. vesiculosus* (Pearson *et al.* Unpublished data). A detailed description of the procedure for identifying single-copy genes from reference transcriptomes is provided in Appendix I). Three alternate mapping methods were tested to evaluate their different performances. Stampy (Lunter and Goodson, 2011)

was tested in a hybrid mode, in which it combines the use of a hash table data structure with the BWA algorithm as a first stage to map the reads. Alternatively, both BWA and Bowtie2 mappers are based on the Burrows-Wheeler transform (Burrows and Wheeler, 1994). The software BWA was tested with the BWA-MEM (Li, 2013) algorithm, which performs a local alignment and with parameter setting for tuning the performance to achieve higher accuracy. Bowtie2 (Langmead and Salzberg, 2012) was tested using both local and end-to-end alignments. In the end-to-end read alignment, the algorithm includes all the characters in the read when searching for alignments, whereas in the local read alignment mode, it may trim some read characters from one or both ends of the alignment, maximizing the alignment score (Langmead and Salzberg, 2012). Based on the percentage of properly paired reads mapped, the latter was chosen for read mapping, using a local alignment and *very-sensitive* option.

2.3 SNP calling and alignment generation

SNP calling and generation of the consensus sequence was done using SAMtools v0.1.19 (Li *et al.*, 2009) and BCFtools (Li, 2011). First, the phasing of the alleles was performed, with the option for dropping reads with ambiguous phase (*samtools phase -AF*), followed by the generation of the consensus sequences (*samtools mpileup -u*). Finally, the variants were called (per-sample genotypes), using a Bayesian inference (*bcftools view* -cg).

In order to obtain multiple sequence alignments for each locus, a pipeline was built for aligning and removing both artifacts and poor alignments for downstream analyses. The transcripts were aligned using TranslatorX (Abascal *et al.*, 2010). This program is based on the principle of back-translation, in which the cDNA sequences are translated into amino-acids and the amino-acid alignment is used to guide the alignment of the nucleotide sequences as codons. Additionally, the GBlocks (Castresana, 2000) option was used to identify poorly aligned regions and those with missing data at the beginning and/or end of alignments. The default options for GBlocks were used, with the exception that gap positions were not allowed (*-b5=n*), and highly divergent regions where positional homology could not be precisely determined were removed (Abascal *et al.*, 2010). This step was performed with a pipeline (*locus_pipe.py*, written by Cymon J. Cox; Appendix II).

A total of 1238 aligned loci were obtained with in-frame codon data with no gaps, ambiguities or stop codons. After filtering loci by removing those with ≤ 60 amino-acids (180 bp), the dataset was reduced to 1000 loci for downstream analyses.

2.4 Network exploratory visualization

Given the close relationships and complex spatial genetic structure observed for *Fucus spp.* in previous phylogeographic studies, the relationships between populations of the focal species (*F. guiryi*, *F. spiralis* and *F. vesiculosus*) were first viewed in a splits network, used as a visualization tool to examine potential conflicting signals, since this method is expected to give a better representation of relationships between taxa in which hybridization is suspected to occur (Huson and Scornavacca, 2011). The splits network was constructed with SplitsTree4 (Huson and Bryant, 2006), using the concatenated dataset with bi-allelic sites. The splits networks was built from the distances between taxa using the Neighbour-Net method (Bryant and Moulton, 2004), in which the distances were estimated based on the proportion of positions at which sequences differ (uncorrected-p distances method; Huson and Bryant, 2006). For the visualization of the network, the Equal Angle (Dress and Huson, 2004) algorithm was used to transform and weight the splits.

2.5 Phylogenetic analyses

2.5.1 Supermatrix approach

Supermatrix approaches to estimate species trees have been widely used in phylogenomics, even if its use with smaller amounts of loci has been strongly discouraged (Edwards *et al.*, 2007). To compare species tree methods to concatenation, we first analyzed the dataset as a single concatenated alignment. For concatenation analyses, aligned transcripts were concatenated into a single supermatrix alignment with a perl script (*catfasta2phyml.pl*, available at github.com/nylander/catfasta2phyml). Bi-allelic sites were then collapsed into a single consensus sequence with a python script (*otus.py,* written by Cymon J. Fox; Appendix III) using p4 (Foster, 2004). Additionally, due to computational constraints, only the informative sites were kept for these analyses.

For the concatenated sequence matrix, we estimated a phylogenetic tree using both maximum likelihood (ML) and Bayesian methods. Maximum likelihood (ML) analyses were performed with RAxML v8.2.8 (Stamatakis, 2014) using the General Time Reversible model (GTR; Tavaré, 1986) and variable sites modeled according to the Gamma distribution. The rapid hill-climbing tree search algorithm (Stamatakis *et al.*, 2008) was used to search for the best scoring tree and perform the bootstrap analysis. One hundred inferences were performed with a complete random parsimony starting tree and ML estimate of base frequencies. The best scoring tree was obtained with a

gamma-based optimization on the best tree. Node confidence was estimated by performing three independent runs (1000 replicates) of rapid bootstrap inferences, with ML estimate of alpha-parameter and the Broyden-Fletcher-Goldfarh-Shanno (BFGS; Head and Zerner, 1985) algorithm to optimize GTR rate parameters. To provide support values for the ML tree, a 50 percent majority rule tree was built with the bootstrap inferences (using the script *makeConsensusTree.py*, available at gyra.ualg.pt).

Bayesian inference analysis was conducted with MrBayes v3.2.6 (Ronquist *et al.*, 2012) on the same dataset used for ML analysis. The GTR model with variable sites modeled according to the Gamma distribution was selected. Two independent runs of Markov chain Monte Carlo (MCMC) (Altekar *et al.*, 2004) analysis were performed, each with four Metropolis-coupled chains and an incremental heating temperature of 0.10. Analysis were run for 5.0×10^6 generations, with parameters sampled every 1.0×10^6 generations and a burn-in of 25% for diagnosis. Average standard deviation of split frequencies and acceptance rates of swaps between Metropolis-coupled chains were checked and stationarity of both runs was analysed with Tracer v1.6.0 (Rambaut *et al.*, 2013). After discarding the first 10% of samples, a 50% majority rule consensus tree was built from the posterior distribution of both runs.

Additionally, a phylogenetic analysis including the invariable sites was performed, using the reversible Polymorphism-Aware Phylogenetic Model (revPoMo; Schrempf *et al.*, 2016). This model can be distinguished from the classical phylogenetic models by the fact that, in addition to the parameters that describe the mutational process, it has an extra parameter (θ) representing the proportion of polymorphic sites (De Maio *et al.*, 2015). In this way, it allows for the incorporation of within-species genetic variation (De Maio *et al.*, 2015). Additionally, by considering both present and ancestral polymorphisms, it accounts for incomplete lineage sorting (ILS) (Schrempf *et al.*, 2016). Following De Maio *et al.* (2015), a counts file was generated from the concatenated dataset of the 1000 loci and was subsequently used as input for the revPoMo, implemented in the ML software IQTREE v1.3.11 (Nguyen *et al.*, 2015). The GTR model was implemented as the substitution model, together with the PoMo model (reversible PoMo with tree inference) and estimation of frequencies and.an ultrafast bootstrap (1000 replicates) (Minh *et al.*, 2013) was performed, The output is the consensus tree.

2.5.2 Supertree approach

In contrast to the concatenation approach, species trees methods assume that gene trees are independent from each other, incorporating gene tree discordance in the

estimation of the species tree (Mirarab *et al.*, 2014; De Maio *et al.*, 2015). Thus, to compare between these two approaches, we used ASTRAL (Mirabab *et al.*, 2014), with the same dataset as for concatenation, which is an alternative to extremely computationally intensive methods, such as *BEAST. Supertree methods are modeled by the coalescent and, thus, they incorporate uncertainties caused by ILS through the coalescent but they do not incoportate introgression (Heled and Drummond, 2010), which can then remain as a source of phylogenetic noise. ASTRAL uses an algorithm that finds the species tree that agrees with the largest number of quartet trees induced by a set of unrooted gene trees, an approach called the Maximum Quartet Support Species Tree (MQSST) (Mirarab *et al.*, 2014).

Optimal gene trees were first estimated with RAxML v4.8.0, using the GTRGAMMA model and the rapid hill-climbing algorithm. Ten independent searches were conducted using random maximum parsimony starting trees, and a final gamma-based optimization was conducted on the likelihood of the best tree. These 1000 best ML gene trees were rooted with *F. serratus* and used as input for reconstructing the species trees with ASTRAL v4.8.0 (Mirarab and Warnow, 2015), which allows the inclusion of multiple individuals per species. Following Mirarab *et al.* (2014) support for the species tree was obtained with 100 bootstraps.

2.6 Detection of incongruence among loci

Detecting incongruence between gene trees presents a major challenge since it may have several potential causes. Particularly, modeling variation in evolutionary histories of hybrid lineages may become a complex process, since hybridization may not be the only source of discordant phylogenies (Cui *et al.*, 2013). This is especially relevant when analyzing multigene datasets.

2.6.1 Analysis of gene tree - species tree discordance with BCA

Analyses of gene tree-species tree discordance were performed with Bayesian concordance analysis (BCA). This method is based on the information provided by the posterior distributions for each gene tree, taking into account the expected degree of concordance among genes to correct each gene's posterior (Ané *et al.*, 2007; Baum, 2007). On a second MCMC stage, it estimates the proportion of the genes that support a given clade, the concordance factor (CF), bounded by a credibility interval. This interval takes into account the statistical uncertainty regarding the individual gene trees (using the posterior distribution) and the amount of overlap provides clues concerning the degree of concordance for a particular gene (Baum, 2007). Hence, CFs give a

measure of the genomic support for each clade. A primary concordance tree is the obtained considering only the clades with the largest CFs, revealing the clades that are true for a large proportion of genes (Ané *et al.*, 2007; Larget *et al.*, 2010). BUCKy v1.4.4 was used for this approach, which makes no assumptions about source(s) of discordance (Larget *et al.*, 2010).

For single-gene analysis, the best-fit model of molecular evolution was estimated for each transcript by running the program MODELGENERATOR (Keane *et al.*, 2006) with the empirically tuned Akaike Information Criterion (AIC_2; Posada and Crandall, 2001a). Transcript alignments were then analysed with MrBayes v3.2.6 to obtain the posterior probability (PP) of each topology for each locus individually. Two independent runs of MCMC analysis were performed, each with four Metropolis-coupled chains and an incremental heating temperature of 0.025. Analysis were run for 7.0×10^5 MCMC generations, with parameters sampled every 1.0×10^2 generations and a burn-in of 25% for diagnosis. A few randomly chosen parameter files from each run were checked for convergence (average split frequencies) and mixing (swaps between chains) diagnoses. For each locus, the tree samples from the two runs were combined and the PP for all topologies was calculated after discarding 25% of the total trees as burn-in.

For concordance analysis, several hypotheses were tested based on the resulting topologies from previous phylogenomic analyses. In order to understand the potential role of *F. vesiculosus* in the evolutionary history of the *F. guiryi* sympatric populations, subsets of this species were selected for each of the hypotheses to be analyzed (Hypotheses 1 - 3: considering either *F. vesiculosus* VC, North or South; Hypothesis 4: considering all populations of *F. vesiculosus*; Hypotheses 5 - 7: considering two of the three groups; Appendix IV). For each taxon group in each hypothesis, one allele was randomly sampled using the UNIX command *shuf* and ten independent replicates were performed in order to have statistical support. Concordance analysis was performed with 1.0×10^5 generations, three chains, four independent runs and a chain swap every 50 generations. Different values for the *a priori* level of discordance among loci (α) and for the heating parameter (alpha-multiplier) were tested. The best parameters were defined as the ones giving low CF standard deviation (SD < 0.001) and chain swap between 20 and 60%. Hence, the α was set to 0.1 and the alpha-multiplier to four. Sample-wide cutoff CF for display was set to 0.05. In order to estimate 95% confidence intervals (CI) considering the ten replicates, the standard deviation (SD) for each interval was estimated as:

$$SD = \sqrt{(1000)} \times \frac{upper\ CI - lower\ CI}{3.92};$$

the standard error (SE) was calculated as:

$$SE = \frac{SD}{\sqrt{1000}}..$$

Additionally, the global mean for the ten CFs and a pooled estimate for the global CI was also calculated. These two values were used to estimate the global upper and lower CIs for the ten replicates.

2.6.2 Testing for introgression

Because BUCKy analysis makes no explicit assumptions about the nature of the discordance between gene trees (although, e.g., inferences can be drawn concerning deviations from expectations under ILS), a complementary approach was used to test whether discordance could be better explained by introgression, rather than simple ILS. As a complement to model-based methods, a widely used approach for detecting introgression over recent years is statistical testing (Green *et al.*, 2010; Martin *et al.*, 2014). A genome-wide test for admixture was performed to detect (ancient) admixture between the diverged lineages. These methods consider individual sites throughout the genome (Green *et al.*, 2010; Durand *et al.*, 2011).

The concatenated dataset with bi-allelic sites was used and several tests were performed in order to assess the proportion of genome admixture. Assuming a four-taxon phylogeny of three populations and an outgroup with topology (((P$_1$, P$_2$), P$_3$), O), the *D* statistic compares the occurrence of two incongruent SNP patterns, ABBA and BABA, in which "A" is the ancestral allele, defined by the outgroup, and "B" the derived allele. At ABBA sites P$_2$ shares a derived allele with P$_3$, whereas at BABA sites P$_1$ shares a derived allele with P$_3$ (Martin *et al.*, 2014). Under the null hypothesis of no gene flow and random mating, the frequencies of these patterns across the genome are expected not to differ significantly (Durand *et al.*, 2011). Hence, by estimating the asymmetry in the relative abundance of these patterns, *D* provides a test for an excess of shared derived polymorphism between populations. In this study population samples were used, where $C_{ABBA}(i)$ and $C_{BABA}(i)$ represent the frequency of the derived allele at each site in each population (Durand *et al.*, 2011; Martin *et al.*, 2014):

$$C_{ABBA}(i) = (1 - \hat{p}_{i1})\hat{p}_{i2}\hat{p}_{i3}(1 - \hat{p}_{i4})$$
$$C_{BABA}(i) = \hat{p}_{i1}(1 - \hat{p}_{i2})\hat{p}_{i3}(1 - \hat{p}_{i4})$$

Where $\hat{p}_{ij}$ is the frequency of the derived allele at site *i* in population *j*.

Following Martin *et al.* (2014), the proportion of the genome shared through introgression (f) was estimated as the proportion of haplotypes in the recipient population that trace their ancestry through the donor population (P_D). In a conservative approach, the $\hat{f}_d$ statistic assumes that complete introgression from P_D to the recipient population (either P_2 or P_3) would lead to complete homogenization of allele frequencies. This allows considering bidirectional introgression on a site-by-site basis, setting the donor population at each site as that which has the higher frequency of the derived allele ("B"). Given *S* as the difference between sums of ABBAs and BABAs (Martin *et al.*, 2014), the $\hat{f}_d$ statistic compares the observed value of *S* to a value estimated under a scenario of complete introgression from P_3 to P_2, being defined as:

$$\hat{f}_d = \frac{S(P_1, P_2, P_3, O)}{S(P_1, P_D, P_D, O)}$$

The analysis was performed with HybridCheck (Ward and Oosterhout, 2016). This program implements both D and $\hat{f}_d$ statistics, but for $\hat{f}_d$ it considers both scenarios of complete introgression between P_3 and either P_2 or P_1 (Ward and Oosterhout, 2016). For statistical support, HybridCheck performs a jackknife procedure dividing the alignment into non-overlapping segments and then estimates a *p*-value based on the binomial distribution, the number of sites that have a higher ABBA score and number of sites that have a higher BABA score. These binomial *p*-values computed for each block are used with Fisher's combined probability formula to calculate an overall binomial based *p*-value for the entire alignment (Ward and Oosterhout, 2016).

2.7 Divergence time analysis

In order to have an estimate of the divergence time for the *Fucus* lineages, a multilocus species tree analysis was carried out using the multispecies coalescent model implemented in BEAST v1.7.5 (Heled and Drummond, 2010; Drummond *et al.*, 2012). *BEAST method applies a MCMC algorithm to perform inference of both gene and species trees from molecular sequences (Drummond *et al.*, 2012), providing a Bayesian implementation of the multispecies coalescent that improves the accuracy of species phylogeny reconstruction (Heled and Drummond, 2010).

Based on the output from BUCKy analysis, a subset of loci was chosen in order to get a cluster in which all loci share the species tree topology, as given by the

phylogenies previously estimated. The choice was based on the posterior probability for each locus of supporting the target topology, given all loci's data (Larget *et al.*, 2010). The loci having a PP greater than 50% of supporting the topology were chosen for the analysis. The subset of transcripts was run with IQTREE (Nguyen *et al.*, 2015) and the consensus tree was visually inspected in FigTree v1.3.1 (Rambaut, 2013). Only loci that had a coherent topology with the cluster to be analyzed and no signals of introgressed individuals (non-polyphyletic lineages) were retained. Additionally, the outgroup species *F. serratus* was excluded since it appeared within the ingroup in several loci.

A test of recombination was performed for each locus with the software RDP4 (Martin *et al.*, 2015), using seven automated detection methods: the original RDP method (Martin and Rybicki, 2000), BOOTSCAN (Martin *et al.*, 2005), Maximum χ^2 (Maynard Smith, 1992), CHIMAERA (Posada and Crandall, 2001b), GENECONV (Padidam *et al.*, 1999), Sister Scan (Gibbs *et al.*, 2000) and 3SEQ (Boni *et al.*, 2007). Loci showing signs of recombination events were discarded. Fifteen loci were used to reconstruct the species tree. BEAST analyses were performed using an uncorrelated, lognormal relaxed molecular clock and a Yule speciation model (Gernhard, 2008) with a piecewise constant population-size model. The nucleotide substitution models were selected following the models obtained in the single-gene Bayesian analyses, with estimated base frequencies. The molecular clock was calibrated incorporating as normal prior the mean evolutionary rate of 3.6×10^{-9} with 9.6×10^{-10} for the standard deviation, following Bengtsson-Palme *et al.* (2013).

MCMC analyses were run for 2.0×10^8 generations, with parameters logged every 2.0×10^4 generations. The remaining parameters were used as default. Output from BEAST was examined for chain stationarity and convergence and the effective sample sizes for each parameter of the model in Tracer v1.6.0 (Rambaut *et al.*, 2013). The maximum clade credibility (MCC) tree was summarized using TreeAnnotator v1.8.3 (Drummond *et al.*, 2012), after discarding the first 40% of samples as burn-in and setting the high posterior probability threshold to 0.5 for the median node heights. The MCC tree was viewed in FigTree and rooted with root age of 2.3×10^6 years, following Cánovas *et al.* (2011).

3. Results

3.1 Quality control of the short-read data

After verifying with FastQC, clean reads obtained from the sequence provider were found to be of high quality (Table 2), with high percentage of good quality reads (Q score = 20, corresponding to a base call accuracy of 99%) and homogeneous distribution of GC content. Further quality trimming was not necessary.

Table 2. Clean reads obtained from RNA-sequencing. Reads (M): millions of read pairs (100 bp paired-end); Bases (Mb): total megabases of sequence; Q20(%): percentage of nucleotides with Q score ≥ 20, corresponding to a base call accuracy ≥ 99%; GC(%): average GC content.

Species	Individual	Reads(M)	Bases(M)	Q20(%)	GC(%)
F. serratus	VC1	17	3341	98.83	53.45
	VC2	15	3019	98.77	53.61
F. ceranoides	AR1	12	2412	98.25	53.56
	AR2	16	3231	98.77	52.98
	AR3	12	2279	98.57	53.06
	VC1	20	3891	98.12	54.08
	VV1	16	3084	98.31	53.56
	VV2	11	2106	97.98	53.82
	VV3	16	3127	98.64	53.56
	MI1	17	3241	98.67	52.78
	MI2	15	2874	98.39	53.91
F. guiryi	CA1	12	2335	98.27	53.17
	CA2	11	2141	98.01	53.68
	CA3	16	3121	98.72	53.22
	DU1	12	2303	97.38	53.82
	DU2	15	2947	98.24	54.00
	DU3	15	2871	97.38	53.82
	ES2	17	3258	98.73	53.68
	ES4	17	3321	98.86	53.47
	ES5	15	3015	98.73	53.62
	TA1	17	3294	98.62	54.07
	TA2	16	3184	98.63	53.83
	TA7	17	3407	98.21	54.30
	VC1	28	5045	98.36	53.01
	VC2	31	5519	98.32	53.29
	VC3	32	5695	98.38	52.38
	MF1	20	3995	98.63	53.57
F. spiralis	LG1	30	5410	98.42	53.26
	LG2	31	5613	98.44	53.69
	LG3	29	5218	98.42	53.60
	DU1	15	2879	98.29	53.92
	DU2	19	3669	98.43	53.70
	VC1	32	5637	98.46	53.21
	VC2	29	5202	98.40	52.82
	VC3	30	5431	98.40	53.24
F. vesiculosus	AR1	15	2987	97.94	53.18
	AR4	20	3985	98.69	53.67
	AR5	11	2086	98.24	53.43
	CZn1	18	3598	98.61	53.24
	CZn2	14	2842	97.57	53.55
	CZn3	16	3108	98.41	53.61
	CZv1	12	2367	98.33	53.74
	CZv2	17	3425	98.76	53.47
	CZv3	15	2950	98.70	53.35
	DU1	15	3017	98.26	53.46
	DU2	14	2739	98.18	53.59
	DU3	16	3091	98.34	53.60
	RF1	15	2969	98.16	53.94
	RF3	15	3013	98.28	53.55
	RF6	16	3077	98.72	53.12
	TJ1	27	4780	98.51	52.75
	TJ2	30	5377	98.55	53.23
	VC1	31	5513	98.57	53.59
	VC2	17	3415	98.16	53.39
	VC3	16	3071	98.55	53.39
	VC4	20	3975	98.59	53.47
	VC5	28	5065	98.45	53.41
	VC6	18	3591	98.51	53.43
	VV2	13	2522	97.64	53.61
	VV3	16	3061	98.65	53.31
	VV5	15	2992	98.29	54.03

The median coverage obtained from read mapping .BAM files, and expressed as the within-sample normalized transcript expression measure (number of fragments per kilobase per million mapped reads; FPKM), ranged between 326.9 and 368.7 for *Fucus serratus* and *F. spiralis* populations, respectively (Appendix V).

After removing loci with less than 60 predicted amino acids (180 bp) from the initial single-copy dataset, a dataset of 1000 transcripts was used for the analyses (Appendix VI). The alignments for these loci included five species with a total length of 734,595 nucleotide sites (20,612 parsimony informative sites) containing 38,592 SNPs. Locus lengths ranged between 222 and 6096 bp median 1266bp; Fig. 4).

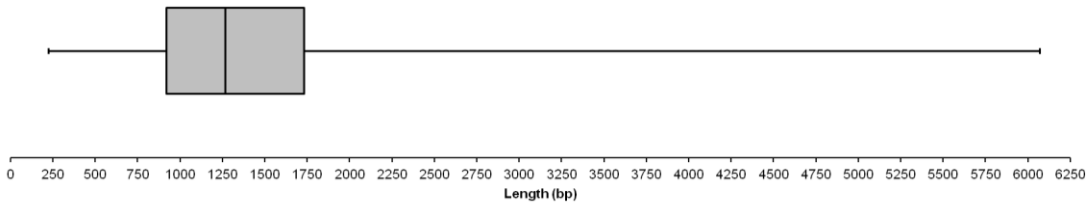

Figure 4. Length distribution (base pairs) of 1000 transcripts from *Fucus spp.*used in the analyses.

3.2 Visualization of the relationships for the focal lineages

Given the complex relationships expected between the species, including potential horizontal gene transmission, a splits network was first used for visualization of the arrangement of individuals within populations for the focal lineages *F. guiryi*, *F. spiralis* and *F. vesiculosus*. The SplitsTree network (Fig. 5) reveals several major features of the relationships among the taxa. First, the higher diversity within *F. vesiculosus* compared with all hermaphrodite taxa is evident, in particular the divergence between northern (N. Spain to UK) and southern (southern Iberia) populations. Second, the population from Viana do Castelo forms a distinct cluster, and is the main source of conflicts (reticulate structures) formed between this population and sympatric *F. guiryi* (northern populations plus one individual from Essaouira, Morocco). Finally, three distinct hermaphroditic clusters are formed; sympatric *F. guiryi*, which is well-separated from allopatric (southern) *F. guiryi* and *F. spiralis*.

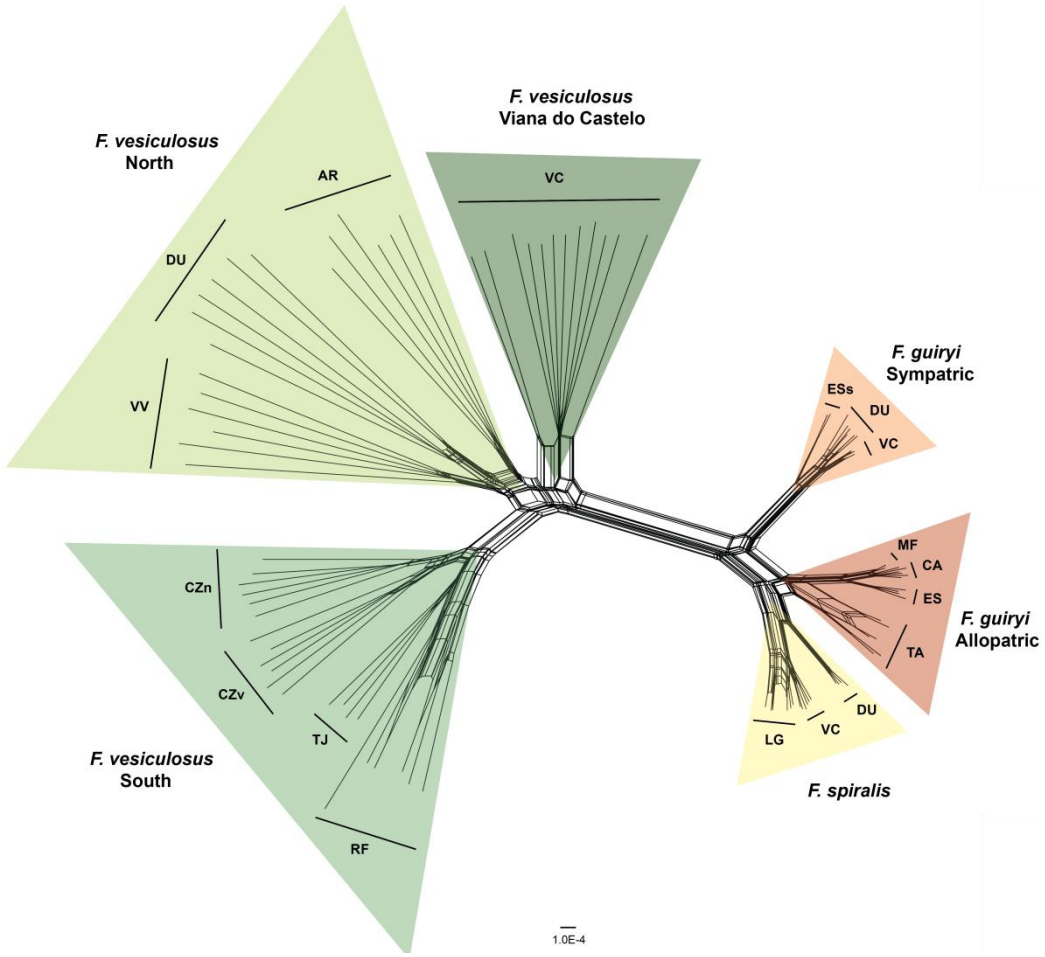

Figure 5. Neighbour-Net splits network constructed from a concatenation of 1000 transcripts for *F. vesiculosus*, *F. spiralis* and *F. guiryi*. Populations are indicated with codes corresponding to locations in Table 1. Colours correspond to the major groups displayed by the network.

Further potential admixture is suggested by reticulate structures between sympatric *F. guiryi* and both the *F. vesiculosus* population from Viana do Castelo (hereafter referred as *F. vesiculosus* VC) and allopatric *F. guiryi* populations. Moreover, longer branches separate the two groups of *F. guiryi* than branches between *F. guiryi* Allopatric and *F. spiralis*. These patterns reveal deep geographic structuring within lineages and, on the other hand, may also indicate (historical) gene flow between lineages.

3.3 Species tree reconstruction

Several species tree methods based on concatenation (the supermatrix approach) were compared with a coalescent-based supertree approach that uses information from gene trees to estimate the true species tree.

Concatenation methods analyzed within both ML (RAxML) and Bayesian (MrBayes) frameworks yielded phylogenetic trees with the same topology and full support for all branches at the population level (Figs. 6, 7). Neither *F. guiryi* nor *F.*

vesiculosus lineages were recovered as monophyletic entities. The former appeared in two separate clades, with full support for the sympatric populations (Durgan and Viana do Castelo) and one individual from Essaouira grouping together as sister to a clade containing the remaining populations of *F. guiryi* grouping with *F. spiralis*. *F. vesiculosus* was polyphyletic, with a clade representing the northern (sympatric) populations (Durgan, Viveiro and Ares) branching first, whereas all southern (allopatric) populations clustered together in a separate clade. Noteworthy was full support for the placement of a single population of *F. vesiculosus* from Viana do Castelo as sister to the hermaphroditic clade containing both *F. guiryi* lineages and *F. spiralis*.

These phylogenetic patterns mirror those observed with the splits network, revealing a clear separation of *F. guiryi* populations into two diverged lineages, with *F. guiryi* sympatric populations more closely related to *F. vesiculosus* VC population and basal to other hermaphroditic lineages. All nodes in both methods give strong support for relationships in these lineages (Bayesian analysis, PP = 1; ML analysis, bootstrap support > 90%).

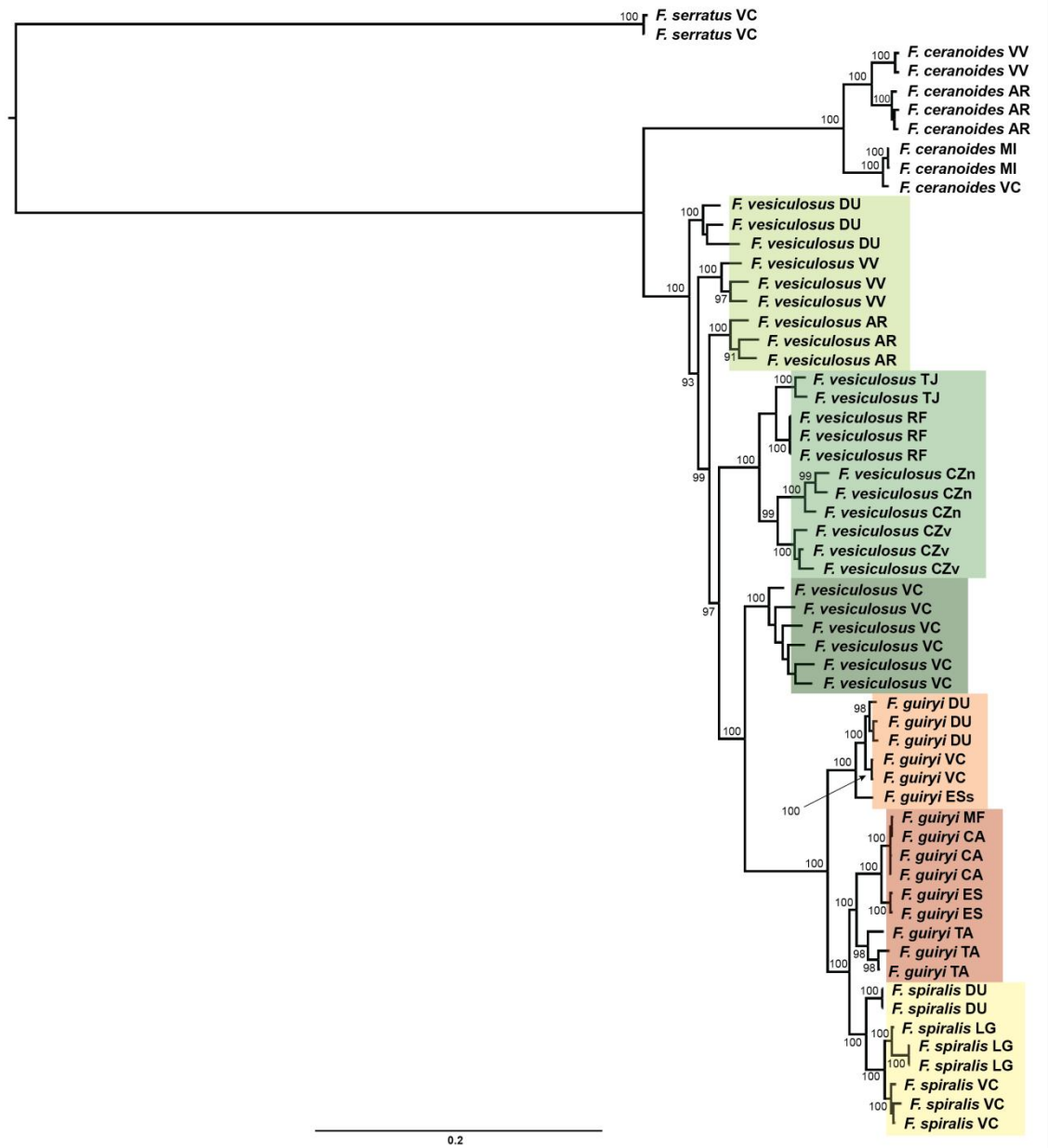

Figure 6. Majority-rule consensus tree resulting from Maximum likelihood analysis of the concatenated dataset (1000 transcripts) for the five lineages of *Fucus spp.* Nodal support generated by 1000 rapid bootstraps with GTRGAMMA model. Colors correspond to the major groups in Figure 5. Codes correspond to locations in Table 1.

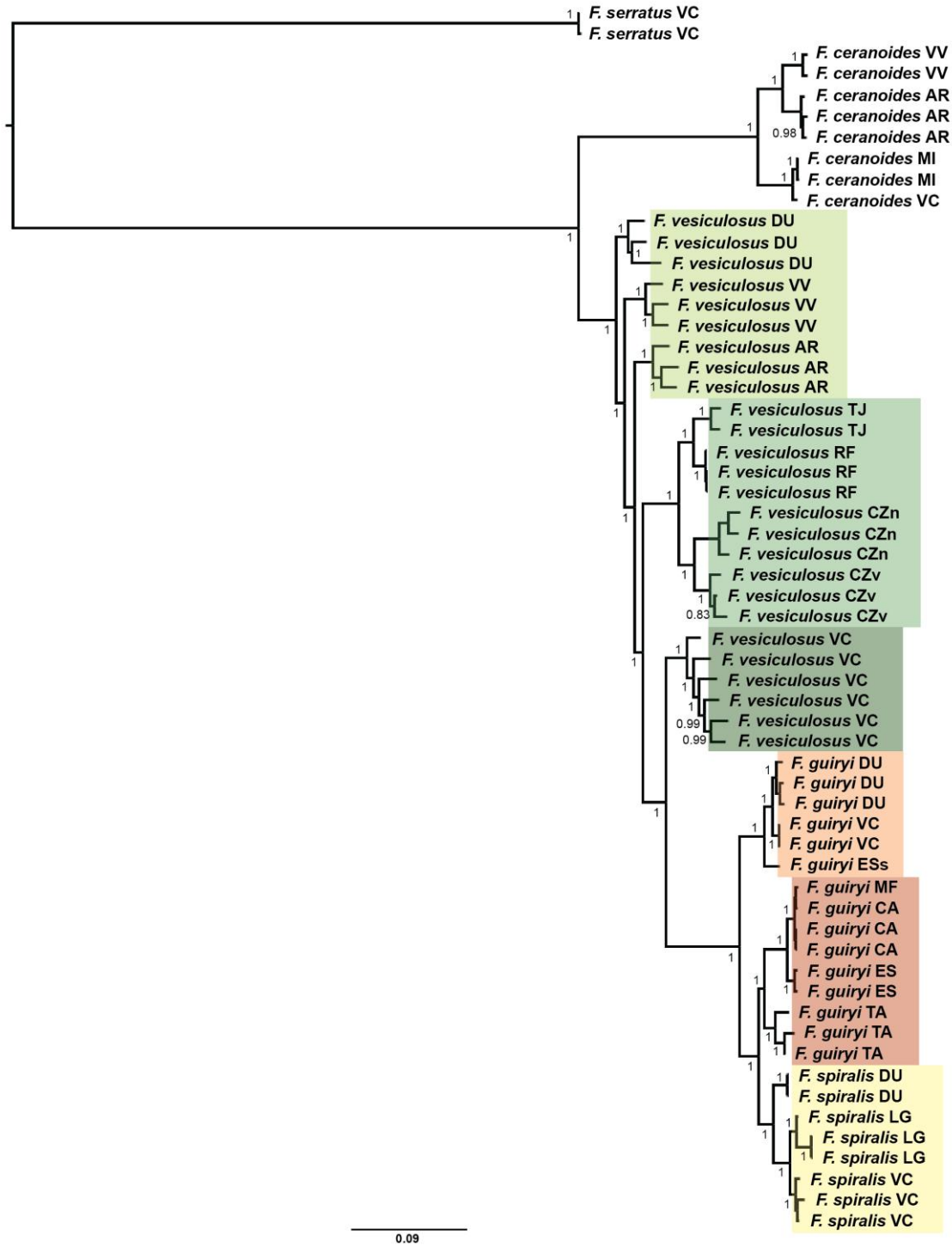

Figure 7. Majority-rule consensus tree resulting from Bayesian analysis of the concatenated dataset (1000 transcripts) for the five lineages of *Fucus spp.* Posterior probabilities are given for the nodes. Colors correspond to the major groups in Figure 5. Codes correspond to locations in Table 1.

A third approach based on a concatenated dataset (of allelic data in this case) and using a polymorphism-aware model (revPoMo; Schrempf *et al.*, 2016) recovered a very similar topology with regard to major clades (Fig. 8). The only difference compared with ML or Bayesian supermatrix methods was the order of branching within the northern

populations of *F. vesiculosus* - Viveiro and Durgan - which grouped together, although with fairly low (66%) bootstrap support.

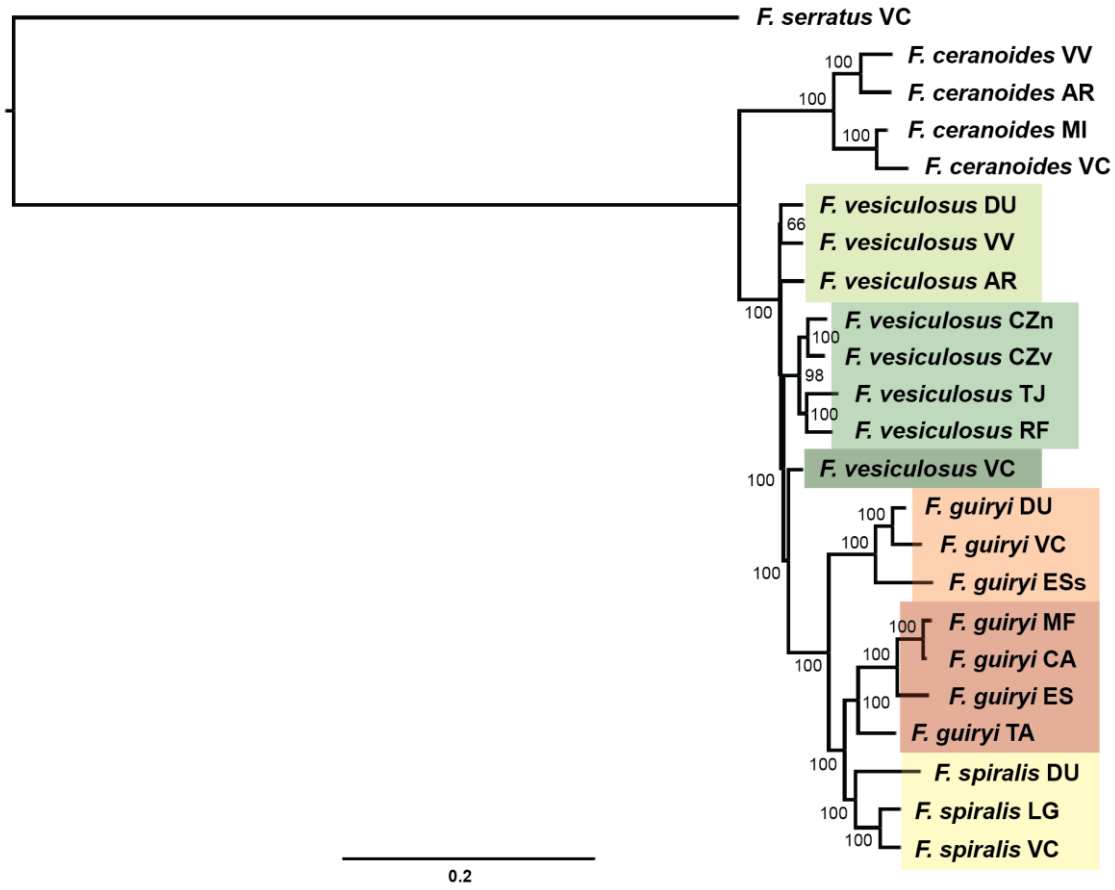

Figure 8. Consensus tree resulting from polymorphism-aware Maximum likelihood analysis of the concatenated dataset (1000 transcripts) for the five lineages of *Fucus spp.* Nodal support generated by 1000 rapid bootstraps with revPoMo+GTR model. Colors correspond to the major groups in Figure 5. Codes correspond to locations in Table 1.

A coalescent-based species tree analysis recovered a similar overall topology for these relationships (Fig. 9), with the major difference being the grouping together of *F. vesiculosus* north populations in a single clade. However, it is noteworthy that the node separating *F. vesiculosus* southern populations from *F. vesiculosus* VC had low bootstrap support (23%), indicating possible ambiguity or gene tree conflict at this node that was not detected using any of the supermatrix approaches. High confidence in poorly-supported (or wrong) species tree topologies is a drawback reported for concatenation methods in the literature (Kubatko and Degnan, 2007). In contrast, the *F. vesiculosus* VC population was again recovered as sister to the hermaphroditic clade (BS support = 84%), as in concatenation methods. Furthermore, a similar pattern was observed for *F. guiryi*/*F. spiralis* populations as for concatenation analyses, in which strong support was found for the hermaphroditic clade, for the divergence

between lineages of *F. guiryi,* and for the sister relationship between *F. guiryi* allopatric populations and *F. spiralis* (100% bootstrap support in all cases).

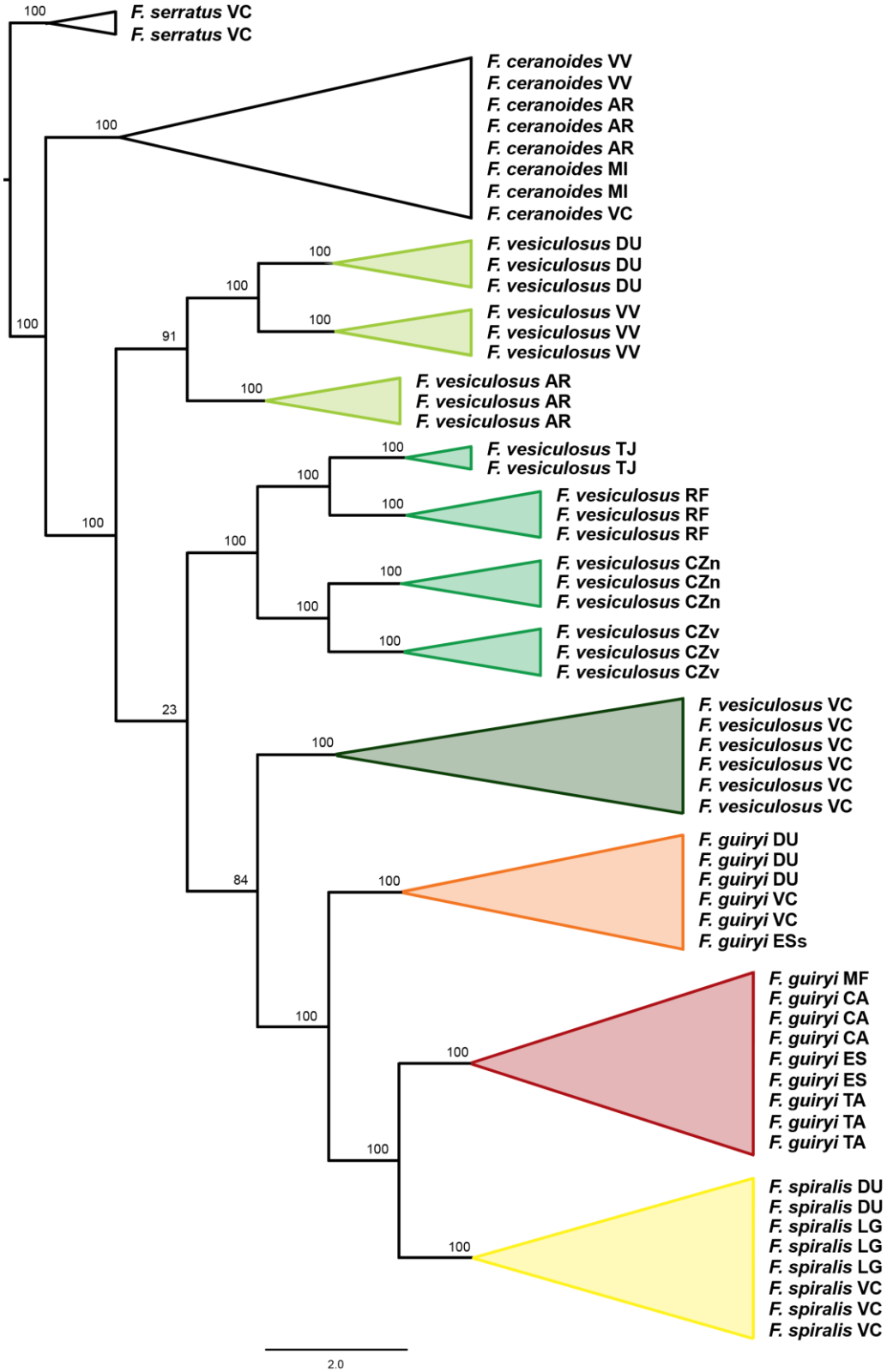

Figure 9. Species tree constructed with ASTRAL based on 1000 best ML gene trees. Colors correspond to the major groups in Figure 5. Codes correspond to locations in Table 1.

Overall, a general concordance between analyses was observed when reconstructing the species tree for the three *Fucus* lineages (*F. vesiculosus, F. guiryi,* and *F. spiralis*). Phylogenetic analyses strongly supported a clear separation of *F. guiryi* into two divergent lineages. Additionally, a deep biogeographic structuring was revealed for *F. vesiculosus*, with separation of northern and southern populations. Likewise, a closer relationship between *F. vesiculosus* VC and the hermaphroditic lineages than to the other northern populations of this lineage was consistently observed, which may be indicative of gene flow, particularly between *F. vesiculosus* VC and the *F. guiryi* sympatric lineages.

3.4 Detection of incongruence among loci

Gene tree discordance may result from several causes, including incomplete lineage sorting (ILS) (Pollard *et al.*, 2006), undetected paralogy, gene flow and introgressive hybridization (Degnan and Rosenberg, 2009). In order to detect conflicting signals within *Fucus* relationships, BUCKy was used to identify instances of major discordance between gene trees and the consensus species tree.

Given the polyphyly recovered by *F. vesiculosus* and *F. guiryi* populations, and doubts regarding the relationships between sympatric and allopatric populations of *F. guiryi,* and additionally between this lineage and both *F. vesiculosus* and *F. spiralis*, the analyses were performed considering different subsets of populations (Appendix IV), reflecting the different clusters retrieved from species tree analyses.

When all populations from *F. vesiculosus* were considered (Fig. 10A, B), 5 of 10 replicate BUCKy runs produced primary concordance trees (PCT) with topologies placing *F. vesiculosus* VC as sister to the hermaphrodite clade (3 replicates with topology as shown in Fig. 10B), the same pattern as that recovered by both the concatenation and supertree methods discussed above. However, a further 4 replicates recovered *F. vesiculosus* as a monophyletic group (Fig. 10A).

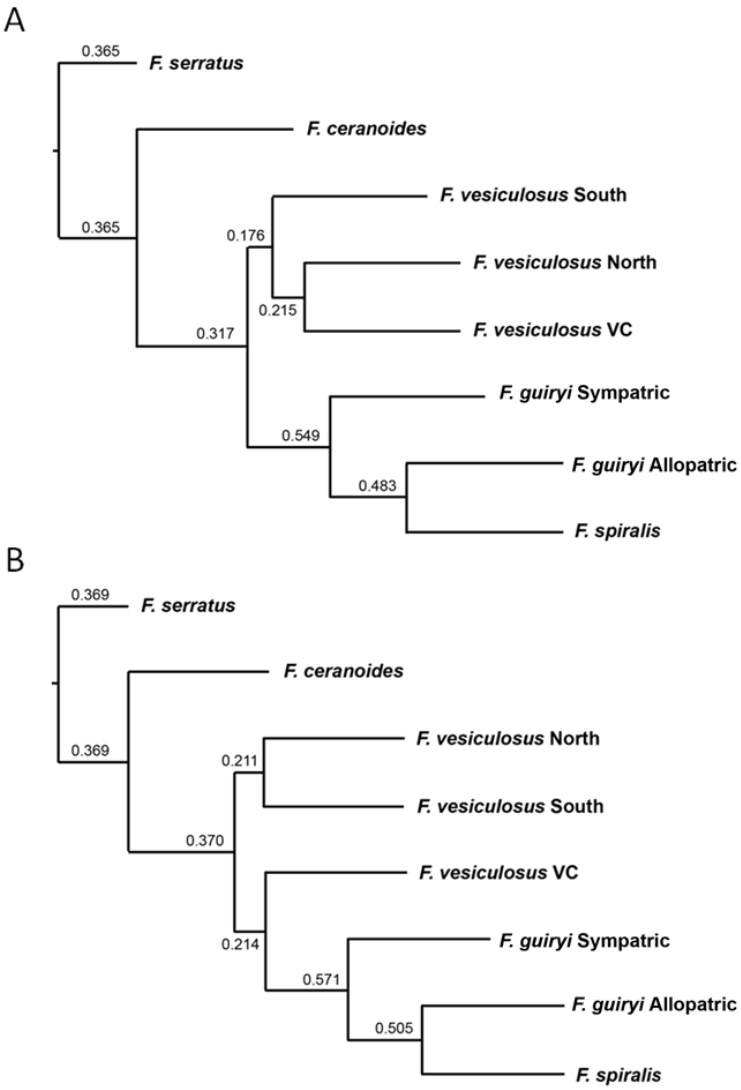

Figure 10. Primary concordance trees obtained with Bayesian Concordance Analysis for the five lineages of *Fucus spp.* including all *F. vesiculosus* groups (*F. vesiculosus* North, *F. vesiculosus* South and *F. vesiculosus* VC). Nodal support is given by sample-wide concordance factors (CF). Names for the major groups correspond to Figure 5. The tree topologies represent the dominant topologies found based on ten replicate runs with randomly-selected alleles. A. Topology supported by four replicates; B. Topology supported by three replicates.

To disentangle the potential role of *F. vesiculosus* in the evolutionary history of the hermaphrodite lineages, and of sympatric *F. guiryi* in particular, alternative hypotheses were tested using subsets of populations from this lineage (Fig. 11A, B, C).

A

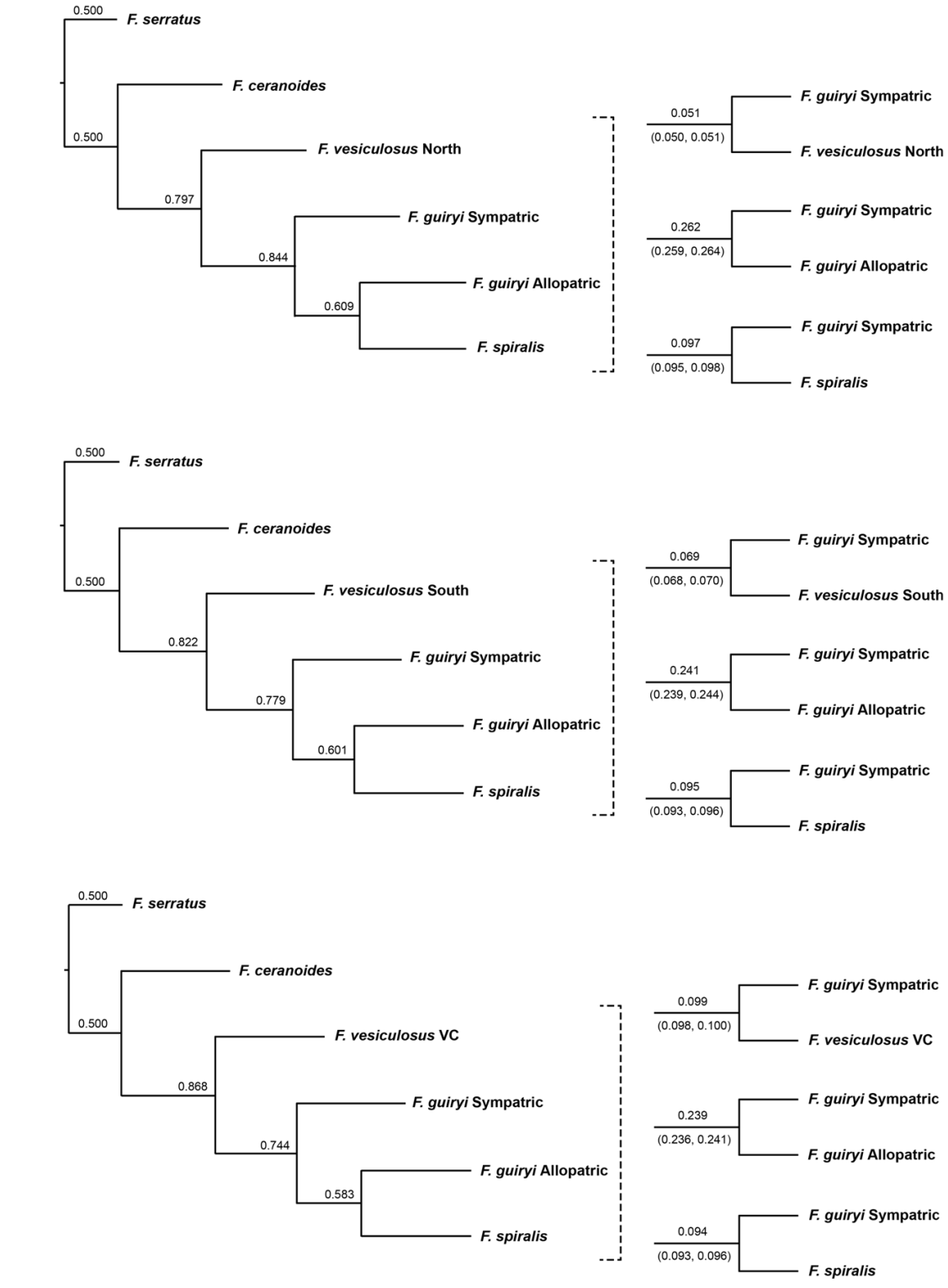
0.500
F. serratus
F. ceranoides
0.500
F. vesiculosus North
0.797
F. guiryi Sympatric
0.844
F. guiryi Allopatric
0.609
F. spiralis
0.051
(0.050, 0.051)
F. guiryi Sympatric
F. vesiculosus North
0.262
(0.259, 0.264)
F. guiryi Sympatric
F. guiryi Allopatric
0.097
(0.095, 0.098)
F. guiryi Sympatric
F. spiralis
0.500
F. serratus
F. ceranoides
0.500
F. vesiculosus South
0.822
F. guiryi Sympatric
0.779
F. guiryi Allopatric
0.601
F. spiralis
0.069
(0.068, 0.070)
F. guiryi Sympatric
F. vesiculosus South
0.241
(0.239, 0.244)
F. guiryi Sympatric
F. guiryi Allopatric
0.095
(0.093, 0.096)
F. guiryi Sympatric
F. spiralis
0.500
F. serratus
F. ceranoides
0.500
F. vesiculosus VC
0.868
F. guiryi Sympatric
0.744
F. guiryi Allopatric
0.583
F. spiralis
0.099
(0.098, 0.100)
F. guiryi Sympatric
F. vesiculosus VC
0.239
(0.236, 0.241)
F. guiryi Sympatric
F. guiryi Allopatric
0.094
(0.093, 0.096)
F. guiryi Sympatric
F. spiralis

B

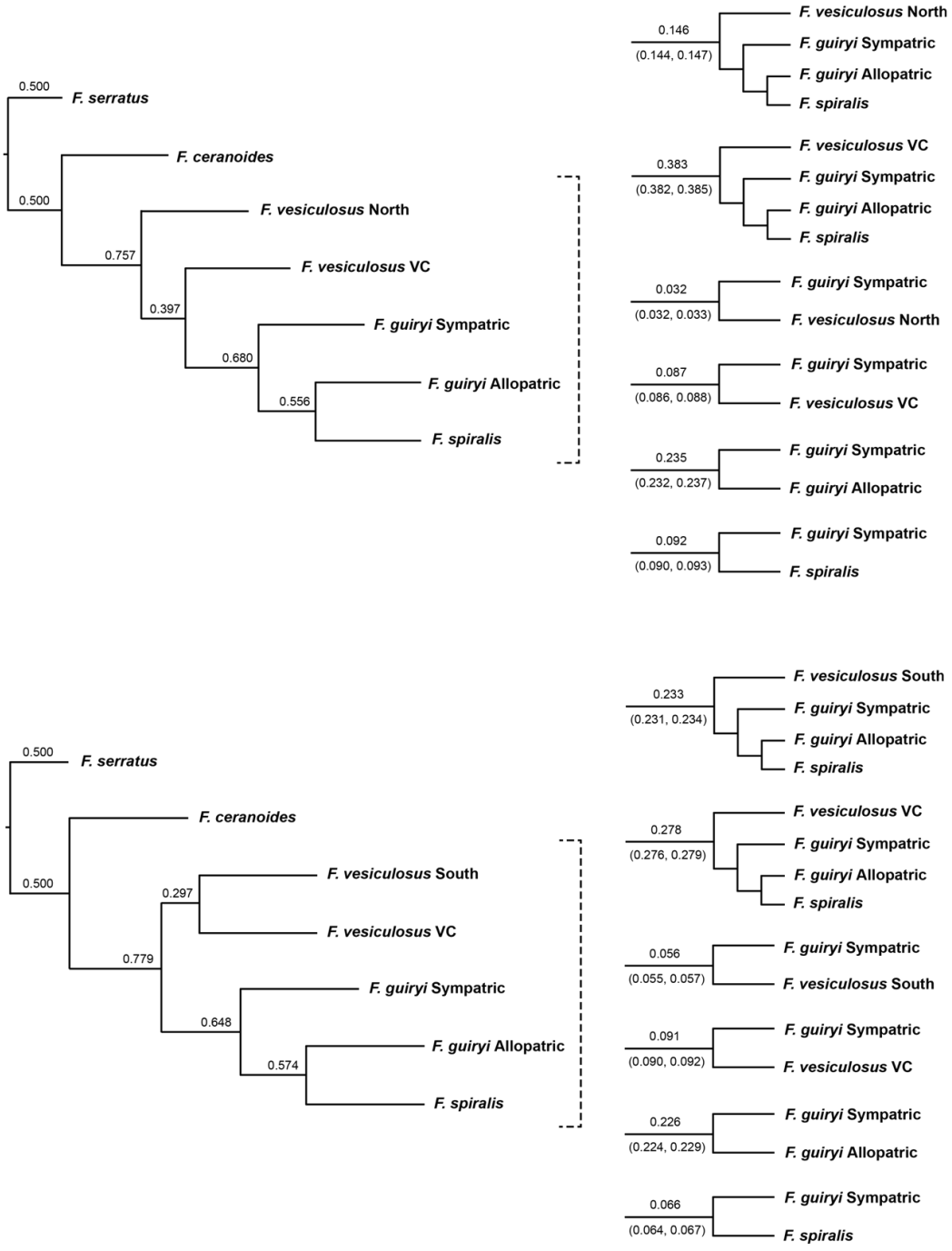
0.500
F. serratus
F. ceranoides
0.500
F. vesiculosus North
0.757
F. vesiculosus VC
0.397
F. guiryi Sympatric
0.680
F. guiryi Allopatric
0.556
F. spiralis
0.146
(0.144, 0.147)
F. vesiculosus North
F. guiryi Sympatric
F. guiryi Allopatric
F. spiralis
0.383
(0.382, 0.385)
F. vesiculosus VC
F. guiryi Sympatric
F. guiryi Allopatric
F. spiralis
0.032
(0.032, 0.033)
F. guiryi Sympatric
F. vesiculosus North
0.087
(0.086, 0.088)
F. guiryi Sympatric
F. vesiculosus VC
0.235
(0.232, 0.237)
F. guiryi Sympatric
F. guiryi Allopatric
0.092
(0.090, 0.093)
F. guiryi Sympatric
F. spiralis
0.500
F. serratus
F. ceranoides
0.500
F. vesiculosus South
0.297
F. vesiculosus VC
0.779
F. guiryi Sympatric
0.648
F. guiryi Allopatric
0.574
F. spiralis
0.233
(0.231, 0.234)
F. vesiculosus South
F. guiryi Sympatric
F. guiryi Allopatric
F. spiralis
0.278
(0.276, 0.279)
F. vesiculosus VC
F. guiryi Sympatric
F. guiryi Allopatric
F. spiralis
0.056
(0.055, 0.057)
F. guiryi Sympatric
F. vesiculosus South
0.091
(0.090, 0.092)
F. guiryi Sympatric
F. vesiculosus VC
0.226
(0.224, 0.229)
F. guiryi Sympatric
F. guiryi Allopatric
0.066
(0.064, 0.067)
F. guiryi Sympatric
F. spiralis

C

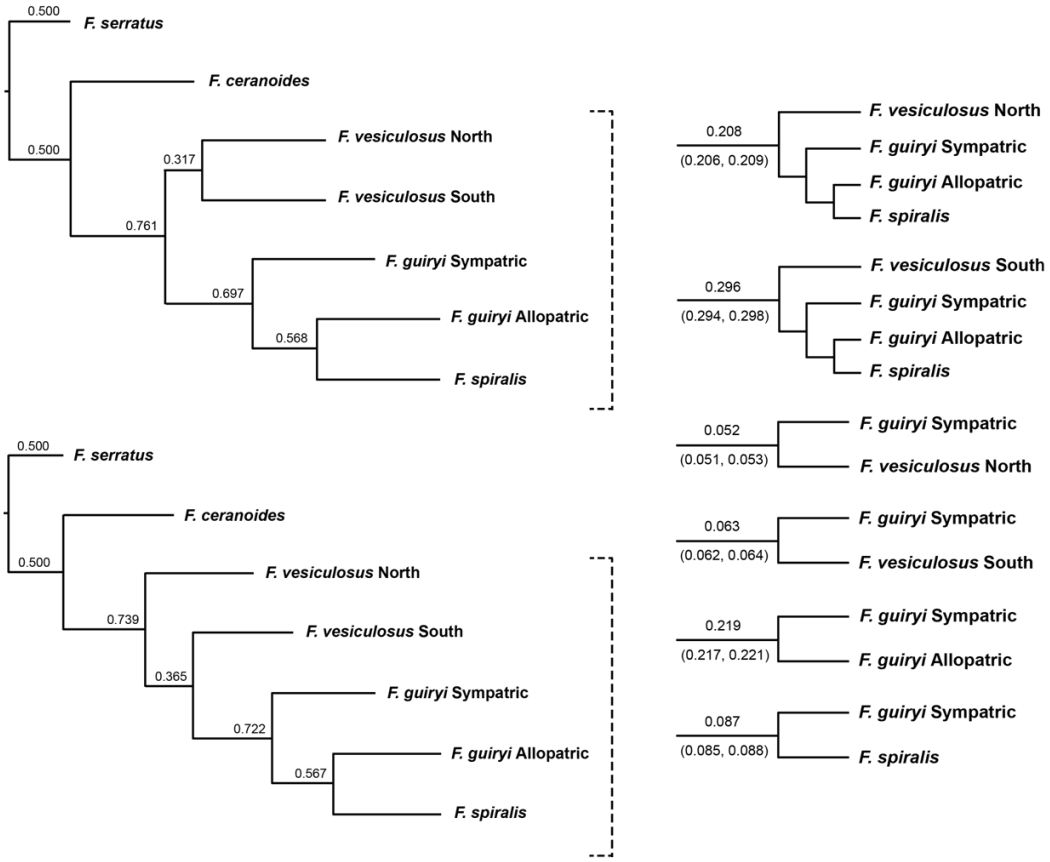

Figure 11. Left side of each panel: primary concordance trees (PCT) obtained with Bayesian Concordance Analysis for the five lineages of *Fucus spp.* Nodal support is given by sample-wide concordance factors (CF). Right side of each panel: alternative splits are given for sample-wide CF and credibility intervals (95% CI; n = 10 independent runs with randomly selected alleles). Names for the major groups correspond to Figure 5. A. Analysis including only one of the *F. vesiculosus* groups - *F. vesiculosus* North (top), *F. vesiculosus* South (center), or *F. vesiculosus* VC (bottom); B. Analysis including *F. vesiculosus* from Viana do Castelo with either the North (top) or South (bottom) group of *F. vesiculosus*; C. Analysis excluding *F. vesiculosus* from Viana do Castelo, with the topologies supported by six replicates (top) and four replicates (bottom).

By examining alternative splits to the PCTs for these hypotheses, several patterns of discordance were identified, depending on the groups of populations involved. While CFs on PCTs were similar when single groups of *F. vesiculosus* were considered (*F. vesiculosus* North, *F. vesiculosus* South or *F. vesiculosus* VC; Fig. 11A), analysis of alternative splits in the PCT revealed two important results. First, the split grouping *F. guiryi* Sympatric with *F. vesiculosus* VC (CF = 0.099; Fig. 11A, bottom) was significantly greater than for other groups of *F. vesiculosus*. Non-overlapping CFs for these splits indicates that ILS cannot fully explain these patterns. Second, CFs for the alternative splits grouping *F. guiryi* Sympatric with *F. guiryi* Allopatric were much (ca. 2.5 x) greater than those for splits grouping *F. guiryi* Sympatric with *F. spiralis.*

Therefore, alternative splits within the hermaphroditic clade do not support ILS as the only source of discordance within this clade, which would predict equal probabilities of allele sharing between *F. guiryi* Sympatric and the two sister taxa *F. guiryi* Allopatric and *F. spiralis.* The results instead suggest that hybridization/introgression has occurred between the *F. guiryi* Sympatric and *F. guiryi* Allopatric lineages.

When considering either *F. vesiculosus* North or South with *F. vesiculosus* VC (Fig. 11B), higher concordance was obtained for splits grouping the latter with either the hermaphrodite clade or with *F. guiryi* Sympatric populations alone. The differences in CFs were very obvious for comparisons with *F. vesiculosus* North (0.383 vs. 0.146; Fig. 11B, top), but was also significant (i.e. CFs were non-overlapping) for comparisons with *F. vesiculosus* South (Fig. 11B, bottom).

Overall, these results suggest patterns of discordance in the species tree that cannot be explained by ILS alone, and provide considerable evidence to support a role for introgressive hybridization involving *F. guiryi* Sympatric and both *F. guiryi* Allopatric and *F. vesiculosus*. Support for the hermaphroditic clade was strong, with *F. guiryi* allopatric clearly grouping with *F. spiralis*. An important result was the finding that the proportion of genome sharing between *F. guiryi* Sympatric and *F. vesiculosus* showed a geographical pattern for the latter species, being significantly greater in analyses including the population from Viana do Castelo in northwest Iberia, followed by southern populations, and was lowest for northern populations (Fig. 11A), despite the presence of *F. guiryi* Sympatric populations throughout this geographic range.

3.5 Testing for introgression

The vast phylogenetic discordances described above allows putting forward relevant hypothesis for the evolutionary history of the lineages and the possible influence of hybridization, but it does not completely inform about the nature of the discordance - ILS or introgression. We therefore tested whether ILS alone could explain phylogenetic patterns or there was evidence for gene flow using the *D* (Green *et al.*, 2010) and $\hat{f}_d$ (Martin *et al.*, 2014) statistics. In a situation of ILS, an equal proportion of ancestral and derived alleles are expected to contribute for the close phylogenetic relatedness of two populations, while introgression leads to an excess of shared derived alleles between the admixed and source populations. Tests were performed for relationships between *F. guiryi* and *F. vesiculosus* lineages (Fig. 12, Tables 3 - 5).

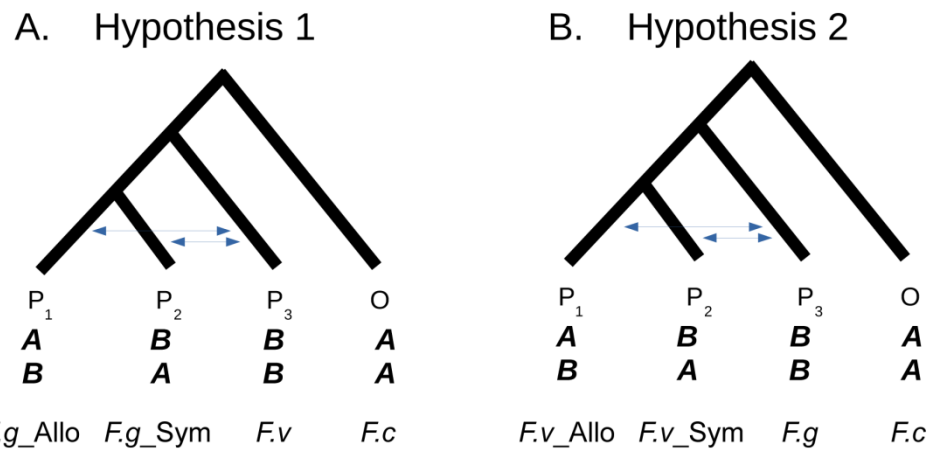

Figure 12. Hypotheses testing with ABBA-BABA tests. A. Test for introgression between *F. vesiculosus* and *F. guryi* Sympatric (ABBA) or *F. guiryi* Allopatric (BABA). B. Test for introgression between *F. guiryi* and sympatric (ABBA) or allopatric (BABA) populations of *F. vesiculosus*. The outgroup in both tests is *F. ceranoides*.

Considering: P_1 = *F. guiryi* Allopatric (CA, TA, ES); P_2 = *F. guiryi* Sympatric (VC, DU, ESs); P_3 = *F. vesiculosus* and O = *F. ceranoides*, where *F. vesiculosus* was the potential donor lineage, and sympatric *F. guiryi* the potential admixed population (Table 3); among *F. guiryi* sympatric populations, the population from Durgan (DU) appeared to have a phylogenetic relationship supported by introgression with both sympatric and allopatric *F. vesiculosus* populations, with the exception for populations from Durgan (DU), Viveiro (VV) and Cadiz (CZ) as given by the significantly higher proportion of ABBA patterns. The proportion of introgression varied between 0.016 and 0.023, as given by the $\hat{f}_d$ statistic. The close phylogenetic relationship given by phylogenetic analyses (Figs. 6 - 9) for both the population of *F. guiryi* from Viana do Castelo (VC) and the individual from Essaouira (ESs) in relation to *F. vesiculosus* appeared to be supported by hybridization, particularly regarding *F. vesiculosus* from Viana do Castelo (VC), with the proportion of introgression varying between 0.031 and 0.073 and 0.026 and 0.068, respectively. Interestingly, hybridization signals were also apparent in *F. guiryi* Sympatric when the donor population was *F. vesiculosus* from Ares (AR), which was not apparent on the phylogenetic analyses with both species tree approaches.

Table 3. Measure of phylogenetic admixture between populations of *F. guiryi* Allopatric (P_1), *F. guiryi* Sympatric (P_2) and *F. vesiculosus* (P_3), for the concatenated dataset (1000 transcripts). ABBA: number of ABBA patterns; BABA: number of BABA patterns; p-value: overall binomial p-value for the D statistic; D: Patterson's D statistic; $\hat{f}_d$(1DD4): proportion of introgression between P_2 and P_3; $\hat{f}_d$(D2D4): proportion of introgression between P_1 and P_3. Significant *p*-values are in bold. Light green: *F. vesiculosus* northern populations (sympatric); dark green: *F. vesiculosus* southern populations (allopatric). Codes correspond to locations in Table 1.

P_1	P_2	P_3	ABBA	BABA	*p*-value	D	f_d(1DD4)	f_d(D2D4)
F. guiryi CA	*F. guiryi* DU	*F. vesiculosus* DU	125	84	0.1075	0.196	0.0225	0.0000
F. guiryi CA	*F. guiryi* DU	*F. vesiculosus* VV	86	92	0.9956	-0.030	0.0000	0.0035
F. guiryi CA	*F. guiryi* DU	*F. vesiculosus* AR	157	96	**1.61E-6**	0.243	0.0385	0.0000
F. guiryi CA	*F. guiryi* DU	*F. vesiculosus* VC	244	104	**1.23E-14**	0.401	0.0813	0.0000
F. guiryi CA	*F. guiryi* DU	*F. vesiculosus* TJ	136	97	**0.0248**	0.169	0.0211	0.0000
F. guiryi CA	*F. guiryi* DU	*F. vesiculosus* RF	180	93	**0.0021**	0.318	0.0412	0.0000
F. guiryi CA	*F. guiryi* DU	*F. vesiculosus* CZ	111	114	0.9941	-0.014	0.0000	0.0022
F. guiryi CA	*F. guiryi* VC	*F. vesiculosus* DU	117	82	0.1716	0.175	0.0178	0.0000
F. guiryi CA	*F. guiryi* VC	*F. vesiculosus* VV	82	89	1.0000	-0.037	0.0000	0.0042
F. guiryi CA	*F. guiryi* VC	*F. vesiculosus* AR	153	95	**0.0019**	0.233	0.0349	0.0000
F. guiryi CA	*F. guiryi* VC	*F. vesiculosus* VC	236	102	**1.15E-7**	0.395	0.0737	0.0000
F. guiryi CA	*F. guiryi* VC	*F. vesiculosus* TJ	143	92	0.1457	0.220	0.0278	0.0000
F. guiryi CA	*F. guiryi* VC	*F. vesiculosus* RF	176	93	0.3967	0.308	0.0382	0.0000
F. guiryi CA	*F. guiryi* VC	*F. vesiculosus* CZ	109	110	0.9922	-0.003	0.0000	0.0007
F. guiryi CA	*F. guiryi* ESs	*F. vesiculosus* DU	119	81	0.3064	0.189	0.0192	0.0000
F. guiryi CA	*F. guiryi* ESs	*F. vesiculosus* VV	81	89	1.0000	-0.044	0.0000	0.0049
F. guiryi CA	*F. guiryi* ESs	*F. vesiculosus* AR	150	94	**0.0011**	0.232	0.0332	0.0000
F. guiryi CA	*F. guiryi* ESs	*F. vesiculosus* VC	232	104	**5.98E-7**	0.381	0.0677	0.0000
F. guiryi CA	*F. guiryi* ESs	*F. vesiculosus* TJ	132	92	0.2886	0.177	0.0203	0.0000
F. guiryi CA	*F. guiryi* ESs	*F. vesiculosus* RF	171	92	0.3162	0.300	0.0349	0.0000
F. guiryi CA	*F. guiryi* ESs	*F. vesiculosus* CZ	99	103	0.9999	-0.022	0.0000	0.0029
F. guiryi TA	*F. guiryi* DU	*F. vesiculosus* DU	90	74	0.3391	0.092	0.0099	0.0000
F. guiryi TA	*F. guiryi* DU	*F. vesiculosus* VV	84	90	1.0000	-0.040	0.0000	0.0051
F. guiryi TA	*F. guiryi* DU	*F. vesiculosus* AR	121	92	**2.71E-5**	0.135	0.0204	0.0000
F. guiryi TA	*F. guiryi* DU	*F. vesiculosus* VC	158	107	**1.36E-12**	0.191	0.0368	0.0000
F. guiryi TA	*F. guiryi* DU	*F. vesiculosus* TJ	119	91	**0.0009**	0.130	0.0162	0.0000
F. guiryi TA	*F. guiryi* DU	*F. vesiculosus* RF	133	89	0.0754	0.200	0.0253	0.0000
F. guiryi TA	*F. guiryi* DU	*F. vesiculosus* CZ	100	115	0.9953	-0.068	0.0000	0.0099
F. guiryi TA	*F. guiryi* VC	*F. vesiculosus* DU	83	74	0.1235	0.058	0.0056	0.0000
F. guiryi TA	*F. guiryi* VC	*F. vesiculosus* VV	80	88	0.9999	-0.048	0.0000	0.0059
F. guiryi TA	*F. guiryi* VC	*F. vesiculosus* AR	115	90	**1.41E-5**	0.123	0.0173	0.0000
F. guiryi TA	*F. guiryi* VC	*F. vesiculosus* VC	150	105	**3.80E-11**	0.176	0.0310	0.0000
F. guiryi TA	*F. guiryi* VC	*F. vesiculosus* TJ	123	84	**0.0108**	0.192	0.0234	0.0000
F. guiryi TA	*F. guiryi* VC	*F. vesiculosus* RF	128	88	**0.0069**	0.189	0.0225	0.0000
F. guiryi TA	*F. guiryi* VC	*F. vesiculosus* CZ	100	112	0.9777	-0.057	0.0000	0.0083
F. guiryi TA	*F. guiryi* ESs	*F. vesiculosus* DU	91	79	0.4908	0.071	0.0073	0.0000
F. guiryi TA	*F. guiryi* ESs	*F. vesiculosus* VV	84	93	1.0000	-0.051	0.0000	0.0066
F. guiryi TA	*F. guiryi* ESs	*F. vesiculosus* AR	119	96	**0.0001**	0.111	0.0159	0.0000
F. guiryi TA	*F. guiryi* ESs	*F. vesiculosus* VC	153	114	**3.88E-9**	0.146	0.0257	0.0000
F. guiryi TA	*F. guiryi* ESs	*F. vesiculosus* TJ	118	91	**0.0128**	0.131	0.0156	0.0000
F. guiryi TA	*F. guiryi* ESs	*F. vesiculosus* RF	128	92	0.0579	0.166	0.0196	0.0000
F. guiryi TA	*F. guiryi* ESs	*F. vesiculosus* CZ	94	110	0.9997	-0.078	0.0000	0.0105

Table 3. *Continued*

P_1	P_2	P_3	ABBA	BABA	*p*-value	D	f_d(1DD4)	f_d(D2D4)
F. guiryi ES	*F. guiryi* DU	*F. vesiculosus* DU	126	83	0.2178	0.208	0.0241	0.0000
F. guiryi ES	*F. guiryi* DU	*F. vesiculosus* VV	84	93	0.9989	-0.047	0.0000	0.0055
F. guiryi ES	*F. guiryi* DU	*F. vesiculosus* AR	157	96	**9.31E-5**	0.243	0.0385	0.0000
F. guiryi ES	*F. guiryi* DU	*F. vesiculosus* VC	242	104	**5.15E-11**	0.399	0.0802	0.0000
F. guiryi ES	*F. guiryi* DU	*F. vesiculosus* TJ	137	95	**0.0289**	0.182	0.0228	0.0000
F. guiryi ES	*F. guiryi* DU	*F. vesiculosus* RF	179	96	**0.0082**	0.299	0.0388	0.0000
F. guiryi ES	*F. guiryi* DU	*F. vesiculosus* CZ	111	110	0.9999	0.004	0.0003	0.0000
F. guiryi ES	*F. guiryi* VC	*F. vesiculosus* DU	117	80	0.6597	0.190	0.0193	0.0000
F. guiryi ES	*F. guiryi* VC	*F. vesiculosus* VV	80	89	1.0000	-0.056	0.0000	0.0062
F. guiryi ES	*F. guiryi* VC	*F. vesiculosus* AR	151	93	**0.0038**	0.236	0.0349	0.0000
F. guiryi ES	*F. guiryi* VC	*F. vesiculosus* VC	234	101	**7.90E-6**	0.395	0.0728	0.0000
F. guiryi ES	*F. guiryi* VC	*F. vesiculosus* TJ	143	88	0.1707	0.236	0.0295	0.0000
F. guiryi ES	*F. guiryi* VC	*F. vesiculosus* RF	174	96	0.4658	0.291	0.0358	0.0000
F. guiryi ES	*F. guiryi* VC	*F. vesiculosus* CZ	109	105	1.0000	0.017	0.0018	0.0000
F. guiryi ES	*F. guiryi* ESs	*F. vesiculosus* DU	119	78	0.8414	0.204	0.0207	0.0000
F. guiryi ES	*F. guiryi* ESs	*F. vesiculosus* VV	78	89	1.0000	-0.063	0.0000	0.0069
F. guiryi ES	*F. guiryi* ESs	*F. vesiculosus* AR	149	92	**0.0078**	0.234	0.0332	0.0000
F. guiryi ES	*F. guiryi* ESs	*F. vesiculosus* VC	230	103	**1.27E-5**	0.380	0.0667	0.0000
F. guiryi ES	*F. guiryi* ESs	*F. vesiculosus* TJ	131	88	0.3591	0.194	0.0218	0.0000
F. guiryi ES	*F. guiryi* ESs	*F. vesiculosus* RF	168	94	0.5846	0.283	0.0325	0.0000
F. guiryi ES	*F. guiryi* ESs	*F. vesiculosus* CZ	98	98	1.0000	-0.002	0.0000	0.0004

When considering: P_1 = *F. vesiculosus* allopatric populations (TJ, RF, CZ); P_2 = *F. vesiculosus* sympatric populations (DU, VV, AR, VC); P_3 = *F. guiryi* Sympatric (DU, VC, ESs); and O = *F. ceranoides*, where *F. guiryi* Sympatric was the potential donor lineage (Table 4), the population of *F. vesiculosus* from Viana do Castelo (VC) was significantly more closely related to all *F. guiryi* Sympatric populations than to *F. vesiculosus* allopatric populations due to introgression (ABBA > BABA), with a proportion of introgression varying between 0.066 and 0.106. Also *F. vesiculosus* from Ares (AR) revealed clear signs of introgression with the sympatric populations of *F. guiryi*.

Table 4. Measure of phylogenetic admixture between populations of *F. vesiculosus* Allopatric (P_1), *F. vesiculosus* Sympatric (P_2) and *F. guiryi* Sympatric (P_3), for the concatenated dataset (1000 transcripts). ABBA: number of ABBA patterns; BABA: number of BABA patterns; p-value: overall binomial p-value for the D statistic; D: Patterson's D statistic; $\hat{f}_d$(1DD4): proportion of introgression between P_2 and P_3; $\hat{f}_d$(D2D4): proportion of introgression between P_1 and P_3. Significant p-values are in bold. Light green: *F. vesiculosus* northern populations (sympatric); dark green: *F. vesiculosus* southern populations (allopatric). Codes correspond to locations in Table 1.

P_1	P_2	P_3	ABBA	BABA	*p*-value	D	f_d(1DD4)	f_d(D2D4)
F. vesiculosus TJ	*F. vesiculosus* DU	*F. guiryi* DU	262	495	**6.77E-60**	-0.308	0.0000	0.0913
F. vesiculosus TJ	*F. vesiculosus* VV	*F. guiryi* DU	291	467	**3.17E-63**	-0.232	0.0000	0.0698
F. vesiculosus TJ	*F. vesiculosus* AR	*F. guiryi* DU	389	376	**4.36E-56**	0.017	0.0060	0.0000
F. vesiculosus TJ	*F. vesiculosus* VC	*F. guiryi* DU	491	310	**1.93E-62**	0.226	0.0881	0.0000
F. vesiculosus TJ	*F. vesiculosus* DU	*F. guiryi* VC	251	502	**1.58E-59**	-0.334	0.0000	0.0969
F. vesiculosus TJ	*F. vesiculosus* VV	*F. guiryi* VC	285	475	**9.97E-63**	-0.249	0.0000	0.0741
F. vesiculosus TJ	*F. vesiculosus* AR	*F. guiryi* VC	381	384	**2.84E-51**	-0.004	0.0000	0.0016
F. vesiculosus TJ	*F. vesiculosus* VC	*F. guiryi* VC	480	318	**9.11E-51**	0.203	0.0773	0.0000
F. vesiculosus TJ	*F. vesiculosus* DU	*F. guiryi* ESs	259	496	**6.78E-58**	-0.313	0.0000	0.0902
F. vesiculosus TJ	*F. vesiculosus* VV	*F. guiryi* ESs	289	468	**1.84E-61**	-0.236	0.0000	0.0689
F. vesiculosus TJ	*F. vesiculosus* AR	*F. guiryi* ESs	383	376	**6.53E-47**	0.010	0.0035	0.0000
F. vesiculosus TJ	*F. vesiculosus* VC	*F. guiryi* ESs	477	309	**1.08E-48**	0.215	0.0789	0.0000
F. vesiculosus RF	*F. vesiculosus* DU	*F. guiryi* DU	245	517	**1.21E-47**	-0.356	0.0000	0.1044
F. vesiculosus RF	*F. vesiculosus* VV	*F. guiryi* DU	289	503	**9.44E-49**	-0.271	0.0000	0.0828
F. vesiculosus RF	*F. vesiculosus* AR	*F. guiryi* DU	387	413	**1.01E-38**	-0.032	0.0000	0.0101
F. vesiculosus RF	*F. vesiculosus* VC	*F. guiryi* DU	470	328	**8.57E-40**	0.178	0.0713	0.0000
F. vesiculosus RF	*F. vesiculosus* DU	*F. guiryi* VC	238	512	**2.10E-50**	-0.365	0.0000	0.1033
F. vesiculosus RF	*F. vesiculosus* VV	*F. guiryi* VC	288	500	**3.69E-54**	-0.268	0.0000	0.0804
F. vesiculosus RF	*F. vesiculosus* AR	*F. guiryi* VC	385	410	**1.15E-45**	-0.032	0.0000	0.0098
F. vesiculosus RF	*F. vesiculosus* VC	*F. guiryi* VC	467	326	**6.91E-45**	0.177	0.0687	0.0000
F. vesiculosus RF	*F. vesiculosus* DU	*F. guiryi* ESs	241	508	**1.27E-52**	-0.356	0.0000	0.0995
F. vesiculosus RF	*F. vesiculosus* VV	*F. guiryi* ESs	287	496	**4.24E-51**	-0.266	0.0000	0.0782
F. vesiculosus RF	*F. vesiculosus* AR	*F. guiryi* ESs	384	406	**4.94E-43**	-0.028	0.0000	0.0086
F. vesiculosus RF	*F. vesiculosus* VC	*F. guiryi* ESs	458	319	**2.70E-43**	0.178	0.0665	0.0000
F. vesiculosus CZ	*F. vesiculosus* DU	*F. guiryi* DU	273	463	**3.26E-52**	-0.259	0.0000	0.0769
F. vesiculosus CZ	*F. vesiculosus* VV	*F. guiryi* DU	294	427	**1.39E-28**	-0.185	0.0000	0.0537
F. vesiculosus CZ	*F. vesiculosus* AR	*F. guiryi* DU	416	360	**6.19E-48**	0.072	0.0263	0.0000
F. vesiculosus CZ	*F. vesiculosus* VC	*F. guiryi* DU	538	314	**3.45E-54**	0.262	0.1055	0.0000
F. vesiculosus CZ	*F. vesiculosus* DU	*F. guiryi* VC	266	465	**2.53E-55**	-0.272	0.0000	0.0790
F. vesiculosus CZ	*F. vesiculosus* VV	*F. guiryi* VC	290	427	**9.19E-29**	-0.191	0.0000	0.0542
F. vesiculosus CZ	*F. vesiculosus* AR	*F. guiryi* VC	410	361	**2.28E-41**	0.064	0.0229	0.0000
F. vesiculosus CZ	*F. vesiculosus* VC	*F. guiryi* VC	532	317	**1.23E-43**	0.253	0.0991	0.0000
F. vesiculosus CZ	*F. vesiculosus* DU	*F. guiryi* ESs	272	464	**1.08E-54**	-0.261	0.0000	0.0756
F. vesiculosus CZ	*F. vesiculosus* VV	*F. guiryi* ESs	292	426	**5.40E-27**	-0.187	0.0000	0.0525
F. vesiculosus CZ	*F. vesiculosus* AR	*F. guiryi* ESs	411	359	**2.22E-41**	0.068	0.0237	0.0000
F. vesiculosus CZ	*F. vesiculosus* VC	*F. guiryi* ESs	524	311	**9.35E-38**	0.255	0.0964	0.0000

When considering: P_1 = *F. vesiculosus* allopatric populations (TJ, RF, CZ); P_2 = *F. vesiculosus* sympatric populations (DU, VV, AR, VC); P_3 = *F. guiryi* Allopatric (CA, TA, ES); and O = *F. ceranoides*, where *F. guiryi* Allopatric was the potential donor lineage (Table 5), only *F. vesiculosus* from Viana do Castelo (VC) revealed a significant

evidence for admixture with *F. guiryi* Allopatric, with the proportion of introgression varying between 0.039 and 0.079.

Table 5. Measure of phylogenetic admixture between populations of *F. vesiculosus* Allopatric (P_1), *F. vesiculosus* Sympatric (P_2) and *F. guiryi* Allopatric (P_3), for the concatenated dataset (1000 transcripts). ABBA: number of ABBA patterns; BABA: number of BABA patterns; p-value: overall binomial p-value for the D statistic; D: Patterson's D statistic; $\hat{f}_d$(1DD4): proportion of introgression between P_2 and P_3; $\hat{f}_d$(D2D4): proportion of introgression between P_1 and P_3. . Significant p-values are in bold. Light green: *F. vesiculosus* northern populations (sympatric); dark green: *F. vesiculosus* southern populations (allopatric). Codes correspond to locations in Table 1.

P_1	P_2	P_3	ABBA	BABA	*p*-value	D	f_d(1DD4)	f_d(D2D4)
F. vesiculosus TJ	*F. vesiculosus* DU	*F. guiryi* CA	237	472	**4.68E-40**	-0.331	0.0000	0.0921
F. vesiculosus TJ	*F. vesiculosus* VV	*F. guiryi* CA	300	431	**3.23E-38**	-0.180	0.0000	0.0530
F. vesiculosus TJ	*F. vesiculosus* AR	*F. guiryi* CA	350	359	**1.40E-29**	-0.013	0.0000	0.0039
F. vesiculosus TJ	*F. vesiculosus* VC	*F. guiryi* CA	390	309	**1.38E-28**	0.115	0.0391	0.0000
F. vesiculosus TJ	*F. vesiculosus* DU	*F. guiryi* TA	259	480	**4.61E-63**	-0.300	0.0000	0.0882
F. vesiculosus TJ	*F. vesiculosus* VV	*F. guiryi* TA	306	447	**3.09E-65**	-0.188	0.0000	0.0578
F. vesiculosus TJ	*F. vesiculosus* AR	*F. guiryi* TA	379	367	**1.79E-52**	0.015	0.0055	0.0000
F. vesiculosus TJ	*F. vesiculosus* VC	*F. guiryi* TA	460	303	**1.70E-58**	0.206	0.0785	0.0000
F. vesiculosus TJ	*F. vesiculosus* DU	*F. guiryi* ES	236	471	**2.50E-41**	-0.332	0.0000	0.0912
F. vesiculosus TJ	*F. vesiculosus* VV	*F. guiryi* ES	304	430	**6.93E-38**	-0.171	0.0000	0.0503
F. vesiculosus TJ	*F. vesiculosus* AR	*F. guiryi* ES	350	356	**1.42E-26**	-0.009	0.0000	0.0026
F. vesiculosus TJ	*F. vesiculosus* VC	*F. guiryi* ES	392	307	**5.16E-27**	0.121	0.0408	0.0000
F. vesiculosus RF	*F. vesiculosus* DU	*F. guiryi* CA	229	455	**1.76E-28**	-0.330	0.0000	0.0867
F. vesiculosus RF	*F. vesiculosus* VV	*F. guiryi* CA	300	422	**1.33E-33**	-0.169	0.0000	0.0480
F. vesiculosus RF	*F. vesiculosus* AR	*F. guiryi* CA	362	361	**6.39E-22**	0.000	0.0002	0.0000
F. vesiculosus RF	*F. vesiculosus* VC	*F. guiryi* CA	401	312	**4.76E-27**	0.126	0.0439	0.0000
F. vesiculosus RF	*F. vesiculosus* DU	*F. guiryi* TA	243	485	**1.17E-44**	-0.333	0.0000	0.0949
F. vesiculosus RF	*F. vesiculosus* VV	*F. guiryi* TA	303	466	**4.43E-52**	-0.212	0.0000	0.0648
F. vesiculosus RF	*F. vesiculosus* AR	*F. guiryi* TA	380	389	**4.42E-41**	-0.012	0.0000	0.0038
F. vesiculosus RF	*F. vesiculosus* VC	*F. guiryi* TA	449	313	**2.11E-40**	0.179	0.0690	0.0000
F. vesiculosus RF	*F. vesiculosus* DU	*F. guiryi* ES	225	458	**1.36E-29**	-0.341	0.0000	0.0889
F. vesiculosus RF	*F. vesiculosus* VV	*F. guiryi* ES	301	425	**1.87E-33**	-0.170	0.0000	0.0484
F. vesiculosus RF	*F. vesiculosus* AR	*F. guiryi* ES	360	364	**2.45E-21**	-0.006	0.0000	0.0019
F. vesiculosus RF	*F. vesiculosus* VC	*F. guiryi* ES	401	315	**1.16E-23**	0.121	0.0420	0.0000
F. vesiculosus CZ	*F. vesiculosus* DU	*F. guiryi* CA	235	469	**4.74E-32**	-0.333	0.0000	0.0943
F. vesiculosus CZ	*F. vesiculosus* VV	*F. guiryi* CA	302	433	**2.31E-32**	-0.178	0.0000	0.0542
F. vesiculosus CZ	*F. vesiculosus* AR	*F. guiryi* CA	363	372	**1.00E-22**	-0.012	0.0000	0.0040
F. vesiculosus CZ	*F. vesiculosus* VC	*F. guiryi* CA	406	325	**9.07E-21**	0.111	0.0385	0.0000
F. vesiculosus CZ	*F. vesiculosus* DU	*F. guiryi* TA	257	477	**2.63E-53**	-0.300	0.0000	0.0912
F. vesiculosus CZ	*F. vesiculosus* VV	*F. guiryi* TA	299	440	**2.45E-32**	-0.191	0.0000	0.0592
F. vesiculosus CZ	*F. vesiculosus* AR	*F. guiryi* TA	389	377	**1.67E-41**	0.016	0.0059	0.0000
F. vesiculosus CZ	*F. vesiculosus* VC	*F. guiryi* TA	487	329	**4.10E-44**	0.194	0.0775	0.0000
F. vesiculosus CZ	*F. vesiculosus* DU	*F. guiryi* ES	233	466	**2.94E-31**	-0.333	0.0000	0.0930
F. vesiculosus CZ	*F. vesiculosus* VV	*F. guiryi* ES	305	428	**2.18E-29**	-0.169	0.0000	0.0509
F. vesiculosus CZ	*F. vesiculosus* AR	*F. guiryi* ES	362	367	**3.41E-19**	-0.006	0.0000	0.0021
F. vesiculosus CZ	*F. vesiculosus* VC	*F. guiryi* ES	407	321	**7.88E-22**	0.119	0.0407	0.0000

Overall, all tests performed revealed clear evidence for introgression (alternative to the null hypothesis of ILS) between the sympatric individuals of *F. guiryi* (Durgan, Viana do

Castelo, plus one individual from Essaouira) and the *F. vesiculosus* population from Viana do Castelo. Additionally, evidence for introgression was also consistently found for the particular case of *F. guiryi* from Durgan with *F. vesiculosus* from Ares and Tejo.

3.6 Divergence time analysis

In order to have an estimate of the divergence events between these lineages, the multispecies coalescent analysis (Heled and Drummond, 2010) was applied, having in consideration that this assumes the incongruence between gene trees to be derived only from incomplete lineage sorting. However, due to computational constraints, only 15 loci were used for this purpose.

The Maximum Clade Credibility (MCC) species tree (Fig. 13) for the multispecies coalescent analysis was similar in topology for the hermaphroditic lineages to both the concatenated (Figs. 6 - 8) and the supertree analyses (Fig. 9).

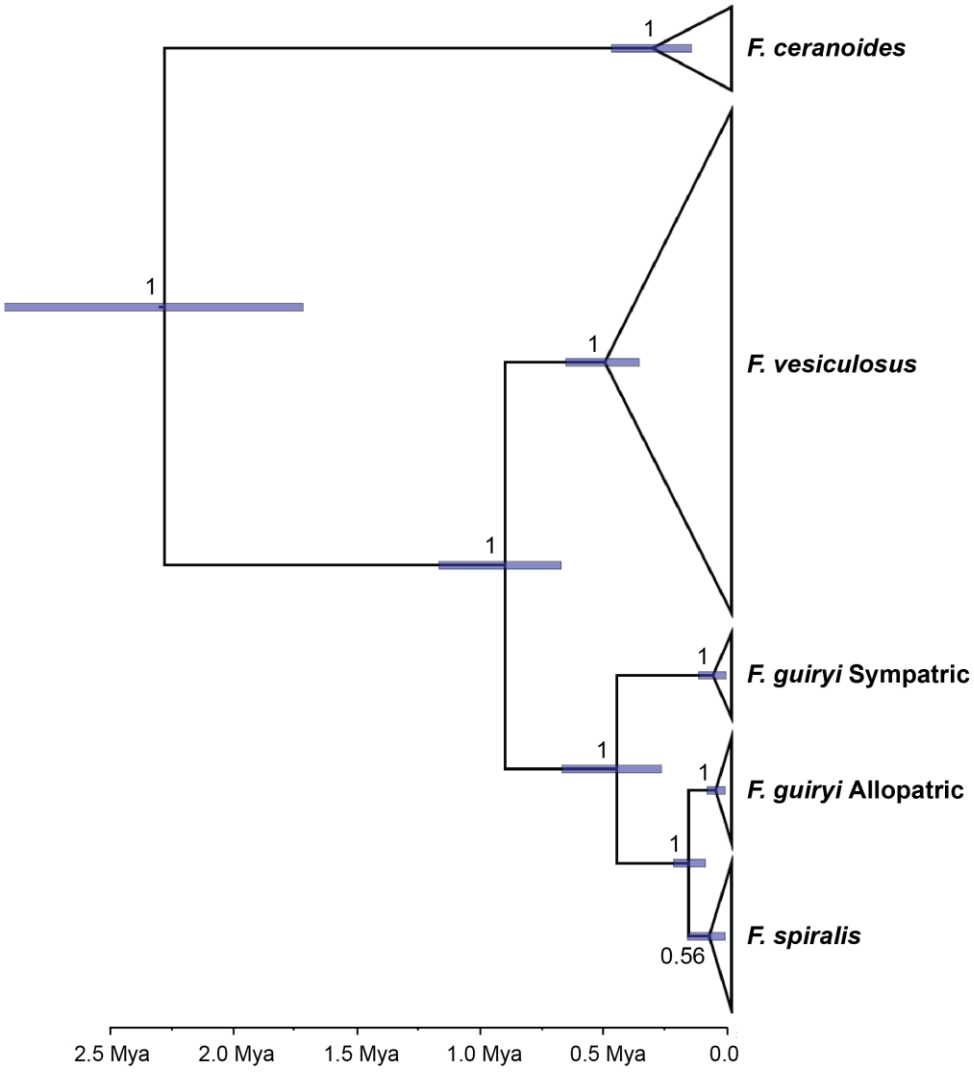

Figure 13. Time-calibrated maximum clade credibility tree with posterior median node heights for *Fucus spp.* resulting from Bayesian analysis of 15 loci. Node support is given for clades with posterior probability greater than 0.50. Blue bars represent 95% HPD node heights. Names for the major groups of *F.guiryi* correspond to Figure 5.

Species tree given by the Bayesian posterior distribution revealed a divergence time between *F. vesiculosus* and the hermaphroditic clade of approximately 1.0 Mya (95% HPD = 1). Within the hermaphroditic clade, divergence was estimated to have occurred first for *F. guiryi* Sympatric, approximately at 0.5 Mya (95% HPD = 1). Additionally, the divergence time estimated for the *F. guiryi* Allopatric - *F. spiralis* clade was approximately 0.25 Mya (95% HPD = 1). From this analysis, it appears that genes that coalesce at the *F. spiralis*/*F. guiryi* Allopatric node diverged more recently than those at the *F. guiryi* Allopatric/*F. guiryi* Sympatric node.

4. Discussion

This thesis reports the first large-scale phylogenomic analysis of divergence in the genus *Fucus*, which has undergone a recent radiation in the North Atlantic (Canóvas *et al.* 2011). We first aimed to estimate the phylogeny of three focal lineages; *Fucus vesiculosus*, *F. spiralis* and *F. guiryi* using different approaches. Based on a curated set of 1000 single-copy loci and population-level transcriptome sampling, we show that species trees constructed with these data and based on both supermatrix (ML, Bayesian and polymorphism-aware ML) and supertree (ASTRAL) methods recovered similar topologies. Secondly, we aimed to understand the impact of secondary introgression in determining phylogenetic incongruence among loci. We found that gene flow affects sympatric populations of *F. guiry* and *F. vesiculosus*, which opens up new perspectives for the study of the functional and adaptive impact of gene flow in this system.

4.1 Species tree estimation

Analyses performed using different approaches recovered the same topology, which holds up for the accurate dataset used, since otherwise would produce conflicting result between supermatrix and supertree approaches (Liu *et al.*, 2009). Hence high support retrieved from concatenated analyses can be trusted as reflecting the real relationships among lineages, notwithstanding the possible variable roles of incomplete lineage sorting and introgression in some instances.

First, species tree analyses provided full support for a new hermaphroditic lineage sister to the group *F. spiralis* - *F. guiryi.* The new lineage is referred to as *F. guiryi* Sympatric as it was sampled exclusively in sympatry (i.e. co-occurring on the same shores) with either *F. vesiculosus* from northern Portugal and Cornwall (UK) or with *F. guiryi* (*sensu* Zardi *et al.*, 2011) in Morocco. This represents an advance compared with previous analyses on the phylogenetic relationships of this genus, in which sympatric populations of *F. guiryi* were either excluded (Cánovas *et al.*, 2011) or, when included, could not be retrieved as a monophyletic entity (Zardi *et al.*, 2011). These previous analyses attested to the recent divergence between these lineages, which prevented an accurate analysis of their relationships with few loci.

Second, *F. vesiculosus* sampled between southern Spain (Cadiz) and the UK was not recovered as a monophyletic entity. A single population from Viana do Castelo in northern Portugal, close to the current boundary between sympatric and allopatric distributions of the species in the eastern Atlantic, were recovered in all analyses as sister (and basal) to the hermaphroditic group containing *F. guiryi* Sympatric, *F. guiryi*

sensu (*sensu* Zardi *et al.*, 2011) and *F. spiralis*. This supports results previously found for this lineage with both microsatellite (Engel *et al.*, 2005; Billard *et al.*, 2010; Moalic *et al.*, 2011) and SNP data (Cánovas *et al.*, 2011) where the northern populations from *F. vesiculosus* (Brittany northwards) were separated from the other sampled populations (NW Iberia southwards). Moreover, analyses based on microsatellite data (Nicastro *et al.*, 2013; Assis *et al.*, 2014) retrieved a separation between northwestern Iberia (from southwest Galicia to northern Portugal) and southern Iberia (central Portugal southwards) and Morocco. However, only in Cánovas *et al.* (2011) were the relationships with the other sister hermaphroditic lineages explored. In the present study, a detailed sampling combined with a large-scale genomic dataset allowed not only for a much more accurate perception of the genetic diversity existing in this lineage, particularly for its distribution in NW Iberia southwards, but also for a clear insight into the relationships between these taxa. Hence, phylogenetic analysis consistently revealed the presence of three monophyletic entities within *F. vesiculosus*, a northern cluster, with populations from Cornwall and North Galicia, a southern cluster, with populations from central Portugal southwards and a third cluster, consisting of a single population from Viana do Castelo. This is further evidence for the cryptic diversity within this lineage, the present distribution of which corresponds with glacial refugia for several marine species (Provan *et al.*, 2005; Maggs *et al.*, 2008), including fucoids (Coyer *et al.*, 2003; Hoarau *et al.*, 2007; Neiva *et al.*, 2012; Assis *et al.*, 2014).

F. vesiculosus from Viana do Castelo was, in all the phylogenetic analyses, sister to the hermaphroditic clade (Figs. 6 - 9). This strongly suggests to be the result from introgressive hybridization with *F. guiryi* Sympatric lineage through secondary contact, which may be found in sympatry here and northwards and, to a lesser extent, from hybridization with the other hermaphroditic lineages, as suggested with both nuclear (Cánovas *et al.*, 2011; Zardi *et al.*, 2011) and mitochondrial DNA (Coyer *et al.*, 2011) data. Interestingly, the other populations from *F. vesiculosus* in sympatry, the northern clade, do not show this signal, which is intriguing, particularly for the population from Durgan (Cornwall) in which the three lineages were collected on the same shore.

Although the phylogenomic analyses provide new insights into the history of diversification in the genus, some of these results may have been influenced by secondary gene flow between the diverging lineages, which phylogenetic tree-construction methods do not take into account. We therefore proceeded to understand the relative impact of potential gene flow in determining the phylogenetic patterns.

4.2 Detection of incongruence among loci

Given the genomic-scale patterns of phylogenetic inference provided by these new analyses, and previous observations suggesting the potential for hybridization between members of this clade (Billard *et al.*, 2010; Zardi *et al.*, 2011; Coyer *et al.*, 2011), we tested gene tree concordance implemented in a Bayesian framework (BUCKy; Ané *et al.*, 2007), and identified alternative splits (those not in the primary concordance tree) with high concordance factors (i.e. > 10%; Cui *et al.*, 2013). These can be considered candidates for the existence of factors other than incomplete lineage sorting (ILS) operating, including potential introgression, which can then be further investigated with other methods, such as the Patterson's *D* statistic (Green *et al.*, 2010).

In particular, while *F. guiryi* Sympatric was sister to the group *F. guiryi* Allopatric and *F. spiralis* on species trees (Fig. 11, left panel), concordance factors (CF) for alternative splits grouping *F. guiryi* Sympatric - *F. guiryi* Allopatric were significantly greater (and about 2.5 x larger) than splits grouping *F. guiryi* Sympatric - *F. spiralis* (Fig. 11, right panel). These results suggest that ILS may not be the sole explanation for allele sharing within the hermaphrodite clade, and the high proportion of genes (24 - 26%) supporting this split suggest possible hybridization/introgression between *F. guiryi* Sympatric and *F. guiryi* Allopatric. In contrast, alternative splits grouping *F. guiryi* Sympatric with *F. spiralis* had concordance factors lower than 10%.

The results consistently give higher support for the alternative split between *F. vesiculosus* VC being sister to *F. guiryi* Sympatric (CF ≈ 10%), compared to the other clades of *F. vesiculosus* (CFs 5 - 7%), suggesting that this population was involved in introgression with *F. guiryi* Sympatric. Moreover, the fact that one individual from the allopatric population of Morocco (*F. guiryi* ESs) consistently grouped with *F. guiry* Sympatric might support the hypothesis suggested in Coyer *et al.* (2011), for an origin for the *F. guiryi* Sympatric lineage through the migration northwards of *F. guiryi* Allopatric - after divergence and geographical segregation from *F. spiralis* - and hybridization with *F. vesiculosus* from Viana do Castelo. Furthermore, despite previous findings (Coyer *et al.*, 2011) of haplotype sharing between *F. guiryi* Sympatric (= *F. spiralis* Low; Coyer *et al.*, 2011), *F. spiralis* (= *F. spiralis* High; Coyer *et al.*, 2011) and *F. vesiculosus*, results in the present study do not support hybridization (with a significant genomic signal) of *F. spiralis* with either *F. vesiculosus* or *F. guiryi* Allopatric, although that hypothesis cannot be ruled out.

4.3 Testing for introgression

In order to understand whether the phylogenetic incongruence among loci is due to gene flow we tested for an excess of derived allele sharing between potential admixed and donor relative to the parental populations using the *D* statistic (Green *et al.*, 2010; Martin *et al.*, 2014). We used the combined inference of phylogenetic discordance from BUCKy and deviations to null expectations from Patterson's *D* statistic to understand the impact of introgression in the *Fucus* system, and concluded that hybridization is a likely contributor to gene tree discordance among species.

The difference observed between allele patterns was consistent with the occurrence of introgression between *F. guiryi* Sympatric and *F. vesiculosus* population from Viana do Castelo in all cases. These results support the idea that the conflicting signals observed with Bayesian concordance analysis and the high support given for these relationships, when compared to other groups of *F. vesiculosus*, as given by the concordance factors for the alternative splits (Figs. 11A, B), could be attributed to hybridization between these two groups. Interestingly, the results showed evidence for introgression also for the *F. guiryi* individual of Morocco (allopatric population) that grouped in the phylogenetic analyses with the populations from the sympatric range of distribution. A previous study found evidence (microsatellite markers) for admixture between *F. spiralis* and *F. vesiculosus* in individuals from Morocco (Moalic *et al.*, 2011), which could possibly correspond to the *F. guiryi* allopatric group (since the lineage was not defined at the time of publication). Hence, results showed that introgression likely contributes to the closer phylogenetic relationship observed in the Bayesian analysis, where higher concordance was generally observed in all tests for the alternative split between *F. guiryi* Sympatric and *F. vesiculosus* South, when compared to *F. vesiculosus* North (Figs. 11A, center; 11B, bottom and 11C). Concerning *F. vesiculosus*, both populations from Viana do Castelo (VC) and Ares (AR) revealed signals of hybridization with *F. guiryi* (Tables 4, 5), although the pattern was more consistent for *F. vesiculosus* from Viana do Castelo.

The proportion of introgression observed, as given by the $\hat{f}_d$ statistic, was in general low. Given previous suggestions of occurrence of hybridization between *F. guiryi* and *F. vesiculosus* based on both nuclear (e.g., Billard *et al.*, 2010; Zardi *et al.*, 2011) and mitochondrial (Coyer *et al.*, 2011) markers, a higher proportion of introgression could be expected between these two species. Such low values may be possibly due to the fact that this statistic is based on the conservative assumption that complete introgression would lead to homogenization of allele frequencies, with the frequencies of the derived allele being identical in the two taxa, hence leading to the

underestimation of the amount of introgression that likely has occurred (Martin *et al.*, 2014). The identical derived allele frequencies will unlikely be the case given their different reproductive mating system; *F. vesiculosus* is an outcrossing species whereas *F. guiryi* is a predominantly selfing species (Monteiro *et al.*, 2012). However, additional analyses would be required regarding the populations´ parameters (e.g., Hardy-Weinberg equilibrium, effective population size) that could guide expectations or predictions in this regard. Moreover, whether *F. guiryi* sympatric lineage arose exclusively due to introgression or it is a divergent lineage that was in addition affected by introgression from *F. vesiculosus* remains unclear. If the latter hypothesis is true, then the low proportion of admixture estimated with this analysis would be more likely to reflect the evolutionary history of this lineage. Alternatively, the origin of *F. guiryi* sympatric lineage due to introgression would probably result in a high proportion of admixture between the two lineages. Nevertheless, both statistics applied are coherent and undoubtedly support introgression as a factor involved in the evolution of these two lineages.

Further analysis, such as testing for the direction of introgression (e.g. D_{FOIL} test; Pease and Hahn, 2015) and the admixed origin of populations (f3; Reich *et al.*, 2009), would likely help in understanding the dynamics of gene flow between these taxa.

4.4 Time divergence estimates

The multispecies coalescent analyses (Fig. 13) yielded a similar topology for the hermaphroditic clade to the species tree obtained with the other methods (Figs. 6 - 9), where the *F. guiryi* Allopatric and the *F. guiryi* Sympatric each formed a distinct monophyletic group. This coherence was not observed for *F. vesiculosus*, which formed a monophyletic clade, contrary to the other tree topologies. However, results cannot be compared as they were based on completely different datasets; the multispecies coalescent analyses were performed with only 15 loci against the 1000 loci used in the previous ones. The divergence time estimated for *F. vesiculosus* was similar, but slightly more recent, to that previously found in a multigene phylogeny using 13 partial gene sequences (Cánovas *et al.*, 2011), although in that study *F. vesiculosus* was not monophyletic. Additionally, the divergence time estimated for the *F. guiryi* Sympatric group was approximately 0.5 Mya, however this date must be considered merely as a rough approximation, since for this analysis all loci in which there were signals of hybridization (i.e. the group was polyphyletic) were excluded, as this method does not account for hybridization in the conflicting signals between gene

trees. Moreover, the constant population-size model was applied, which assumes no variation in population sizes over time; this is unlikely to reflect the demographic history of this lineage along its evolution.

5. Conclusion

This thesis reports the first large-scale phylogenomic analysis of divergence in Lineage 2 (*sensu* Coyer *et al.*, 2006) of the genus *Fucus*, which has undergone a recent radiation in the North Atlantic (Canóvas *et al.*, 2011). Using extensive transcriptomic sampling of 1000 single-copy loci, population-level phylogenetic relationships were fully resolved, revealing phylogenetic incongruence at biogeographic scales. A new taxonomic entity within the hermaphroditic clade was shown, sister to the group of southern *F. guiryi* and northern *F. spiralis* (allopatric and sympatric, respectively with respect to *F. vesiculosus*). This basal hermaphroditic lineage corresponded to populations of *F. guiryi* ocurring (mainly) in sympatry with extant *F. vesiculosus* populations.

Phylogenies using both supermatrix and supertree methods strongly confirmed previous evidence of polyphyly within *F. vesiculosus,* between the group of populations from southern Iberia and those to the north of NW Iberia (in allopatry and sympatry with other *Fucus spp.*, respectively). Furthermore, a single population of *F. vesiculosus* in NW Iberia (Viana do Castelo) showed a sister relationship with sympatric *F. guiryi* ranging from Morocco to the UK. We show, using Bayesian concordance analysis and tests for introgression, that phylogenetic incongruence between loci found for lineages of *F. vesiculosus*, *F. guiryi* and *F. spiralis* was due to localized events of introgressive hybridization between *F. vesiculosus* in NW Iberia and the *F. guiryi* sympatric lineage. Clear signals of this introgression event could also be found in a population of the *F. guiryi* sympatric lineage in present-day allopatry (Morocco).

Additional signals suggesting allele sharing between both sympatric and allopatric *F. guiryi* and southern *F. vesiculosus* likely reflect the polyphyletic nature and cryptic diversity within *F. vesiculosus,* and we hypothesize that the hermaphroditic clade diverged from the southern *F. vesiculosus* clade following a north-south split within *F. vesiculosus*. This thesis opens up new perspectives for the study of the functional and adaptive impact of gene flow in this system.

6. References

Abascal F, Zardoya R, Telford MJ (2010) TranslatorX: multiple alignment of nucleotide sequences guided by amino acid translations. *Nucleic Acids Research*, gkq291.

Abbott R, Albach D, Ansell S, Arntzen JW, Baird SJE, Bierne N, *et al.* (2013) Hybridization and speciation. *Journal of Evolutionary Biology*, **26**, 229-246.

Allendorf FW, Leary RF, Spruell P, Wenburg JK (2001) The problems with hybrids: setting conservation guidelines. *Trends in Ecology and Evolution*, **16**, 613-622.

Altekar G, Dwarkadas S, Huelsenbeck JP, Ronquist F (2004) Parallel Metropolis-coupled Markov chain Monte Carlo for Bayesian phylogenetic inference. *Bioinformatics*, **20**, 407-415.

Ané C, Larget B, Baum DA, Smith SD, Rokas A (2007) Bayesian estimation of concordance among gene trees. *Molecular Biology and Evolution*, **24**, 412-426.

Andrews S (2011) FastQC: a quality control tool for high throughput sequence data. Available from http://www.bioinformatics.babraham.ac.uk/projects/fastqc

Arano B, Llorente G, Garcia-Paris M, Herrero P (1995) Species translocation menaces Iberian waterfrogs. *Conservation Biology*, **9**, 196-198.

Arnold ML, Buckner CM, Robinson JJ (1991) Pollen-mediated introgression and hybrid speciation in Louisiana irises. *Proceedings of the National Academy of Sciences*, **88**, 1398-1402.

Arnold ML (1997) *Natural Hybridization and Evolution*. Oxford University Press, Oxford.

Arnold ML, Martin NH (2010) Hybrid fitness across time and habitats. *Trends in Ecology and Evolution*, **25**, 530-536.

Assis J, Serrão EA, Claro B, Perrin C, Pearson GA (2014) Climate-driven range shifts explain the distribution of extant gene pools and predict future loss of unique lineages in a marine brown alga. *Molecular Ecology*, **23**, 2797-2810.

Avise JC, Wollenberg K (1997) Phylogenetics and the origin of species. *Proceedings of the National Academy of Sciences*, **94**, 7748-7755.

Baack E, Rieseberg L (2007) A genomic view of introgression and hybrid speciation. *Current Opinion in Genetics & Development*, **17**, 513-518.

Baum DA (2007) Concordance trees, concordance factors, and the exploration of reticulate genealogy. *Taxon*, **56**, 417-426.

Ballard JWO, Whitlock MC (2004) The incomplete natural history of mitochondria. *Molecular Ecology*, **13**, 729-744.

Bengtsson-Palme J, Ryberg M, Hartmann M, Branco S, Wang Z, Godhe A, Amend A (2013) Improved software detection and extraction of ITS1 and ITS2 from ribosomal ITS sequences of fungi and other eukaryotes for analysis of environmental sequencing data. *Methods in Ecology and Evolution*, **4**, 914-919.

Billard E, Serrão E, Pearson GA, Destombe C, Valero M (2010) *Fucus vesiculosus* and *spiralis* species complex: a nested model of local adaptation at the shore level. *Marine Ecology Progress Series*, **405**, 163-174.

Boni MF, Posada D, Feldman MW (2007) An exact nonparametric method for inferring mosaic structure in sequence triplets. *Genetics*, **176**, 1035-1047.

Bryant D, Moulton V (2004) Neighbor-Net: an agglomerative method for the construction of phylogenetic networks. *Molecular Biology and Evolution*, **21**, 255-265.

Bull V, Beltrán M, Jiggins CD, McMillan WO, Bermingham E, J (2006) Polyphyly and gene flow between non-sibling *Heliconius* species. *BMC Biology*, **4**, 1.

Burrows M, Wheeler DJ (1994) A block-sorting lossless data compression algorithm. *Technical report 124*, Palo Alto, CA, Digital Equipment Corporation.

Cánovas FG, Mota CF, Serrão EA, Pearson GA (2011) Driving south: a multigene phylogeny of the brown algal family Fucaceae reveals relationships and recent drivers of a marine radiation. *BMC Evolutionary Biology*, **11**, 371.

Castresana J (2000) Selection of conserved blocks from multiple alignments for their use in phylogenetic analysis. *Molecular Biology and Evolution*, **17**, 540-552.

Choleva L, Musilova Z, Kohoutova-Sediva A, Paces J, Rab P, Janko K (2014) Distinguishing between incomplete lineage sorting and genomic introgressions: complete fixation of allospecific mitochondrial DNA in a sexually reproducing fish (*Cobitis*; Teleostei), despite clonal reproduction of hybrids. *PLoS ONE*, **9**, e80641.

Coyer JA, Peters AF, Hoarau G, Stam WT, Olsen JL (2002) Hybridiszation of the marine seaweeds, *Fucus serratus* and *F. evanescens* (Heterokontophyta; Phaeophyceae) in a century-old zone of secondary contact. *Proceedings of the Royal Society of London. Series B*, **269**, 1829-1834.

Coyer JA, Peters AF, Stam WT, Olsen JL (2003) Post-ice age recolonization and differentiation of *Fucus serratus* L. (Phaeophyceae; Fucaceae) populations in Northern Europe. *Molecular Ecology*, **12**, 1817-1829.

Coyer JA, Hoarau G, Oudot-Le Secq MP, Stam WT, Olsen JL (2006) A mtDNA-based phylogeny of the brown algal genus *Fucus* (Heterokontophyta; Phaeophyta). *Molecular Phylogenetics and Evolution*, **39**, 209-222.

Coyer JA, Hoarau G, Costa JF, Hogerdijk B, Serrão EA, Billard E, Valero M, Pearson GA, Olsen JL (2011) Evolution and diversification within the intertidal brown macroalgae *Fucus spiralis/F. vesiculosus* species complex in the North Atlantic. *Molecular Phylogenetics and Evolution*, **58**, 283-296.

Crispo E, Bentzen P, Reznick DN, Kinnison MT, Hendry AP (2006) The relative influence of natural selection and geography on gene flow in guppies. *Molecular Ecology*, **15**, 49-62.

Cui R, Schumer M, Kruesi K, Walter R, Andolfatto P, Rosenthal GG (2013) Phylogenomics reveals extensive reticulate evolution in *Xiphophorus* fishes. *Evolution*, **67**, 2166-2179.

Darwin C (1859) *On the Origin of Species by Means of Natural Selection, or the Preservation of Favoured Races in the Struggle for Life*. John Murray, London, England.

De Maio N, Schrempf D, Kosiol C (2015) PoMo: An allele frequency-based approach for species tree estimation. *Systematic Biology*, **64**, 1018-1031.

Degnan J, Rosenberg N (2009) Gene tree discordance, phylogenetic inference and the multispecies coalescent. *Trends in Ecology and Evolution*, **24**, 332-340.

Dowling TE, Childs MR (1992) Impact of hybridization on a threatened trout of the southwestern United States. *Conservation Biology*, **6**, 355-364.

Dress AW, Huson DH (2004) Constructing splits graphs. *IEEE/ACM transactions on Computational Biology and Bioinformatics*, **1**, 109-115.

Drummond AJ, Suchard MA, Xie D, Rambaut A (2012) Bayesian phylogenetics with BEAUti and the BEAST 1.7. *Molecular Biology and Evolution*, **29**, 1969-1973.

Durand EY, Patterson N, Reich D, Slatkin M (2011) Testing for ancient admixture between closely related populations. *Molecular Biology and Evolution*, **28**, 2239-2252.

Edwards SV, Liu L, Pearl DK (2007) High-resolution species trees without concatenation. *Proceedings of the National Academy of Sciences*, **104**, 5936-5941.

Engel CR, Daguin C, Serrão EA (2005) Genetic entities and mating system in hermaphroditic *Fucus spiralis* and its close dioecious relative *F. vesiculosus* (Fucaceae, Phaeophyceae). *Molecular Ecology*, **14**, 2033-2046.

Foster PG (2004) Modelling compositional heterogeneity. *Systematic Biology*, **53**, 485-495.

Galtier N, Nabholz B, Glémin S, Hurst GDD (2009) Mitochondrial DNA as a marker of molecular diversity: a reappraisal. *Molecular Ecology*, **18**, 4541-4550.

Gernhard T (2008) The conditioned reconstructed process. *Journal of Theoretical Biology*, **253**, 769-778.

Gibbs MJ, Armstrong JS, Gibbs AJ (2000) Sister-Scanning: a Monte Carlo procedure for assessing signals in recombinant sequences. *Bioinformatics*, **16**, 573-582.

Gompert Z, Forister ML, Fordyce JA, Nice CC (2008) Widespread mito-nuclear discordance with evidence for introgressive hybridization and selective sweeps in *Lycaeides*. *Molecular Ecology*, **17**, 5231-5244.

Grant PR, Grant BR (2010) Conspecific versus heterospecific gene exchange between populations of Darwin's finches. *Philosophical Transactions of the Royal Society of London B: Biological Sciences*, **365**, 1065-1076.

Green RE, Krause J, Briggs AW *et al.* (2010) A draft sequence of the Neandertal genome. *Science*, **328**, 710-722.

Hamilton JA, Miller JM (2016) Adaptive introgression as a resource for management and genetic conservation in a changing climate. *Conservation Biology*, **30**, 33-41.

Harley CD, Helmuth BS (2003) Local-and regional-scale effects of wave exposure, thermal stress, and absolute versus effective shore level on patterns of intertidal zonation. *Limnology and Oceanography*, **48**, 1498-1508.

Head JD, Zerner MC (1985) A Broyden-Fletcher-Goldfarb-Shanno optimization procedure for molecular geometries. *Chemical Physics Letters*, **122**, 264-270.

Hedrick PW (2013) Adaptive introgression in animals: examples and comparison to new mutation and standing variation as sources of adaptive variation. *Molecular Ecology*, **22**, 4606-4618.

Heled J, Drummond AJ (2010) Bayesian inference of species trees from multilocus data. *Molecular Biology and Evolution*, **27**, 570-580.

Hewitt GM (2011) Quaternary phylogeography: the roots of hybrid zones. *Genetica*, **139**, 617-638.

Hoarau G, Coyer JA, Veldsink JH, Stam WT, Olsen JL (2007) Glacial refugia and recolonization pathways in the brown seaweed *Fucus serratus. Molecular Ecology*, **16**, 3606-3616.

Hoskin CJ, Higgie M, McDonald KR, Moritz C (2005) Reinforcement drives rapid allopatric speciation. *Nature*, **437**, 1353-1356.

Huson DH, Bryant D (2006) Application of phylogenetic networks in evolutionary studies. *Molecular Biology and Evolution*, **23**, 254-267.

Huson DH, Scornavacca C (2011) A survey of combinatorial methods for phylogenetic networks. *Genome Biology and Evolution*, **3**, 23-35.

Johannesson K, Rolán-Alvarez E, Ekendahl A (1995) Incipient reproductive isolation between two sympatric morphs of the intertidal snail *Littorina saxatilis*. *Evolution*, **49**, 1180-1190.

Keller I, Wagner CE, Greuter L, Mwaiko S, Selz OM, Sivasundar A, Seehausen O (2013) Population genomic signatures of divergent adaptation, gene flow and hybrid speciation in the rapid radiation of Lake Victoria cichlid fishes. *Molecular Ecology*, **22**, 2848-2863.

Keane TM, Creevey CJ, Pentony MM, Naughton TJ, Mclnerney JO (2006) Assessment of methods for amino acid matrix selection and their use on empirical data shows that ad hoc assumptions for choice of matrix are not justified. *BMC Evolutionary Biology*, **6**, 1.

Kliman RM, Hey J (1993) Reduced natural selection associated with low recombination in *Drosophila melanogaster*. *Molecular Biology and Evolution*, ***10***, 1239-1258.

Kubatko LS, Degnan JH (2007) Inconsistency of phylogenetic estimates from concatenated data under coalescence. *Systematic Biology*, **56**, 17-24.

Larget BR, Kotha SK, Dewey CN, Ané C (2010) BUCKy: gene tree/species tree reconciliation with Bayesian concordance analysis. *Bioinformatics*, **26**, 2910-2911.

Langmead B, Salzberg SL (2012) Fast gapped-read alignment with Bowtie 2. *Nature Methods,* **9**, 357-359.

Lewis RJ, Neushul M (1995) Intergeneric hybridization among five genera of the family Lessoniaceae (Phaeophyceae) and evidence for polyploidy in a fertile *Pelagophycus*× *Macrocystis* hybrid. *Journal of Phycology*, **31**, 1012-1017.

Li H, Handsaker B, Wysoker A, Fennell T, Ruan J, Homer N, Marth G, Abecasis G, Durbin R (2009) The Sequence Alignment/Map format and SAMtools. *Bioinformatics*, **25**, 2078-2079.

Li H (2011) A statistical framework for SNP calling, mutation discovery, association mapping and population genetical parameter estimation from sequencing data. *Bioinformatics*, **27**, 2987-2993.

Li H (2013) Aligning sequence reads, clone sequences and assembly contigs with BWA-MEM. arXiv:1303.3997v1 [q-bio.GN].

Liu L, Yu LL, Kubatko L, Pearl DK, Edwards SV (2009) Coalescent methods for estimating phylogenetic trees. *Molecular Phylogenetics and Evolution*, **53**, 320-328.

Lunter G, Goodson M (2011) Stampy: a statistical algorithm for sensitive and fast mapping of Illumina sequence reads. *Genome Research*, **21**, 936-939.

Macholán M, Baird SJ, Munclinger P, Dufková P, Bímová B, Piálek J (2008) Genetic conflict outweighs heterogametic incompatibility in the mouse hybrid zone?. *BMC Evolutionary Biology*, **8**, 1.

Maddison WP, Knowles LL (2006) Inferring phylogeny despite incomplete lineage sorting. *Systematic Biology*, **55**, 21-30.

Maggs CA, Castilho R, Foltz D, Henzler C, Jolly MT, Kelly J, Viard F (2008) Evaluating signatures of glacial refugia for North Atlantic benthic marine taxa. *Ecology*, **89**, S108-S122.

Mallet J (2005) Hybridization as an invasion of the genome. *Trends in Ecology and Evolution*, **20**, 229-237.

Mallet J (2007) Hybrid speciation. *Nature*, **446**, 279-283.

Mallet J (2009) Rapid speciation, hybridization and adaptive radiation in the *Heliconius melpomene* group. In: *Speciation and Patterns of Diversity* (eds Butlin RK, Bridle JR, Schluter D), pp. 177-194. Cambridge University Press, Cambridge, UK.

Martin DP, Rybicki E (2000) RDP: detection of recombination amongst aligned sequences. *Bioinformatics*, **16**, 562-563.

Martin DP, Posada D, Crandall KA, Williamson C (2005) A modified BOOTSCAN algorithm for automated identification of recombinant sequences and recombination breakpoints. *AIDS Research Human Retroviruses*, **21**, 98-102.

Martin DP, Murrell B, Golden M, Khoosal A, Muhire B (2015) RDP4: detection and analysis of recombination patterns in virus genomes. *Virus Evolution*, **1**.

Martin SH, Davey JW, Jiggins CD (2014) Evaluating the use of ABBA-BABA statistics to locate introgressed loci. *Molecular Biology and Evolution*, **32**, 244-257.

Martinsen GD, Whitham TG, Turek RJ, Keim P (2001) Hybrid populations selectively filter gene introgression between species. *Evolution*, **55**, 1325-1335.

Maynard Smith J (1992) Analyzing the mosaic structure of genes. *Journal of Molecular Evolution*, **34**, 126-129.

Mayr E (1963) *Animal Species and Evolution*. Harvard University Press, Cambridge, Massachusetts.

Melo-Ferreira J, Boursot P, Randi E, Kryukov A, Suchentrunk F, Ferrand N, Alves PC (2007) The rise and fall of the mountain hare (*Lepus timidus*) during Pleistocene glaciations: expansion and retreat with hybridization in the Iberian Peninsula. *Molecular Ecology*, **16**, 605-618.

Meng C, Kubatko LS (2009) Detecting hybrid speciation in the presence of incomplete lineage sorting using gene-tree incongruence: a model. *Theoretical Population Biology*, **75**, 35-45.

Miller LM, Close T, Kapuscinski AR (2004) Lower fitness of hatchery and hybrid rainbow trout compared to naturalized populations in Lake Superior tributaries. *Molecular Ecology*, **13**, 3379-3388.

Minh BQ, Nguyen MA, von Haeseler A (2013) Ultrafast approximation for phylogenetic bootstrap. *Molecular Biology and Evolution*, **30**, 1188-1195.

Mirarab S, Reaz R, Bayzid MS, Zimmermann T, Swenson MS, Warnow T (2014) ASTRAL: genome-scale coalescent-based species tree estimation. *Bioinformatics*, **30**, i541-i548.

Mirarab S, Warnow T (2015) ASTRAL-II: coalescent-based species tree estimation with many hundreds of taxa and thousands of genes. *Bioinformatics*, **12**, i44–i52.

Moalic Y, Arnaud-Haond S, Perrin C, Pearson GA, Serrão, EA (2011) Travelling in time with networks: Revealing present day hybridization versus ancestral polymorphism between two species of brown algae, *Fucus vesiculosus* and *F. spiralis*. *BMC Evolutionary Biology*, **11**, 33.

Montanari SR, Hobbs JPA, Pratchett MS, van Herwerden L (2016) The importance of ecological and behavioural data in studies of hybridization among marine fishes. *Reviews in Fish Biology and Fisheries*, **26**, 181-198.

Monteiro CA, Serrão EA, Pearson GA (2012) Prezygotic barriers to hybridization in marine broadcast spawners: reproductive timing and mating system variation. *PloS One*, **7**, e35978.

Monteiro CA, Paulino C, Jacinto R, Serrão EA, Pearson GA (2016) Temporal windows of reproductive opportunity reinforce species barriers in a marine broadcast spawning assemblage. *Scientific Reports*, **6**, 29198.

Neiva J, Pearson GA, Valero M, Serrão EA (2010) Surfing the wave on a borrowed board: range expansion and spread of introgressed organellar genomes in the seaweed *Fucus ceranoides* L. *Molecular Ecology*, **19**, 4812-4822.

Neiva J, Pearson GA, Valero M, Serrão EA (2012) Fine-scale genetic breaks driven by historical range dynamics and ongoing density-barrier effects in the estuarine seaweed *Fucus ceranoides* L. *BMC Evolutionary Biology*, **12**, 78.

Neiva J, Serrão EA, Assis J, Pearson GA, Coyer JA, Olsen JL, Valero M (2016) Climate oscillations, range shifts and phylogeographic patterns of North Atlantic Fucaceae. In: *Seaweed Phylogeography* (eds Hu Z-M, Fraser C), pp. 279-308. Springer Netherlands.

Nguyen LT, Schmidt HA, von Haeseler A, Minh BQ (2015) IQ-TREE: A fast and effective stochastic algorithm for estimating maximum-likelihood phylogenies. *Molecular Biology and Evolution*, **32**, 268-274.

Nicastro KR, Zardi GI, Teixeira S, Neiva J, Serrão EA, Pearson GA (2013) Shift happens: trailing edge contraction associated with recent warming trends threatens a distinct genetic lineage in the marine macroalga *Fucus vesiculosus*. *BMC Biology*, **11**, 1.

Padidam M, Sawyer S, Fauquet CM (1999) Possible emergence of new geminiviruses by frequent recombination. *Virology*, **265**, 218-225.

Pardo-Diaz C, Salazar C, Baxter SW, Merot C, Figueiredo-Ready W, Joron M, McMillan O, Jiggins CD (2012) Adaptive introgression across species boundaries in *Heliconius* butterflies. *PLoS Genetics*, **8**, e1002752.

Payseur BA, Rieseberg LH (2016) A genomic perspective on hybridization and speciation. *Molecular Ecology*, **25**, 2337-2360.

Pease JB, Hahn MW (2015) Detection and polarization of introgression in a five-taxon phylogeny. *Systematic Biology*, **64**, 651-662.

Pease JB, Guerrero RF, Sherman NA, Hahn MW, Moyle LC (2016) Molecular mechanisms of postmating prezygotic reproductive isolation uncovered by transcriptome analysis. *Molecular Ecology*, **25**, 2592-2608.

Pearson GA, Kautsky L, Serrão E (2000) Recent evolution in Baltic *Fucus vesiculosus*: reduced tolerance to emersion stresses compared to intertidal (North Sea) populations. *Marine Ecology Progress Series*, **202**, 67-79.

Pearson GA, Lago-Leston A, Valente M, Serrão E (2006) Simple and rapid RNA extraction from freeze-dried tissue of brown algae and seagrasses. *European Journal of Phycology*, **41**, 97-104.

Pearson GA, Lago-Leston A, Mota C (2009) Frayed at the edges: selective pressure and adaptive response to abiotic stressors are mismatched in low diversity edge populations. *Journal of Ecology*, **97**, 450-462.

Pereyra RT, Bergström L, Kautsky L, Johannesson K (2009) Rapid speciation in a newly opened postglacial marine environment, the Baltic Sea. *BMC Evolutionary Biology*, **9**, 70.

Petit RJ, Excoffier L (2009) Gene flow and species delimitation. *Trends in Ecology and Evolution*, **24**, 386-393.

Pfenninger M, Reinhardt F, Streit B (2002) Evidence for cryptic hybridization between different evolutionary lineages of the invasive clam genus *Corbicula* (Veneroida, Bivalvia). *Journal of Evolutionary Biology*, **15**, 818-829.

Pollard DA, Iyer VN, Moses AM, Eisen MB (2006) Widespread discordance of gene trees with species tree in *Drosophila*: evidence for incomplete lineage sorting. *PLoS Genetics*, **2**, e173.

Posada D, Crandall KA (2001a) Selecting the best-fit model of nucleotide substitution. *Systematic Biology*, **50**, 580-601.

Posada D, Crandall KA (2001b) Evaluation of methods for detecting recombination from DNA sequences: Computer simulations. *Proceedings of the National Academy Sciences*, **98**, 13757-13762.

Provan J, Wattier RA, Maggs CA (2005) Phylogeographic analysis of the red seaweed *Palmaria palmata* reveals a Pleistocene marine glacial refugium in the English Channel. *Molecular Ecology*, **14**, 793-803.

Rambaut A (2013) FigTree v1.3.1. Available from http://tree.bio.ed.ac.uk/software/figtree/

Rambaut A, Suchard MA, Xie D, Drummond AJ (2013) Tracer v1.6.0 Available from http://beast.bio.ed.ac.uk/software/tracer/

Ryan ME, Johnson JR, Fitzpatrick BM (2009) Invasive hybrid tiger salamander genotypes impact native amphibians. *Proceedings of the National Academy of Sciences*, **106**, 11166-11171.

Reich D, Thangaraj K, Patterson N, Price AL, Singh L (2009) Reconstructing Indian population history. *Nature*, **461**, 489-494.

Reisenbichler RR, Rubin SP (1999) Genetic changes from artificial propagation of Pacific salmon affect the productivity and viability of supplemented populations. *ICES Journal of Marine Science: Journal du Conseil*, **56**, 459-466.

Richards ZT, Hobbs JPA (2015) Hybridization on coral reefs and the conservation of evolutionary novelty. *Current Zoology*, **61**, 132-145.

Rieseberg LH, Choi HC, Ham D (1991) Differential cytoplasmic versus nuclear introgression in *Helianthus*. *Journal of Heredity*, **82**, 489-493.

Rieseberg LH, Van Fossen C, Desrochers AM (1995) Hybrid speciation accompanied by genomic reorganization in wild sunflowers. *Nature*, **375,** 313-316.

Rieseberg L, Raymond O, Rosenthal DM *et al.* (2003) Major ecological transitions in wild sunflowers facilitated by hybridization. *Science*, **301**, 1211-1216.

Riley SP, Shaffer H, Voss S, Fitzpatrick BM (2003) Hybridization between a rare, native tiger salamander (*Ambystoma californiense*) and its introduced congener. *Ecological Applications*, **13**, 1263-1275.

Rhymer JM, Simberloff D (1996) Extinction by hybridization and introgression. *Annual Review of Ecology and Systematics*, **27**, 83-109.

Rolán-Alvarez E, Johannesson K, Erlandsson J (1997) The maintenance of a cline in the marine snail *Littorina saxatilis*: the role of home site advantage and hybrid fitness. *Evolution*, **51**, 1838-1847.

Ronquist F, Teslenko M, van der Mark P, Ayres DL, Darling A, Höhna S, Larget B, Liu L, Suchard M, Huelsenbeck JP (2012). MrBayes 3.2: efficient Bayesian phylogenetic inference and model choice across a large model space. *Systematic Biology*, **61**, 539-542.

Schrempf D, Minh BQ, De Maio N, von Haeseler A, Kosiol C (2016) Reversible polymorphism-aware phylogenetic models and their application to tree inference. *Journal of Theoretical Biology*, **407**, 362-370.

Schumer M, Rosenthal GG, Andolfatto P (2014) How common is homoploid hybrid speciation? *Evolution*, **68**, 1553-1560.

Schwenk K*,* Brede N*,* Streit B (2008) Extent, processes and evolutionary impact of interspecific hybridization in animals*. Philosophical Transactions of the Royal Society of London B: Biological Sciences,* **363***,* 2805-2811*.*

Serrão EA, Brawley SH, Hedman J, Kautsky L, Samuelsson G (1999) Reproductive success of *Fucus vesiculosus* (Phaeophyceae) in the Baltic Sea. *Journal of Phycology*, **35**, 254-269.

Stamatakis A, Hoover P, Rougemont J (2008) A rapid bootstrap algorithm for the RAxML web servers. *Systematic Biology*, **57**, 758-771.

Stamatakis A (2014) RAxML version 8: a tool for phylogenetic analysis and post-analysis of large phylogenies. *Bioinformatics*, **30**, 1312-1313.

Stölting KN, Nipper R, Lindtke D, Caseys C, Waeber S, Castiglione S, Lexer C (2013) Genomic scan for single nucleotide polymorphisms reveals patterns of divergence and gene flow between ecologically divergent species. *Molecular Ecology*, **22**, 842-855.

Tavaré S (1986) Some Probabilistic and Statistical Problems in the Analysis of DNA Sequences. In: *Some Mathematical Questions in Biology: DNA Sequence Analysis* (eds Miura RM), volume 17, pp. 57-86. American Mathematical Society, Rhode Island.

Than C, Ruths D, Nakhleh L (2008) PhyloNet: a software package for analyzing and reconstructing reticulate evolutionary relationships. *BMC Bioinformatics*, **9**, 322.

Twyford AD, Ennos RA (2012) Next-generation hybridization and introgression. *Heredity*, **108**, 179-189.

Ward BJ, Oosterhout C (2016) Hybridcheck: software for the rapid detection, visualization and dating of recombinant regions in genome sequence data. *Molecular Ecology Resources*, **16**, 534-539.

Wielstra B, Arntzen JW, van der Gaag KJ, Pabijan M, Babik W (2014) Data concatenation, bayesian concordance and coalescent-based analyses of the species tree for the rapid radiation of *Triturus* newts. *PloS One*, **9**, e111011.

Yu Y, Barnett RM, Nakhleh L (2013) Parsimonious inference of hybridization in the presence of incomplete lineage sorting. *Systematic Biology*, **62**, 738-751.

Zardi GI, Nicastro KR, Canovas F, Ferreira Costa J, Serrão EA, Pearson GA (2011) Adaptive traits are maintained on steep selective gradients despite gene flow and hybridization in the intertidal zone. *PLoS One*, **6**, e19402.

Zardi GI, Nicastro KR, Serrão EA, Jacinto R, Monteiro CA, Pearson GA (2015) Closer to the rear edge: ecology and genetic diversity down the core-edge gradient of a marine macroalga. *Ecosphere*, **6**, 23.

Zhang W, Dasmahapatra KK, Mallet J, Moreira GR, Kronforst MR (2016) Genome-wide introgression among distantly related *Heliconius* butterfly species. *Genome Biology*, **17**, 1-15.

7. Appendices

Appendix I. Identification of single-copy loci in *Fucus*

Background

To accurately infer phylogenetic relationships among taxa it is critical that sequences chosen for analysis are true orthologous loci that diverged as a result of speciation, rather than paralogues arising from gene duplication events (Dufayard, 2005). This is a challenging task, particularly for data where positional information in the annotated genome (e.g., that might establish synteny or intron-exon structure) is lacking. Such information is lacking for transcriptome data, and here the aim was to apply a conservative approach based on reciprocal BLAST analysis to screen reference transcriptomes for single-copy loci prior to downstream phylogenomic analyses.

Two high-quality references were available, from *Fucus vesiculosus* (Pearson *et al.* unpubl data) and *F. ceranoides* (EMBL-EBI ENA Accession PRJEB11969). Both transcriptomes have been curated to remove potentially non brown-algal transcripts by BLAST comparisons (Altschul *et al.*, 1990) against genome data for the brown alga *Ectocarpus siliculosus* (Cock *et al.*, 2010).

Methods

Local BLAST databases (*F_ves* and *F_cer*) were made using *F. vesiculosus* and *F. ceranoides* reference transcriptome sequences ("*fves_HK_nucl.fasta*" and "*fcer_HK_nucl.fasta*"). A total of 4 BLASTn analyses were performed (2 self *versus* self and 2 interspecific). Loci that uniquely matched a single database entry were retained. The BLAST commands and command line UNIX code to extract unique hits is shown below.

1) BLASTn analyses:

```
$ blastn -query fves_HK_nucl.fasta -db Fves -outfmt 6 -out
  Fves_SELF.csv -max_target_seqs 4 -evalue 0.0001 -num_threads 10

$ blastn -query fcer_HK_nucl.fasta -db Fcer -outfmt 6 -out
  Fcer_SELF.csv -max_target_seqs 4 -evalue 0.0001 -num_threads 10

$ blastn -query fves_HK_nucl.fasta -db Fcer -outfmt 6 -out
  Fves_vs_Fcer.csv -max_target_seqs 4 -evalue 0.0001 -num_threads 10

$ blastn -query fcer_HK_nucl.fasta -db Fves -outfmt 6 -out
  Fcer_vs_Fves.csv -max_target_seqs 4 -evalue 0.0001 -num_threads 10
```

2) Write unique hit locus identifiers to file:

```
$ cut -f1 Fves_SELF.csv | sort | uniq -c | grep -e '\s1\s'| sed -r
  's/\s+1\s+//' > fves_uniqhit_self.txt

$ cut -f1 Fcer_SELF.csv | sort | uniq -c | grep -e '\s1\s'| sed -r
  's/\s+1\s+//' > fcer_uniqhit_self.txt

$ cut -f1 Fves_vs_Fcer.csv | sort | uniq -c | grep -e '\s1\s'| sed -r
  's/\s+1\s+//' > fves_uniqhit_fcer.txt

$ cut -f1 Fcer_vs_Fves.csv | sort | uniq -c | grep -e '\s1\s'| sed -r
  's/\s+1\s+//' > fcer_uniqhit_fves.txt
```

3) Join the locus lists from 2) above to obtain the unique hit loci (in the second column) common to both self and interspecies blasts. These are putative single-copy genes by separate analysis of each species:

```
$ join -j 2 fves_uniqhit_self.txt fves_uniqhit_fcer.txt >
  fves_singlecopy_candidates.txt

$ join -j 2 fcer_uniqhit_self.txt fcer_uniqhit_fves.txt >
  fcer_singlecopy_candidates.txt
```

4) Extract single-copy candidate loci with unique BLASTn hits in all comparisons:

use grep and a pattern list file (fves_singlecopy_candidate.txt and fcer_singlecopy_candidate.txt
files) to extract records from the blast.csv files

lines with fves singlecopy in Fcer_vs_Fves blast

```
$ grep -Ff fves_singlecopy_candidates.txt Fcer_vs_Fves.csv |wc -l
    2364
```

write to a temp file

```
$ grep -Ff fves_singlecopy_candidates.txt Fcer_vs_Fves.csv > temp
```

grep lines that are also fcer singlecopy and count number of records returned

```
$ grep -Ff fcer_singlecopy_candidates.txt temp | wc -l
    2027
```

write result to file and clean up

```
$ grep -Ff fves_singlecopy_candidates.txt temp >
  Fv_v_Fc_singlecopyblast.csv && rm temp
```

Repeat for Fves_vs_Fcer blast

```
$ grep -Ff fcer_singlecopy_candidates.txt Fves_vs_Fcer.csv |wc -l
    2579
$ grep -Ff fcer_singlecopy_candidates.txt Fves_vs_Fcer.csv > temp
$ grep -Ff fves_singlecopy_candidates.txt temp | wc -l
    2027
$ grep -Ff fves_singlecopy_candidates.txt temp >
  Fc_v_Fc_singlecopyblast.csv && rm temp
```

Results

Using this conservative approach, we identified a common set of 2027 transcript loci with unique hits in self- and interspecific BLASTs. These are therefore good candidates for single-copy genes in the *Fucus* genome, and were selected for downstream phylogenomic analyses.

References

Altschul SF, Gish W, Miller W, Myers EW, Lipman DJ (1990) Basic local alignment search tool. *Journal of Molecular Biology*, **215,** 403-410.

Cock JM *et al.* (2010) The *Ectocarpus* genome and the independent evolution of multicellularity in brown algae. *Nature*, **465,** 617-621.

Dufayard J, Duret L, Penel S, Gouy M, Rechenmann F, Perrière G (2005) Tree pattern matching in phylogenetic trees: automatic search for orthologs or paralogs in homologous gene sequence databases. *Bioinformatics*, **21**, 2596-2603.

Appendix II. Pipeline for aligning and removing poorly aligned regions for the 1000 transcripts

Locus_pipe.py, written by Cymon J. Cox

```
#! /usr/bin/env python

desc = """
1. Write locus alignments
2. Run TranslocatorX on them (including Gblocks)
3. Clean to remove any further ambiguities, gaps or stop codons
at any codon sites

This leaves only solid blocks of in-frame codon aligned data
with no gaps, ambiguities, stop anywhere.
"""
```

```
import argparse
import sys
import subprocess
import os
from Bio import SeqIO
import textwrap
#import p4
#p4.var.doCheckForBlankSequences = False
#p4.var.doCheckForDuplicateSequences = False

from locus_alignments_from_transcriptomes import main as
align_loci
from TranslatorX_functions import run_TranslatorX
from remove_gapped_and_ambiguous_codons import main as
clean_loci

##############################################
SUPERFLUOUS_TRANSX_FILES = [
"%s_transX.aa_ali.fasta",
"%s_transX.aa_ali.fasta-gb.txts",
"%s_transX.aa_based_codon_coloured-gb.html",
"%s_transX.aa_based_codon_coloured.html",
"%s_transX.aa_cleanali.fasta",
"%s_transX.aaseqs",
"%s_transX.aaseqs.fasta",
"%s_transX.html",
"%s_transX.mafft.log",
"%s_transX.nt12_ali.fasta",
"%s_transX.nt12_cleanali.fasta",
"%s_transX.nt1_ali.fasta",
"%s_transX.nt1_cleanali.fasta",
"%s_transX.nt2_ali.fasta",
"%s_transX.nt2_cleanali.fasta",
"%s_transX.nt3_ali.fasta",
"%s_transX.nt3_cleanali.fasta"]
##############################################

def main(data_filenames, locus_names, out_dir):

    if not os.path.exists(out_dir):
        os.makedirs(out_dir)

    align_loci(data_filenames, locus_names, outdir=out_dir,
            overwrite=True, csv_log=True, quiet=False)

    f = open(locus_names, 'r')
    loci = f.read().splitlines()
    f.close()

    os.chdir(out_dir)
    for locus in loci:
        print "\tAligning %s with TranslatorX" % locus,
        r = run_TranslatorX("%s.fasta" % locus, code=1, gbl="-
b5=n")
        if r[0] == "":
```

```
            print "\tTranslatorX failed - perhaps cannot find
input file..."
            print
            continue
        else:
            (returncode, stderr, stdout) = r
        if returncode != 0:
            if "Gblocks alignment:  0 positions" in stderr:
                print "\tGblocks alignment:  0 positions saved"
                print
                continue
            else:
                print "\tError running TranslatorX - see
transX_stdout.text..."
                print "\treturncode = %s" % returncode
                of = open("transX_stdout.text", "a")
                of.write(stdout)
                of.write(stderr)
                of.close()
                print
                continue
        else:
            print "done."
            for f in SUPERFLUOUS_TRANSX_FILES:
                os.remove(f % locus)
            # Clean out all ambigous, gapped, or stop codons if
present - even when
            # not constant - by removing the codon site (3 nucs
at which it occurs)
            clean_loci("%s_transX.nt_cleanali.fasta" % locus,
quiet=False)

if __name__ == "__main__":

    parser = argparse.ArgumentParser(

formatter_class=argparse.RawDescriptionHelpFormatter,
            description=textwrap.dedent(desc),
            )
    parser.add_argument(dest="data_filenames",
                        help="File listing input data files (one
per line)"
                        )
    parser.add_argument(dest="locus_names",
                        help="File listing locus names (one per
line)"
                        )
    parser.add_argument("-d", "--output_dir",
                        dest="outdir",
                        help="Output directory name Default:
locus_alignments",
                        default="locus_alignments"
                        )
    args = parser.parse_args()
    main(args.data_filenames, args.locus_names, args.outdir)
```

Appendix III. Pipeline for collapsing aligned alleles into a single consensus sequence

Otus.py, written by Cymon J. Cox

```
#! /usr/bin/env python

"""
Collapse allele data in an alignment to a single consensus
sequence
"""

import os
import sys, subprocess
from p4 import *
from p4.SequenceList import Sequence
var.doCheckForDuplicateSequences = False

#From p4
#equates = {'b': 'cgt', 'd': 'agt', 'h': 'act', 'k': 'gt', 'm':
'ac', 'n': 'acgt', 's': 'cg', 'r': 'ag', 'w': 'at', 'v': 'acg',
'y': 'ct'}
equates = {'cgt': 'b',
        'agt': 'd',
        'act': 'h',
        'gt': 'k',
        'ac': 'm',
        'acgt': 'n',
        'cg': 's',
        'ag': 'r',
        'at': 'w',
        'acg': 'v',
        'ct': 'y'
        }

def main(the_alignment):

    read(the_alignment)
    a = var.alignments[0]
    a.makeSequenceForNameDict()

    labels = [i.rsplit("_")[0] for i in a.taxNames]
    #print labels
    assert len(labels) == 146
    otus = set(labels)
    assert len(otus) == (len(labels)/2)
```

```
    new_seqs = []

    for otu in sorted(otus):

        s1 = a.sequenceForNameDict[otu + "_0"]
        s2 = a.sequenceForNameDict[otu + "_1"]

        if s1.sequence == s2.sequence:
            s = Sequence()
            s.name = otu
            s.sequence = s1.sequence
            s.dataType = s1.dataType
            new_seqs.append(s)
        else:
            ns = []
            for i in range(len(s1.sequence)):
                if s1.sequence[i] == s2.sequence[i]:
                    ns.append(s1.sequence[i])
                else:
                    b = [s1.sequence[i], s2.sequence[i]]
                    b.sort()
                    ns.append(equates["".join(b)])
            s = Sequence()
            s.name = otu
            s.sequence = "".join(ns)
            s.dataType = s1.dataType
            new_seqs.append(s)

    a.sequences = new_seqs
    assert len(a.sequences) == 71
    nn = a.fName.split(".")[0] + "_OTUS.nex"
    a.writeNexus(fName=nn, writeDataBlock=1, interleave=0,
flat=1, append=0, userText='')

    var.alignments = []


child = subprocess.Popen(["ls -1"], stdout=subprocess.PIPE,
            stderr=subprocess.PIPE, shell=True)
stdoutdata, stderrdata = child.communicate()
matrices =  stdoutdata.split("\n")[:-1]

skip = []

for mat in matrices:
    if mat in skip:
        print "SKIPPING %s" % mat
        continue
    print "Doing mat: %s" % mat,
    main(mat)
    print "done."
```

Appendix IV. Groups of taxa used for testing for incongruence between gene trees using BUCKy

Hypothesis 1, taxa for analysis including only *F. vesiculosus* North (=Sympatric):
F. ceranoides
F. guiryi
*F. guiryi*I
F. serratus
F. spiralis
*F. vesiculosus*N

Hypothesis 2, taxa for analysis including only *F. vesiculosus* VC (=Sympatric, Viana do Castelo):
F. ceranoides
F. guiryi
*F. guiryi*I
F. serratus
F. spiralis
*F. vesiculosus*VC

Hypothesis 3, taxa for analysis including only *F. vesiculosus* South (=Allopatric):
F. ceranoides
F. guiryi
*F. guiryi*I
F. serratus
F. spiralis
*F. vesiculosus*S

Hypothesis 4, taxa for analysis including all *F. vesiculosus* groups (North, South and VC):
F. ceranoides
F. guiryi

*F. guiryi*I
F. serratus
F. spiralis
*F. vesiculosus*N
*F. vesiculosus*S
*F. vesiculosus*VC

Hypothesis 5, taxa for analysis including populations from *F. vesiculosus* North and VC:
F. ceranoides
F. guiryi
*F. guiryi*I
F. serratus
F. spiralis
*F. vesiculosus*N
*F. vesiculosus*VC

Hypothesis 6, taxa for analysis including populations from *F. vesiculosus* South and VC:
F. ceranoides
F. guiryi
*F. guiryi*I
F. serratus
F. spiralis
*F. vesiculosus*S
*F. vesiculosus*VC

Hypothesis 7, taxa for analysis including populations from *F. vesiculosus* North and South:
F. ceranoides
F. guiryi
*F. guiryi*I
F. serratus
F. spiralis
*F. vesiculosus*N
*F. vesiculosus*S

Appendix V. Coverage obtained for read mapping

Coverage obtained for read mapping for the major groups of *Fucus spp.*, given by the within-sample normalized transcript expression measure. FPKM: number of fragments per kilobase of transcript per million mapped reads. A: *F. ceranoides*; B: *F. serratus*; C: *F. guiryi* Sympatric; D: *F. guiryi* Allopatric; E: *F. spiralis*; F: *F. vesiculosus* Sympatric; G: *F. vesiculosus* Allopatric.

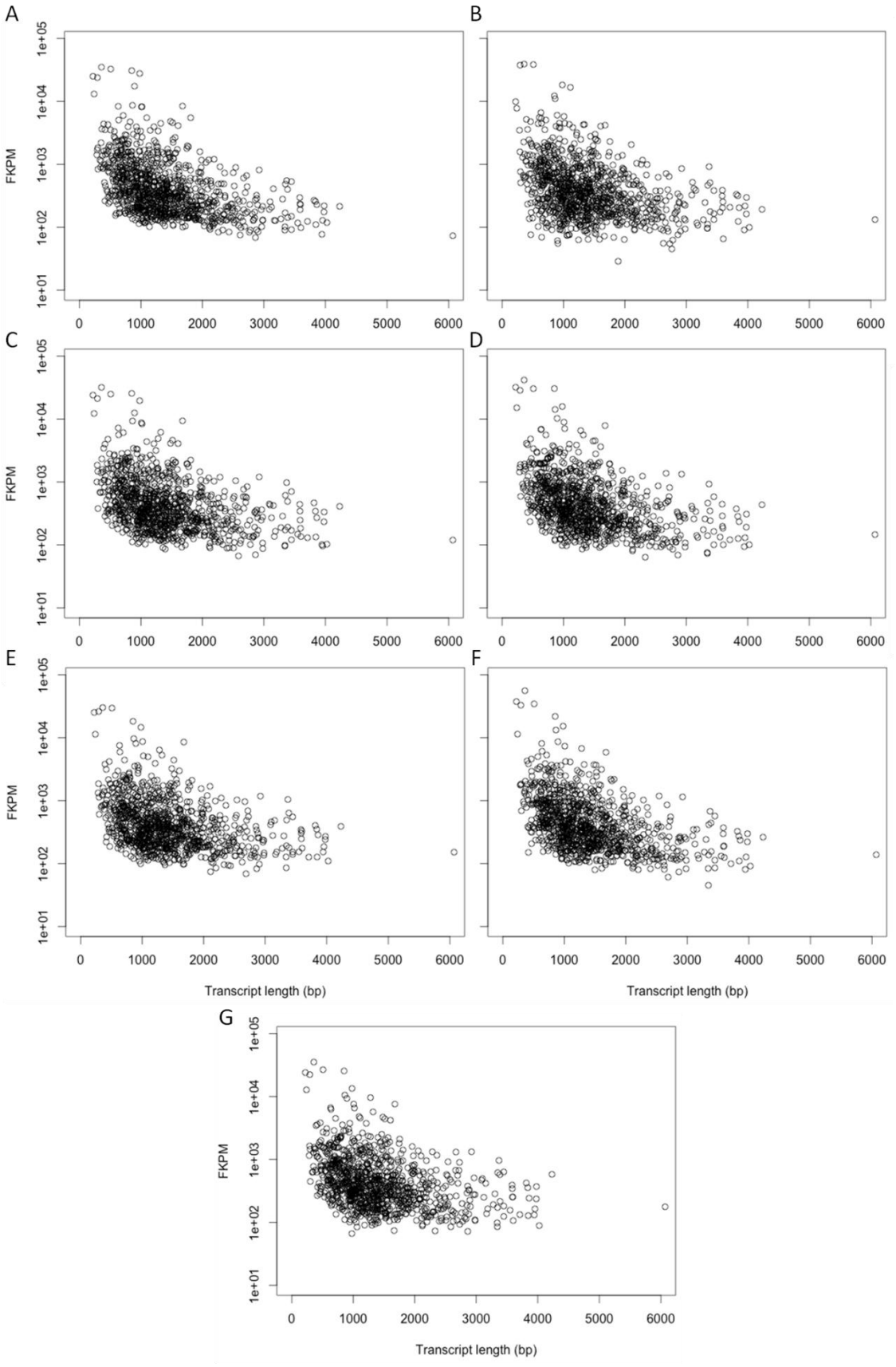
A
B
C
D
E
F
G
FKPM
1e+01
1e+02
1e+03
1e+04
1e+05
0
1000
2000
3000
4000
5000
6000
Transcript length (bp)

Appendix VI. Statistics for transcript alignments

Statistics for the 1000 transcript alignments used in the analyses. All alignments contain 49 taxa. nChar: length of the transcript; Constant: number of invariable sites; Variable: number of variable sites; Informative: number of parsimony informative sites; GC(%): GC content; nSNP: number of SNPs.

Transcript	nChar	Constant	Variable	Informative	GC (%)	nSNP
FcF_L10151_514-1752-	963	924	39	35	0.53	62
FcF_L1020_793-1726-	798	777	21	11	0.6	29
FcF_L1050_396-1993-	1449	1430	19	18	0.6	23
FcF_L1090_127-879+	681	664	17	14	0.59	17
FcF_L110_2183-3114+	816	813	3	3	0.6	3
FcF_L1108_1641-2752+	633	619	14	13	0.62	24
FcF_L1121_1-3976+	762	748	14	13	0.57	28
FcF_L1159_2140-4660-	1170	1109	61	59	0.6	81
FcF_L1176_7-2540+	345	327	18	17	0.61	29
FcF_L118_1230-2229-	654	643	11	10	0.62	59
FcF_L1188_211-1765-	1038	969	69	64	0.54	89
FcF_L11961_170-643-	255	247	8	6	0.58	10
FcF_L120_284-2960+	540	526	14	13	0.61	21
FcF_L1210_1034-1674-	597	582	15	15	0.58	22
FcF_L1221_73-877+	633	612	21	19	0.62	43
FcF_L1223_1-2105+	1896	1868	28	26	0.6	43
FcF_L1258_1282-5096-	1002	977	25	23	0.59	39
FcF_L1264_38-409+	315	306	9	8	0.59	12
FcF_L1279_1991-2279-	213	209	4	2	0.59	9
FcF_L1283_1-1969+	1317	1272	45	36	0.62	64
FcF_L1290_612-1204-	516	510	6	6	0.55	10
FcF_L1294_1984-4282-	588	571	17	14	0.61	34
FcF_L1297_389-3061+	1332	1309	23	15	0.59	55
FcF_L1303_2447-4786-	762	740	22	21	0.57	45
FcF_L1312_1-2216+	462	449	13	12	0.56	17
FcF_L132_1-1782+	1527	1475	52	47	0.61	74
FcF_L132_2704-4504-	1608	1553	55	49	0.6	82
FcF_L1338_1-979+	891	845	46	40	0.57	56
FcF_L1356_262-1880+	1572	1541	31	28	0.54	38
FcF_L1361_1-1085+	945	881	64	53	0.6	82
FcF_L1370_305-961+	639	632	7	3	0.58	11
FcF_L138_580-2318+	1230	1206	24	20	0.58	40
FcF_L1385_612-2014-	849	824	25	22	0.54	40
FcF_L1406_2014-4545-	1110	1088	22	20	0.56	36
FcF_L1431_1-1560+	1431	1394	37	30	0.57	63

FcF_L1450_909-2316-	1104	1078	26	22	0.61	41
FcF_L1452_362-1518+	1068	1053	15	14	0.6	15
FcF_L1473_1636-2590-	279	276	3	3	0.55	10
FcF_L1475_2586-4397-	1020	965	55	50	0.6	70
FcF_L1480_1-646+	555	549	6	6	0.57	9
FcF_L1490_861-2572-	846	818	28	22	0.58	50
FcF_L1497_294-1915+	873	829	44	40	0.61	54
FcF_L1500_3541-4295+	681	660	21	16	0.58	34
FcF_L1521_2646-5428-	450	409	41	31	0.6	58
FcF_L1531_1-1800+	1251	1183	68	65	0.58	101
FcF_L1533_1-754+	678	653	25	18	0.59	39
FcF_L1557_852-2292-	1224	1173	51	49	0.56	65
FcF_L1560_413-1972-	1260	1241	19	17	0.59	22
FcF_L1564_1700-4434-	1608	1570	38	33	0.56	57
FcF_L1564_1-981+	525	497	28	26	0.59	41
FcF_L1566_737-1678-	765	744	21	21	0.58	23
FcF_L1568_1-782+	627	606	21	20	0.57	27
FcF_L1568_841-2322-	1212	1158	54	47	0.53	79
FcF_L1598_1-968+	348	330	18	15	0.54	26
FcF_L161_47-1597+	609	586	23	20	0.6	38
FcF_L1638_1487-3377-	342	342	0	0	0.6	3
FcF_L1668_2284-3562-	216	211	5	4	0.64	7
FcF_L1673_1-993+	891	857	34	29	0.54	62
FcF_L1676_130-1532+	1377	1337	40	32	0.57	63
FcF_L1681_338-1660-	756	716	40	32	0.64	61
FcF_L1682_122-3276+	1224	1196	28	24	0.57	39
FcF_L1723_1857-3474-	1395	1355	40	34	0.54	45
FcF_L1727_3962-5165-	981	963	18	18	0.59	36
FcF_L1735_1335-2434+	990	981	9	9	0.59	9
FcF_L1738_426-3776-	2124	2080	44	39	0.58	77
FcF_L1739_1408-1824-	393	385	8	7	0.56	12
FcF_L1752_2762-4231-	1257	1234	23	21	0.59	36
FcF_L1754_381-1035-	594	564	30	26	0.55	32
FcF_L1757_2776-3543-	678	660	18	16	0.58	19
FcF_L1777_253-747+	351	339	12	10	0.64	18
FcF_L1787_1-1749+	1530	1493	37	34	0.61	57
FcF_L1789_598-2409-	1503	1475	28	23	0.6	73
FcF_L1792_1-3305+	1560	1519	41	39	0.61	70
FcF_L1792_4423-5438-	888	853	35	32	0.6	47
FcF_L1805_226-705+	471	464	7	6	0.58	12
FcF_L1810_844-2936-	1437	1405	32	28	0.6	68
FcF_L1813_90-1225-	528	516	12	12	0.58	27
FcF_L1816_1-686+	600	580	20	17	0.6	24
FcF_L1833_1073-3180+	1026	988	38	33	0.63	70
FcF_L1842_1-704+	660	627	33	26	0.56	47

FcF_L187_1-1857+	942	915	27	25	0.57	50
FcF_L188_349-714+	327	321	6	6	0.53	6
FcF_L1880_1-3549+	375	359	16	15	0.58	23
FcF_L1895_1587-3201-	963	931	32	25	0.59	38
FcF_L1903_2299-5153-	744	725	19	16	0.58	32
FcF_L1933_81-1840+	1626	1605	21	19	0.54	28
FcF_L1939_1-507+	408	396	12	9	0.6	18
FcF_L1941_1624-3166-	861	838	23	19	0.59	39
FcF_L1960_149-982+	372	362	10	9	0.6	15
FcF_L1960_2491-3751-	885	860	25	24	0.63	42
FcF_L1971_1050-1594-	336	331	5	5	0.61	12
FcF_L20_2586-4137-	633	622	11	11	0.6	81
FcF_L2036_828-1396-	492	483	9	8	0.55	13
FcF_L2038_1-1499+	309	294	15	13	0.58	24
FcF_L2042_37-1686+	828	802	26	26	0.57	39
FcF_L2099_311-1698-	1143	1109	34	22	0.57	61
FcF_L2106_2301-5006-	459	448	11	5	0.56	39
FcF_L2113_1-1841+	924	900	24	20	0.55	43
FcF_L2116_1-622+	540	526	14	14	0.57	36
FcF_L2134_194-2135+	300	286	14	13	0.7	21
FcF_L2146_617-4067-	282	276	6	6	0.63	13
FcF_L2152_1-884+	366	345	21	18	0.55	24
FcF_L2159_1-2138+	1776	1730	46	42	0.61	85
FcF_L2160_438-2018+	843	814	29	29	0.61	51
FcF_L2162_310-1778+	624	613	11	9	0.56	23
FcF_L2181_942-1714-	591	574	17	15	0.61	24
FcF_L2184_1-1187+	270	264	6	5	0.64	20
FcF_L2199_1-2575+	1008	985	23	19	0.59	42
FcF_L2234_1-1941+	1839	1779	60	51	0.59	93
FcF_L2235_1043-3293-	714	696	18	13	0.65	38
FcF_L2246_714-1857-	768	744	24	23	0.58	37
FcF_L2250_1262-2860-	1326	1286	40	32	0.59	63
FcF_L2257_1-2142+	1227	1170	57	50	0.62	71
FcF_L2284_746-4328-	1062	1030	32	27	0.57	45
FcF_L2307_895-1970-	996	962	34	27	0.57	53
FcF_L2326_360-830-	432	426	6	4	0.59	8
FcF_L2328_1-925+	840	803	37	31	0.53	52
FcF_L2336_1146-2490-	1098	1055	43	34	0.56	72
FcF_L235_1-1213+	789	759	30	28	0.55	66
FcF_L2358_1-2192+	1383	1344	39	32	0.62	76
FcF_L237_1110-2395-	1158	1120	38	34	0.56	49
FcF_L2378_610-2979-	1146	1105	41	39	0.59	59
FcF_L24_1-1780+	1107	1087	20	17	0.58	29
FcF_L2420_374-1428+	252	237	15	13	0.64	22
FcF_L2426_1214-2444-	732	707	25	18	0.62	54

FcF_L2429_557-1981-	1095	1065	30	28	0.6	42
FcF_L2444_872-1568-	588	578	10	9	0.55	14
FcF_L2461_1-1274-	1161	1143	18	15	0.51	31
FcF_L2480_1008-1904-	801	774	27	22	0.6	45
FcF_L2489_1-1052-	816	777	39	28	0.52	56
FcF_L2506_809-2549-	285	285	0	0	0.6	18
FcF_L2527_189-3311-	693	676	17	16	0.61	30
FcF_L2591_1605-3663-	1260	1225	35	34	0.59	60
FcF_L2595_498-1460-	870	852	18	16	0.59	44
FcF_L2650_117-1297+	1131	1094	37	36	0.58	61
FcF_L2651_1023-4111+	324	318	6	6	0.59	13
FcF_L2654_3334-5279-	696	669	27	24	0.6	38
FcF_L2660_421-1292-	498	482	16	13	0.61	35
FcF_L2678_1-2125+	1374	1330	44	41	0.59	78
FcF_L2678_2495-2836-	324	314	10	9	0.56	17
FcF_L268_1-2883-	1671	1629	42	35	0.51	69
FcF_L2686_641-1161-	480	470	10	8	0.57	12
FcF_L2698_1-1138+	381	381	0	0	0.59	19
FcF_L2717_4127-4753-	606	589	17	13	0.57	18
FcF_L2725_181-2119+	1617	1558	59	51	0.55	87
FcF_L2766_177-2068+	342	339	3	3	0.61	5
FcF_L2804_921-2038-	702	667	35	29	0.6	49
FcF_L2810_347-2005-	1236	1178	58	49	0.55	78
FcF_L2824_41-1072+	645	622	23	20	0.58	45
FcF_L2839_807-1443-	453	439	14	13	0.59	21
FcF_L2852_951-1688-	699	679	20	17	0.58	29
FcF_L2878_1-2525+	555	536	19	16	0.59	31
FcF_L2943_1-1021+	942	913	29	25	0.54	43
FcF_L2944_215-2831+	234	228	6	6	0.59	9
FcF_L2945_214-1776+	897	844	53	47	0.59	71
FcF_L2975_1-905-	213	203	10	9	0.6	18
FcF_L2987_312-1466-	999	969	30	26	0.51	37
FcF_L2994_1929-3930-	909	890	19	13	0.56	27
FcF_L3005_1-2190+	1509	1475	34	31	0.53	59
FcF_L3010_198-1870+	1062	1021	41	39	0.63	64
FcF_L3011_1600-3068-	480	476	4	1	0.62	62
FcF_L3014_1590-2303-	633	608	25	21	0.6	43
FcF_L3033_1148-2431-	279	270	9	8	0.53	18
FcF_L3036_390-1958-	1449	1432	17	14	0.56	24
FcF_L3054_149-851+	630	613	17	16	0.64	22
FcF_L3093_1-2116+	708	687	21	20	0.6	30
FcF_L3095_1-690+	645	637	8	8	0.6	11
FcF_L3099_1782-3123+	933	904	29	22	0.59	55
FcF_L3099_629-1767-	822	792	30	25	0.53	46
FcF_L3121_1040-1987-	825	805	20	17	0.62	37

FcF_L3135_603-1351-	681	667	14	13	0.6	21
FcF_L3143_913-3402+	198	192	6	4	0.63	12
FcF_L3156_97-1029+	876	859	17	11	0.56	21
FcF_L3192_479-1157-	615	597	18	11	0.6	33
FcF_L3212_1-2395+	861	836	25	22	0.56	47
FcF_L3214_1-1355-	327	319	8	8	0.57	15
FcF_L3258_1-1337+	1035	1014	21	18	0.58	39
FcF_L3263_24-830+	696	660	36	29	0.57	58
FcF_L3304_678-1762-	1005	984	21	20	0.6	30
FcF_L3309_276-1649+	1314	1291	23	21	0.59	31
FcF_L3324_436-1668-	1149	1095	54	42	0.55	79
FcF_L3344_206-1422+	846	823	23	18	0.64	39
FcF_L3347_30-743+	690	675	15	11	0.64	23
FcF_L3349_1-2511+	456	444	12	12	0.58	23
FcF_L3391_93-632+	471	459	12	11	0.56	18
FcF_L3396_276-861-	468	447	21	17	0.55	32
FcF_L3401_988-3913-	1746	1707	39	33	0.58	55
FcF_L3412_253-2014+	501	495	6	6	0.61	18
FcF_L3448_189-2153+	1770	1724	46	40	0.58	63
FcF_L3458_1244-1634-	303	297	6	6	0.54	15
FcF_L3480_1-600+	534	524	10	8	0.54	23
FcF_L3489_287-1069+	669	654	15	15	0.6	25
FcF_L3493_1-820+	744	707	37	31	0.56	58
FcF_L3505_976-2837-	321	313	8	8	0.62	15
FcF_L352_957-1838-	687	665	22	21	0.53	24
FcF_L3535_21-1805+	309	296	13	13	0.57	21
FcF_L3549_1-911+	822	793	29	20	0.6	38
FcF_L3550_1168-2287-	741	708	33	29	0.59	52
FcF_L359_781-1793-	912	905	7	7	0.59	7
FcF_L3598_1-2860+	1083	1055	28	24	0.58	48
FcF_L360_1430-5277-	519	506	13	11	0.58	27
FcF_L3601_1-1090+	936	904	32	25	0.62	53
FcF_L3604_1-1569+	381	365	16	13	0.61	26
FcF_L3617_467-2095-	846	810	36	32	0.56	61
FcF_L3633_1-927-	852	824	28	26	0.56	36
FcF_L3636_1-2186+	699	668	31	25	0.63	49
FcF_L3647_1252-3431-	657	640	17	14	0.59	30
FcF_L365_57-1423+	786	758	28	25	0.54	35
FcF_L3681_1895-2934-	576	560	16	15	0.62	25
FcF_L3699_1-1228-	969	917	52	39	0.53	63
FcF_L3700_564-1397-	729	694	35	32	0.59	42
FcF_L3710_487-2476-	558	533	25	24	0.58	39
FcF_L3714_1-1133+	366	343	23	14	0.57	36
FcF_L3714_1269-2494-	1053	1032	21	15	0.59	48
FcF_L3722_464-2373+	585	570	15	14	0.57	30

FcF_L3725_1-1086+	966	929	37	34	0.59	63
FcF_L3744_52-1643+	681	647	34	31	0.59	58
FcF_L3753_252-2020+	705	686	19	16	0.62	36
FcF_L3756_26-1274+	663	636	27	25	0.58	64
FcF_L3761_179-2532-	2019	1983	36	32	0.54	60
FcF_L3770_434-1762-	792	775	17	17	0.57	37
FcF_L3783_1-1263+	843	805	38	35	0.57	54
FcF_L3793_107-2733+	561	536	25	18	0.57	42
FcF_L3819_110-1872+	354	347	7	6	0.59	17
FcF_L382_1226-1741-	333	329	4	3	0.55	7
FcF_L3825_157-849-	636	625	11	9	0.58	13
FcF_L3831_79-1822+	1107	1081	26	25	0.6	45
FcF_L3834_1-1992-	390	377	13	9	0.58	16
FcF_L3835_166-923-	726	703	23	20	0.62	33
FcF_L3891_186-2237+	792	770	22	19	0.56	33
FcF_L39_2416-3509-	873	852	21	18	0.6	36
FcF_L3907_208-2008-	228	225	3	2	0.57	15
FcF_L3927_890-3158-	1644	1607	37	35	0.52	57
FcF_L3930_132-1564-	822	787	35	32	0.54	60
FcF_L3942_54-1068+	873	839	34	27	0.56	46
FcF_L3943_979-2152-	1017	964	53	46	0.54	70
FcF_L3945_65-989-	429	399	30	25	0.6	39
FcF_L3958_379-1482-	966	920	46	38	0.55	70
FcF_L3960_1-2775+	1206	1152	54	46	0.61	74
FcF_L397_1-590+	528	510	18	17	0.59	29
FcF_L3976_1-1985+	1611	1556	55	44	0.57	70
FcF_L3977_278-1272+	936	901	35	31	0.61	57
FcF_L398_1-1268+	1059	1030	29	25	0.6	54
FcF_L3989_481-2107-	1575	1535	40	32	0.61	62
FcF_L4023_182-940+	459	443	16	16	0.6	26
FcF_L4054_1-1164+	492	473	19	17	0.57	33
FcF_L4078_1-569+	519	498	21	21	0.57	31
FcF_L408_100-1538+	282	271	11	10	0.62	14
FcF_L4103_1-1088+	711	670	41	34	0.54	62
FcF_L4124_158-1007+	759	721	38	34	0.58	45
FcF_L4163_57-1852+	522	484	38	29	0.57	56
FcF_L418_1-703+	537	508	29	22	0.59	37
FcF_L4195_1-834+	723	711	12	10	0.51	20
FcF_L420_1084-3234-	1533	1487	46	41	0.58	68
FcF_L4206_566-1678-	801	773	28	23	0.62	44
FcF_L4213_1-1151+	900	863	37	32	0.52	47
FcF_L4214_1058-2037-	804	791	13	11	0.57	20
FcF_L4226_4084-4752-	600	581	19	18	0.59	28
FcF_L4235_274-1856+	1419	1402	17	14	0.61	40
FcF_L4260_135-1957+	711	689	22	22	0.63	42

FcF_L4263_70-1348+	231	224	7	7	0.61	15
FcF_L4275_1-1407+	435	413	22	20	0.64	33
FcF_L4275_1848-3581-	1323	1283	40	33	0.61	70
FcF_L4277_600-1227+	276	273	3	3	0.59	10
FcF_L4291_1-999+	906	882	24	16	0.59	31
FcF_L4291_2053-3055-	633	602	31	26	0.62	45
FcF_L4300_1230-2471-	954	936	18	15	0.53	37
FcF_L4344_92-1071+	198	195	3	2	0.57	8
FcF_L4347_1639-2646-	414	394	20	15	0.57	32
FcF_L4363_1-796+	309	300	9	8	0.57	14
FcF_L4364_1-1339+	423	414	9	9	0.57	22
FcF_L4366_847-1943-	675	656	19	18	0.59	32
FcF_L4392_964-1691-	597	592	5	5	0.54	7
FcF_L4400_1-1604+	666	640	26	21	0.59	48
FcF_L4400_1858-3128-	909	874	35	26	0.57	55
FcF_L4409_208-1084-	645	612	33	27	0.57	53
FcF_L4414_82-2260+	501	479	22	19	0.57	38
FcF_L4423_670-2156-	1056	1030	26	24	0.61	48
FcF_L4432_136-1548-	477	460	17	15	0.65	33
FcF_L4433_490-1178-	603	567	36	23	0.59	50
FcF_L4440_373-3255-	1299	1266	33	28	0.58	56
FcF_L4480_1776-2581-	681	670	11	10	0.62	12
FcF_L4538_1-1206+	624	613	11	10	0.61	19
FcF_L4541_76-1352+	585	567	18	16	0.57	23
FcF_L455_74-2741+	912	881	31	30	0.56	51
FcF_L4553_1-1069+	627	603	24	22	0.54	35
FcF_L4580_1-479+	348	340	8	6	0.54	16
FcF_L459_1-2816+	363	345	18	17	0.53	24
FcF_L4595_201-1511+	363	353	10	10	0.57	21
FcF_L4617_177-1615+	1131	1091	40	37	0.57	56
FcF_L4619_74-721+	624	608	16	15	0.61	35
FcF_L4627_1-947+	570	557	13	9	0.54	27
FcF_L4659_174-2092-	408	399	9	9	0.58	29
FcF_L47_223-1247+	936	926	10	10	0.61	11
FcF_L4701_1237-3735+	297	282	15	15	0.6	21
FcF_L4706_360-1629-	669	657	12	10	0.62	40
FcF_L4710_88-1496+	477	461	16	12	0.57	30
FcF_L4732_710-3373-	534	518	16	12	0.57	33
FcF_L474_301-1832+	438	420	18	15	0.53	27
FcF_L479_855-4832-	1356	1306	50	44	0.56	73
FcF_L480_1-573+	498	483	15	12	0.56	16
FcF_L4832_4959-5659-	633	615	18	18	0.54	20
FcF_L4835_614-1374-	684	659	25	23	0.56	38
FcF_L4837_473-1216-	285	276	9	7	0.56	16
FcF_L4838_1-1409+	1233	1177	56	53	0.6	93

FcF_L4846_1-1334-	1050	1003	47	41	0.62	71
FcF_L4865_1-823+	717	666	51	41	0.61	72
FcF_L4879_1-1115+	909	907	2	2	0.39	47
FcF_L4891_1-1021+	849	808	41	31	0.55	53
FcF_L491_1286-2329-	717	698	19	17	0.62	36
FcF_L4919_455-1592-	726	709	17	15	0.6	34
FcF_L4944_843-1729-	843	811	32	27	0.63	51
FcF_L4981_706-1262-	531	526	5	4	0.57	11
FcF_L4998_74-1365+	1008	985	23	21	0.53	40
FcF_L5010_238-843+	270	262	8	7	0.61	17
FcF_L5041_1-1354+	804	777	27	25	0.57	58
FcF_L5053_501-1474-	582	559	23	18	0.6	40
FcF_L5070_552-2078-	1389	1373	16	14	0.53	20
FcF_L5079_613-1720-	1023	1008	15	12	0.53	31
FcF_L5094_1-838+	501	475	26	21	0.57	32
FcF_L510_1709-5311-	306	290	16	14	0.59	22
FcF_L5104_867-2747-	591	574	17	16	0.61	25
FcF_L511_631-2119-	1359	1319	40	33	0.56	49
FcF_L5120_752-2240-	741	702	39	33	0.61	59
FcF_L5122_1-1477+	1200	1159	41	37	0.61	65
FcF_L5124_373-3063-	261	247	14	14	0.64	20
FcF_L514_234-1561-	1155	1137	18	16	0.59	18
FcF_L5180_1-2315+	1902	1836	66	55	0.58	116
FcF_L5186_898-2074-	585	553	32	27	0.59	44
FcF_L5190_460-1215-	669	643	26	24	0.61	50
FcF_L5193_809-4085-	246	231	15	14	0.68	20
FcF_L520_1-1308+	1251	1235	16	13	0.57	29
FcF_L5286_212-1160-	699	666	33	27	0.58	53
FcF_L5320_1-1267+	264	257	7	7	0.57	14
FcF_L534_398-3994+	252	231	21	12	0.59	32
FcF_L535_530-1044-	462	455	7	7	0.63	7
FcF_L5351_1523-3095-	204	198	6	6	0.51	14
FcF_L5402_1-2227+	603	591	12	5	0.55	57
FcF_L5431_1-1060+	387	372	15	10	0.62	27
FcF_L5449_1029-1981-	750	731	19	18	0.57	37
FcF_L547_1-1468+	1269	1241	28	26	0.55	47
FcF_L5483_902-2326-	1059	1032	27	24	0.59	35
FcF_L5494_685-2277-	1275	1218	57	47	0.58	83
FcF_L5523_573-3122-	366	347	19	16	0.59	29
FcF_L555_1061-4450-	1251	1225	26	19	0.6	42
FcF_L5556_1-1565+	1359	1312	47	40	0.56	70
FcF_L559_833-1733-	777	771	6	6	0.55	6
FcF_L5594_498-1754-	1026	974	52	49	0.5	61
FcF_L5606_84-1605-	963	933	30	27	0.58	53
FcF_L563_781-2299-	1416	1404	12	11	0.6	13

FcF_L564_1-1273+	1095	1068	27	27	0.59	44
FcF_L564_2622-3205-	501	488	13	9	0.55	17
FcF_L5641_444-1590-	543	519	24	21	0.58	38
FcF_L5648_1-1140+	873	833	40	27	0.59	62
FcF_L5653_196-1583+	843	813	30	21	0.61	57
FcF_L570_1-1731+	438	419	19	18	0.55	32
FcF_L5708_1-791+	198	190	8	8	0.57	11
FcF_L5719_663-1941-	606	585	21	18	0.62	31
FcF_L5738_38-814+	678	642	36	29	0.61	52
FcF_L5763_61-682+	570	549	21	15	0.58	35
FcF_L5764_804-2335-	714	682	32	27	0.59	59
FcF_L5802_698-2894-	531	501	30	23	0.55	45
FcF_L5887_1-1588+	225	216	9	9	0.52	14
FcF_L591_279-1701+	1179	1147	32	29	0.59	44
FcF_L5930_580-2000+	984	957	27	18	0.6	38
FcF_L5984_21-833+	771	746	25	19	0.58	32
FcF_L5993_1-2312+	684	653	31	26	0.57	47
FcF_L5998_1-1327+	579	560	19	14	0.53	71
FcF_L6022_53-848+	432	416	16	8	0.55	26
FcF_L6039_1-1150+	630	604	26	25	0.54	40
FcF_L6067_1-1139+	585	566	19	16	0.59	31
FcF_L6085_1-835+	525	503	22	17	0.63	35
FcF_L6103_752-1621-	723	703	20	18	0.55	41
FcF_L6116_876-1753-	780	744	36	32	0.59	58
FcF_L6117_43-1426+	636	602	34	30	0.57	56
FcF_L621_1807-3358-	1320	1284	36	32	0.58	57
FcF_L6232_1250-2298-	183	172	11	10	0.66	13
FcF_L6233_158-2006-	888	859	29	23	0.64	46
FcF_L6239_1-597+	489	482	7	4	0.57	15
FcF_L6257_479-1727+	357	346	11	8	0.56	25
FcF_L6264_192-1556-	186	180	6	6	0.54	10
FcF_L6312_139-1300-	1047	1012	35	29	0.54	69
FcF_L6355_1208-1621-	384	372	12	11	0.58	18
FcF_L6358_437-2526-	495	477	18	17	0.58	32
FcF_L6371_387-1833-	312	302	10	5	0.61	18
FcF_L6377_161-2088-	726	708	18	15	0.57	33
FcF_L6391_1-871+	651	626	25	17	0.56	38
FcF_L642_1120-3116+	1122	1080	42	42	0.57	57
FcF_L644_108-3300-	759	723	36	28	0.61	64
FcF_L6455_1-423+	246	233	13	12	0.62	17
FcF_L6470_78-788+	234	224	10	9	0.59	16
FcF_L65_969-1828-	627	601	26	22	0.52	38
FcF_L6568_802-2316-	621	601	20	19	0.6	41
FcF_L6596_215-2106+	900	874	26	24	0.59	42
FcF_L661_195-1243+	948	923	25	23	0.62	31

FcF_L664_1409-3389-	1194	1157	37	33	0.57	89
FcF_L664_4039-5478+	1269	1230	39	26	0.58	48
FcF_L6675_191-1507-	228	214	14	14	0.51	18
FcF_L6736_1-1231+	255	253	2	1	0.58	10
FcF_L6814_1019-1971-	873	844	29	25	0.51	53
FcF_L6825_399-1933-	699	669	30	25	0.63	55
FcF_L684_1696-3466-	444	427	17	9	0.53	36
FcF_L6880_363-1360-	855	836	19	17	0.53	33
FcF_L6899_62-959+	843	823	20	13	0.58	39
FcF_L6910_1-1708+	792	768	24	16	0.6	42
FcF_L693_1-597+	483	461	22	15	0.51	47
FcF_L6937_1-2127+	183	179	4	4	0.6	10
FcF_L7012_73-897+	624	596	28	20	0.6	45
FcF_L7085_204-800+	561	547	14	13	0.59	29
FcF_L7108_1-976+	651	611	40	38	0.51	58
FcF_L7126_886-2965-	384	374	10	9	0.59	27
FcF_L7168_494-1485-	759	725	34	30	0.55	53
FcF_L7185_561-1289-	486	473	13	11	0.59	20
FcF_L7194_115-4072+	432	411	21	18	0.62	28
FcF_L7237_597-1795-	321	307	14	13	0.58	27
FcF_L7240_116-1410+	1008	991	17	14	0.59	34
FcF_L726_126-1077+	654	638	16	16	0.57	19
FcF_L726_2084-3043-	882	842	40	32	0.58	62
FcF_L737_674-1800-	309	293	16	10	0.58	25
FcF_L738_149-3520+	1131	1109	22	21	0.59	32
FcF_L7387_1-954+	603	578	25	23	0.62	39
FcF_L7445_333-1606-	801	784	17	14	0.57	37
FcF_L7470_1-912+	735	706	29	17	0.59	60
FcF_L7511_113-1725+	291	285	6	6	0.6	12
FcF_L7515_162-1177+	804	782	22	20	0.6	42
FcF_L752_2216-3453-	1050	1007	43	39	0.56	63
FcF_L7525_350-1713-	645	628	17	15	0.59	26
FcF_L7545_442-963-	393	385	8	7	0.62	23
FcF_L7554_1-1179+	501	484	17	16	0.55	27
FcF_L7659_1-1393+	309	300	9	7	0.59	17
FcF_L7745_324-2658-	261	253	8	7	0.59	22
FcF_L7780_656-2921-	663	633	30	24	0.58	44
FcF_L7803_1-2147+	1059	1034	25	23	0.58	39
FcF_L7815_509-1908-	279	264	15	13	0.56	28
FcF_L782_289-2583+	1239	1211	28	26	0.61	51
FcF_L7826_441-1075-	483	470	13	12	0.56	28
FcF_L784_1-1531+	912	867	45	40	0.61	57
FcF_L785_639-2019-	249	248	1	0	0.55	8
FcF_L7886_82-1077+	639	616	23	20	0.6	41
FcF_L7920_9-1609+	882	859	23	20	0.61	47

FcF_L8031_725-1185-	306	285	21	20	0.52	29
FcF_L8148_312-2473-	204	200	4	4	0.59	9
FcF_L8170_1-1052+	744	717	27	21	0.61	51
FcF_L819_725-2764-	861	840	21	18	0.57	49
FcF_L8190_106-495+	327	320	7	7	0.56	12
FcF_L827_1-1739+	657	629	28	21	0.58	49
FcF_L8277_51-727+	576	559	17	13	0.6	32
FcF_L8314_101-1327+	504	488	16	14	0.59	33
FcF_L849_236-1580+	1056	1034	22	21	0.59	29
FcF_L8505_67-1099+	453	431	22	16	0.63	35
FcF_L853_2238-3260-	750	715	35	33	0.57	61
FcF_L857_371-799-	234	224	10	6	0.57	15
FcF_L8581_500-983-	432	426	6	3	0.51	20
FcF_L8587_80-1117+	711	682	29	20	0.55	50
FcF_L8614_814-3280-	1071	1030	41	38	0.59	63
FcF_L8638_72-1173+	225	214	11	11	0.52	18
FcF_L8657_353-1127+	522	493	29	21	0.63	39
FcF_L866_1887-3663-	531	508	23	21	0.65	31
FcF_L871_1040-2256-	996	953	43	40	0.58	60
FcF_L873_1-1379+	786	751	35	30	0.59	56
FcF_L873_1815-2632-	771	751	20	18	0.58	34
FcF_L8756_753-2080-	204	201	3	3	0.57	7
FcF_L882_1097-1914-	675	639	36	33	0.52	42
FcF_L902_254-2697+	471	455	16	16	0.6	27
FcF_L9086_340-1380-	870	836	34	31	0.57	46
FcF_L9087_1029-2244-	723	697	26	24	0.5	43
FcF_L9204_1-2350+	831	787	44	39	0.52	67
FcF_L9267_1-1379+	243	231	12	10	0.54	26
FcF_L9285_1-1160-	873	830	43	34	0.58	54
FcF_L930_1-3590+	684	664	20	16	0.54	28
FcF_L936_2249-3178-	717	671	46	42	0.56	66
FcF_L9422_489-1047-	438	429	9	8	0.59	19
FcF_L960_1-1901+	972	943	29	28	0.58	78
FcF_L9673_131-2603+	510	484	26	24	0.63	44
FcF_L974_142-876+	690	667	23	19	0.57	31
FcF_L980_596-1905-	1131	1076	55	52	0.6	83
FcM_L10003_570-1526-	606	589	17	12	0.57	31
FcM_L1002_2163-3375-	579	557	22	19	0.54	30
FcM_L1005_2015-2866-	810	790	20	16	0.58	33
FcM_L1008_2503-3203-	666	651	15	13	0.6	38
FcM_L1012_1-790+	501	485	16	14	0.52	38
FcM_L1016_919-2680-	732	710	22	19	0.61	49
FcM_L10351_472-1563-	342	331	11	8	0.57	18
FcM_L1043_5749-7273-	1443	1405	38	35	0.57	47
FcM_L1056_3640-5072-	861	832	29	24	0.65	48

FcM_L1061_898-2630-	1515	1440	75	64	0.56	113
FcM_L1069_281-1561-	1185	1161	24	15	0.56	41
FcM_L1073_272-1697+	1188	1146	42	38	0.59	66
FcM_L1084_118-666+	534	510	24	17	0.61	40
FcM_L11066_1-227+	195	193	2	1	0.56	2
FcM_L1134_154-1271+	897	876	21	18	0.59	41
FcM_L1136_2729-3108-	273	266	7	6	0.54	12
FcM_L1138_3074-3745-	639	628	11	11	0.62	13
FcM_L1141_921-1723-	600	578	22	20	0.58	36
FcM_L1157_1-1483+	243	236	7	6	0.57	13
FcM_L1158_110-1239+	1065	1041	24	21	0.56	26
FcM_L1182_759-2564-	1467	1423	44	37	0.59	70
FcM_L1185_396-1840-	1224	1197	27	26	0.54	43
FcM_L1188_1095-4076-	231	227	4	4	0.58	13
FcM_L1191_226-1580+	1296	1261	35	32	0.58	47
FcM_L1191_2311-3374-	363	340	23	22	0.55	34
FcM_L1193_2162-2807-	582	577	5	5	0.57	5
FcM_L1202_718-2002-	1038	1013	25	25	0.6	25
FcM_L1237_374-1905-	876	845	31	28	0.53	47
FcM_L1240_752-1397-	423	406	17	16	0.56	28
FcM_L1262_917-1712-	648	632	16	16	0.55	20
FcM_L1269_1-1493+	1338	1320	18	15	0.6	20
FcM_L1281_1371-2265-	606	586	20	17	0.49	27
FcM_L1285_198-1127+	486	464	22	13	0.61	29
FcM_L1287_1-924+	642	626	16	16	0.57	36
FcM_L1289_1170-2431-	396	378	18	15	0.61	43
FcM_L1313_532-2260-	1443	1409	34	28	0.55	50
FcM_L1320_6489-8018-	729	707	22	20	0.58	41
FcM_L133_799-1437-	579	567	12	12	0.55	12
FcM_L1342_79-3420+	405	387	18	15	0.62	27
FcM_L1352_74-1326+	1002	961	41	40	0.64	56
FcM_L1358_1-996+	936	903	33	31	0.54	60
FcM_L1362_100-834+	555	544	11	11	0.51	13
FcM_L1365_248-1365-	987	959	28	27	0.55	41
FcM_L1388_4529-4879-	273	259	14	13	0.56	17
FcM_L1394_1318-2204-	678	649	29	27	0.52	57
FcM_L1394_1-769+	690	665	25	22	0.53	46
FcM_L1397_151-1755+	882	860	22	21	0.59	40
FcM_L1415_1-1131+	759	719	40	26	0.59	65
FcM_L1416_726-2155-	1122	1091	31	25	0.61	49
FcM_L1418_1-826+	504	491	13	13	0.55	16
FcM_L1430_136-2868+	552	536	16	14	0.63	35
FcM_L1433_2133-2881-	603	588	15	14	0.54	19
FcM_L1445_3867-4959-	1005	969	36	33	0.59	43
FcM_L1452_1-1890-	1185	1125	60	51	0.59	95

FcM_L1455_189-1377-	303	291	12	11	0.63	18
FcM_L1462_1388-2380-	888	865	23	20	0.6	38
FcM_L1463_263-3712-	1908	1848	60	56	0.56	88
FcM_L1481_79-2341+	1740	1712	28	28	0.57	48
FcM_L1487_292-1041+	738	715	23	17	0.69	32
FcM_L1490_402-2196+	909	885	24	21	0.56	38
FcM_L1508_1242-1664-	381	376	5	5	0.57	5
FcM_L1521_986-1837-	237	222	15	13	0.57	19
FcM_L1562_655-900-	210	205	5	5	0.54	5
FcM_L1565_1-2436+	306	287	19	15	0.54	22
FcM_L1578_1-855+	786	763	23	22	0.54	44
FcM_L159_423-2208-	549	536	13	10	0.58	25
FcM_L1613_1-1018+	738	712	26	24	0.57	38
FcM_L1622_1119-3884-	321	312	9	8	0.62	26
FcM_L1628_1-2721+	1524	1490	34	30	0.58	43
FcM_L1632_1-1267+	1035	1008	27	24	0.6	45
FcM_L1660_190-2253+	1254	1220	34	32	0.58	41
FcM_L1686_61-984+	549	521	28	26	0.58	51
FcM_L1706_4557-5340-	720	708	12	10	0.56	22
FcM_L173_2371-3311+	804	796	8	8	0.62	9
FcM_L175_1-856+	771	762	9	9	0.62	10
FcM_L1760_1-1476+	831	803	28	26	0.58	43
FcM_L1764_1249-2775-	1128	1066	62	59	0.58	94
FcM_L1801_1-2866+	222	212	10	9	0.55	18
FcM_L1805_1928-2865-	879	855	24	21	0.57	32
FcM_L1807_2298-3696+	1005	953	52	43	0.6	73
FcM_L1812_279-2218+	450	436	14	14	0.57	21
FcM_L1813_2174-2926-	633	622	11	10	0.55	14
FcM_L1859_1-653+	525	508	17	13	0.54	24
FcM_L1876_1-1096+	540	508	32	27	0.63	47
FcM_L188_1-1073+	927	899	28	24	0.61	37
FcM_L1888_537-1273-	681	666	15	12	0.58	25
FcM_L1889_269-808+	267	259	8	8	0.54	14
FcM_L1894_1170-1651-	378	370	8	5	0.54	12
FcM_L1902_1-3946+	306	293	13	11	0.5	22
FcM_L1904_228-1606-	1116	1080	36	31	0.61	73
FcM_L1907_1087-2840-	669	649	20	19	0.59	34
FcM_L1908_125-4356+	798	758	40	37	0.64	55
FcM_L1908_5588-6790-	528	504	24	24	0.64	41
FcM_L1970_475-1535-	204	201	3	3	0.51	11
FcM_L1973_1-846+	555	539	16	15	0.58	19
FcM_L1978_1811-2700-	840	818	22	15	0.6	34
FcM_L1986_97-1506+	687	656	31	26	0.6	61
FcM_L1987_292-1670+	1272	1222	50	41	0.62	74
FcM_L1992_285-911+	573	553	20	19	0.54	42

FcM_L1996_202-963+	705	670	35	31	0.64	59
FcM_L1999_1-487+	396	376	20	17	0.57	25
FcM_L2009_1-1611+	822	793	29	26	0.58	46
FcM_L2017_2789-6498-	450	426	24	22	0.52	29
FcM_L2023_463-1484-	912	891	21	20	0.6	42
FcM_L2030_118-2500+	378	367	11	10	0.6	18
FcM_L2039_1718-2871-	510	496	14	11	0.6	17
FcM_L2047_1476-4463-	243	237	6	6	0.54	18
FcM_L206_4996-6305+	195	189	6	4	0.56	15
FcM_L2078_1-1156+	492	466	26	23	0.59	50
FcM_L208_538-2146-	1335	1311	24	23	0.54	33
FcM_L2080_185-1443+	1170	1147	23	16	0.61	26
FcM_L2128_1-400+	345	338	7	5	0.61	8
FcM_L214_1-1681+	1356	1343	13	11	0.61	32
FcM_L2147_108-1369+	1092	1053	39	29	0.56	72
FcM_L2150_167-1341+	1098	1047	51	46	0.56	59
FcM_L2161_1-451+	390	383	7	6	0.52	10
FcM_L217_1-1988+	1587	1522	65	59	0.6	101
FcM_L2173_318-1988+	366	356	10	9	0.58	25
FcM_L2182_122-1386+	1113	1091	22	19	0.59	27
FcM_L2188_1-1408+	951	898	53	46	0.54	78
FcM_L2216_4382-6137-	1029	1005	24	21	0.57	32
FcM_L2218_1377-3533-	591	573	18	16	0.59	26
FcM_L2239_724-2085-	1290	1257	33	26	0.58	51
FcM_L2240_674-1534-	741	724	17	15	0.57	28
FcM_L2280_332-2001+	1056	1032	24	17	0.61	52
FcM_L2291_650-1543-	843	835	8	7	0.57	16
FcM_L2304_564-3057-	654	639	15	15	0.59	30
FcM_L2317_2095-2819-	321	314	7	6	0.62	17
FcM_L2330_134-1566+	909	888	21	14	0.6	39
FcM_L2333_3504-5565-	243	235	8	7	0.46	16
FcM_L234_1-2828+	672	650	22	19	0.51	30
FcM_L2347_61-1387+	1176	1116	60	59	0.58	97
FcM_L2354_511-3492-	969	947	22	20	0.61	37
FcM_L2361_389-1370-	849	838	11	9	0.59	15
FcM_L237_118-1043+	807	779	28	27	0.58	36
FcM_L2374_122-1446+	456	436	20	18	0.57	31
FcM_L2379_576-1792+	1122	1067	55	42	0.61	70
FcM_L2390_270-1267+	966	929	37	36	0.6	43
FcM_L2400_1-1261+	915	868	47	41	0.55	69
FcM_L2405_1136-1564-	405	398	7	6	0.57	12
FcM_L2409_1-1323+	654	621	33	32	0.57	63
FcM_L2435_1-2881+	336	325	11	11	0.61	22
FcM_L2453_221-2351+	276	268	8	6	0.54	17
FcM_L2466_1283-2199-	783	758	25	23	0.55	42

FcM_L247_1-1210+	1080	1047	33	30	0.58	56
FcM_L2483_4922-5508-	486	474	12	10	0.57	14
FcM_L2486_1-1077+	990	968	22	22	0.57	34
FcM_L25_1-2290+	1776	1741	35	33	0.6	55
FcM_L2519_1-2542+	891	857	34	30	0.59	42
FcM_L2531_866-2081-	900	860	40	34	0.56	69
FcM_L2548_461-2281-	1362	1322	40	37	0.54	71
FcM_L2572_1810-3759-	969	947	22	21	0.56	36
FcM_L2582_1-2004+	873	841	32	29	0.57	49
FcM_L2586_3841-4902-	708	693	15	12	0.58	19
FcM_L2642_1-756+	501	481	20	17	0.54	27
FcM_L2650_1-685+	618	600	18	18	0.59	22
FcM_L2652_138-3239+	984	955	29	27	0.59	39
FcM_L2674_637-2722-	1389	1358	31	28	0.58	50
FcM_L269_1-2239+	747	713	34	34	0.55	50
FcM_L2701_2042-3506-	981	916	65	58	0.62	91
FcM_L2704_510-2220-	585	567	18	16	0.56	38
FcM_L2729_614-3203-	228	224	4	2	0.59	16
FcM_L2732_296-1424+	870	829	41	36	0.62	61
FcM_L277_1-1197+	942	898	44	43	0.51	60
FcM_L2822_350-1694-	279	269	10	9	0.59	15
FcM_L2838_513-2883-	1050	1023	27	21	0.56	47
FcM_L2840_1-1462+	699	656	43	33	0.55	63
FcM_L2841_1-2436+	1212	1190	22	20	0.53	60
FcM_L2842_747-4606-	1236	1183	53	42	0.57	99
FcM_L2850_4410-5568-	873	849	24	21	0.6	39
FcM_L2884_103-546+	417	406	11	10	0.58	12
FcM_L2885_2357-4034-	264	257	7	7	0.61	10
FcM_L2916_185-1578-	189	185	4	4	0.54	7
FcM_L2919_83-1759+	1326	1282	44	38	0.55	77
FcM_L2932_859-2513-	1224	1194	30	25	0.58	51
FcM_L2959_1-1998+	969	934	35	33	0.58	50
FcM_L2976_1086-1382-	276	270	6	5	0.56	8
FcM_L298_369-1594-	996	959	37	33	0.51	48
FcM_L2997_199-1139+	315	295	20	19	0.56	41
FcM_L2999_1432-2365-	525	498	27	22	0.52	36
FcM_L3_11113-12696-	1119	1086	33	31	0.57	64
FcM_L3000_90-1186+	969	947	22	19	0.58	54
FcM_L3011_2042-2711-	456	441	15	12	0.62	19
FcM_L3019_428-3774+	609	588	21	19	0.63	32
FcM_L3032_346-1051+	555	536	19	18	0.6	36
FcM_L3044_629-2040-	276	269	7	7	0.61	20
FcM_L3061_88-1691+	600	560	40	38	0.57	56
FcM_L308_1-1427+	333	317	16	12	0.55	19
FcM_L3088_785-1803-	840	808	32	28	0.56	47

FcM_L3100_4518-5968-	1050	1034	16	12	0.63	62
FcM_L3101_1462-2802-	600	573	27	23	0.55	33
FcM_L3105_492-1690-	1062	1037	25	25	0.64	32
FcM_L3109_1224-3106-	492	484	8	5	0.62	23
FcM_L3116_1-1068+	966	931	35	33	0.58	49
FcM_L3123_1226-2045-	246	239	7	5	0.6	13
FcM_L3131_614-2717-	1413	1355	58	46	0.59	89
FcM_L3138_712-2089-	234	228	6	6	0.6	12
FcM_L3185_1255-3886-	375	367	8	4	0.56	14
FcM_L3195_416-1506+	216	209	7	6	0.56	11
FcM_L3197_78-2930+	702	683	19	18	0.53	28
FcM_L3200_1-929+	696	675	21	20	0.54	35
FcM_L3215_367-1676+	1101	1063	38	33	0.54	49
FcM_L3248_206-1161+	786	760	26	23	0.58	37
FcM_L3251_1-1482+	1182	1126	56	53	0.57	84
FcM_L3259_471-1879-	750	727	23	18	0.61	37
FcM_L3262_246-1924-	1437	1380	57	50	0.58	91
FcM_L3280_185-2347-	552	532	20	19	0.59	37
FcM_L3348_4568-5365-	696	690	6	5	0.54	7
FcM_L3366_365-2333+	1728	1684	44	42	0.53	64
FcM_L3384_1080-3584-	1935	1876	59	55	0.56	85
FcM_L3386_1-1365+	1152	1092	60	50	0.56	91
FcM_L3390_2400-4696-	366	354	12	11	0.6	18
FcM_L3413_1929-3601-	774	736	38	32	0.63	58
FcM_L3431_3686-4233-	507	486	21	21	0.58	24
FcM_L3436_1-1606+	1203	1159	44	40	0.57	82
FcM_L3437_1-1102+	927	900	27	20	0.55	43
FcM_L3439_120-1654+	450	431	19	18	0.58	38
FcM_L3445_1-968+	810	767	43	35	0.53	63
FcM_L3451_1-641+	477	454	23	22	0.54	35
FcM_L348_721-1671-	729	714	15	11	0.55	15
FcM_L3492_1378-1901-	495	483	12	11	0.53	15
FcM_L3493_220-2118-	381	373	8	7	0.63	20
FcM_L3496_630-1489-	819	794	25	24	0.57	30
FcM_L3519_469-1769-	1260	1220	40	28	0.63	60
FcM_L3521_1-2698+	1119	1094	25	20	0.62	48
FcM_L3528_89-1196-	606	599	7	7	0.58	11
FcM_L3530_192-3149+	633	615	18	16	0.58	28
FcM_L3537_132-1483+	186	185	1	1	0.59	29
FcM_L3551_297-1201+	657	627	30	27	0.59	47
FcM_L3559_452-1575+	522	509	13	11	0.61	25
FcM_L3584_55-2018+	366	351	15	12	0.55	29
FcM_L3587_390-977-	399	391	8	7	0.53	13
FcM_L3605_555-2817-	213	201	12	11	0.62	15
FcM_L3628_1780-3940-	381	375	6	6	0.65	15

FcM_L3633_47-1123+	201	191	10	9	0.57	17
FcM_L3640_1-297+	240	234	6	6	0.56	6
FcM_L3641_1-2496-	759	714	45	43	0.63	66
FcM_L3662_1192-2327-	984	959	25	21	0.61	40
FcM_L3669_1508-2958-	1347	1318	29	29	0.59	40
FcM_L3672_1-1349+	1098	1068	30	26	0.61	46
FcM_L3681_128-754+	585	573	12	11	0.59	15
FcM_L3687_281-859+	528	499	29	25	0.59	41
FcM_L3695_628-2982-	768	725	43	37	0.59	58
FcM_L3707_1-1319+	558	543	15	15	0.64	28
FcM_L3711_1-1841+	975	934	41	40	0.58	71
FcM_L3713_439-1226+	627	599	28	26	0.57	40
FcM_L3735_970-2615-	990	969	21	18	0.56	37
FcM_L3737_299-1435-	1080	1034	46	42	0.58	67
FcM_L3738_1-898-	756	710	46	33	0.54	68
FcM_L3795_1-1084+	1002	947	55	46	0.58	67
FcM_L3797_757-1474-	672	658	14	13	0.57	23
FcM_L3816_139-2373+	1539	1485	54	44	0.57	75
FcM_L3838_1-1380+	228	220	8	6	0.64	17
FcM_L3859_81-1839+	1272	1218	54	46	0.6	90
FcM_L3873_1099-4683-	1077	1044	33	32	0.58	47
FcM_L3886_338-1034-	585	559	26	18	0.56	48
FcM_L3897_1-1707+	1023	973	50	40	0.57	70
FcM_L3940_595-2016-	714	694	20	18	0.59	52
FcM_L3948_1-620+	543	533	10	10	0.56	16
FcM_L3951_204-1566+	1203	1171	32	30	0.56	55
FcM_L3968_1-614+	438	429	9	7	0.57	32
FcM_L3972_425-1491+	450	434	16	15	0.58	31
FcM_L3975_1-657+	582	558	24	24	0.58	29
FcM_L3990_34-981+	378	363	15	11	0.58	24
FcM_L3998_758-2372-	1293	1232	61	59	0.54	90
FcM_L4001_960-2608-	267	251	16	13	0.61	20
FcM_L4014_778-2561-	300	297	3	1	0.57	38
FcM_L4016_155-1515+	948	932	16	9	0.6	32
FcM_L4017_801-2706-	600	580	20	19	0.57	31
FcM_L4024_334-1260-	894	875	19	14	0.51	26
FcM_L4032_396-1267+	831	808	23	20	0.62	31
FcM_L4034_888-2146-	657	644	13	9	0.55	20
FcM_L4043_487-2601-	303	296	7	6	0.59	18
FcM_L4050_45-1453+	1353	1297	56	47	0.62	83
FcM_L4061_1602-3464-	516	495	21	20	0.6	34
FcM_L4089_598-2234-	906	880	26	23	0.64	50
FcM_L41_196-2127+	549	532	17	17	0.56	31
FcM_L4115_1319-3738-	714	684	30	30	0.62	58
FcM_L4141_760-2414-	1212	1165	47	37	0.61	81

FcM_L4142_287-3676+	789	764	25	25	0.56	44
FcM_L4153_1-2032+	240	236	4	4	0.6	14
FcM_L4162_1-1613+	345	323	22	19	0.61	38
FcM_L4164_211-1307-	825	781	44	33	0.56	79
FcM_L4165_563-2096-	387	370	17	15	0.59	29
FcM_L4170_715-2401-	1491	1436	55	50	0.59	75
FcM_L419_902-1562-	270	254	16	15	0.63	30
FcM_L425_1-2195+	1911	1869	42	32	0.56	72
FcM_L4257_846-4018-	504	479	25	25	0.55	47
FcM_L4268_403-1948-	489	476	13	13	0.58	23
FcM_L4278_1-1448+	984	946	38	37	0.57	54
FcM_L4298_130-2533-	249	231	18	13	0.61	26
FcM_L430_1-612+	516	512	4	4	0.51	7
FcM_L4303_101-1581+	957	913	44	37	0.57	76
FcM_L4305_1007-2178-	522	501	21	18	0.54	46
FcM_L4320_698-2675-	1011	968	43	38	0.64	52
FcM_L433_1113-2580-	1314	1285	29	28	0.59	33
FcM_L4336_1046-2460-	1251	1205	46	40	0.59	75
FcM_L4341_1-1017+	900	872	28	25	0.6	49
FcM_L4362_60-1182+	252	240	12	11	0.56	21
FcM_L4369_1-1639+	1176	1143	33	27	0.56	54
FcM_L4370_249-1603+	1161	1123	38	34	0.65	59
FcM_L4371_492-2015-	915	884	31	29	0.61	63
FcM_L4372_2922-3594-	606	589	17	15	0.59	26
FcM_L4392_1-1033+	414	393	21	19	0.59	31
FcM_L4394_1-1977+	1161	1129	32	22	0.62	86
FcM_L4397_219-1230+	324	318	6	5	0.57	14
FcM_L4409_114-2282-	255	253	2	1	0.58	28
FcM_L4459_631-2101-	309	289	20	16	0.6	28
FcM_L4466_3522-4198-	543	526	17	16	0.61	24
FcM_L4472_410-2264-	729	722	7	6	0.59	29
FcM_L4484_114-848+	474	464	10	5	0.58	25
FcM_L4490_1-2412+	852	820	32	30	0.6	54
FcM_L4492_2694-5601-	312	294	18	9	0.66	29
FcM_L4510_4131-4848-	654	631	23	20	0.55	29
FcM_L4515_191-2048+	651	626	25	23	0.66	49
FcM_L4543_1-906+	612	591	21	18	0.57	27
FcM_L457_1510-7578-	297	286	11	7	0.59	19
FcM_L4602_1-1248+	885	868	17	17	0.59	23
FcM_L4618_655-1436-	720	697	23	17	0.55	32
FcM_L4647_357-1322-	768	734	34	24	0.63	48
FcM_L4654_86-544+	405	396	9	9	0.57	9
FcM_L4658_290-1069+	390	373	17	12	0.6	27
FcM_L4665_283-1269+	942	903	39	37	0.53	47
FcM_L4686_57-719+	633	616	17	13	0.59	30

FcM_L4688_1-1386+	831	789	42	40	0.57	60
FcM_L4698_1-1897+	897	869	28	25	0.62	56
FcM_L4700_86-1449-	528	500	28	26	0.57	44
FcM_L475_1-1796+	486	476	10	7	0.63	24
FcM_L477_331-2407+	1161	1121	40	35	0.58	73
FcM_L4816_165-1274+	180	173	7	7	0.54	9
FcM_L4818_846-1981-	1020	996	24	20	0.59	30
FcM_L4826_424-1053-	465	454	11	10	0.56	17
FcM_L4828_1472-2935+	264	255	9	8	0.54	16
FcM_L4843_2519-3990+	726	700	26	22	0.57	36
FcM_L4857_1-653+	399	386	13	13	0.6	20
FcM_L4860_497-3943-	780	752	28	25	0.59	48
FcM_L4890_1-768+	690	670	20	16	0.57	30
FcM_L4891_435-2560+	603	583	20	16	0.61	39
FcM_L4905_1-1308+	384	364	20	19	0.55	29
FcM_L494_537-1336-	543	526	17	16	0.62	30
FcM_L4942_317-1742-	1335	1308	27	24	0.54	36
FcM_L495_1-1558+	1131	1080	51	44	0.58	75
FcM_L4951_1-1886+	561	542	19	17	0.59	31
FcM_L501_1783-2810-	825	792	33	33	0.55	41
FcM_L501_221-579-	336	322	14	12	0.55	17
FcM_L5046_162-1450+	1011	985	26	25	0.61	48
FcM_L5047_1-1671+	255	245	10	8	0.56	18
FcM_L506_1-1742+	729	710	19	19	0.6	34
FcM_L5069_1-984+	285	265	20	17	0.61	30
FcM_L5082_1-1977+	804	761	43	34	0.54	63
FcM_L5084_1-472+	447	443	4	4	0.51	5
FcM_L5087_522-2526-	1710	1681	29	25	0.53	50
FcM_L515_81-386+	285	278	7	4	0.54	11
FcM_L5152_320-1887+	756	725	31	30	0.58	52
FcM_L5159_970-2201-	1023	993	30	25	0.61	44
FcM_L5165_1-471+	381	375	6	6	0.59	10
FcM_L5195_1-914+	654	629	25	23	0.57	43
FcM_L5207_87-1167+	948	911	37	30	0.63	60
FcM_L5213_1-1284+	1137	1095	42	39	0.61	67
FcM_L5222_102-1498+	1122	1088	34	33	0.65	63
FcM_L5229_251-1584+	963	925	38	37	0.55	56
FcM_L5230_1076-2163-	246	242	4	4	0.55	8
FcM_L5231_266-3614-	330	324	6	6	0.56	20
FcM_L5242_217-1433+	1128	1096	32	26	0.61	46
FcM_L5245_1-971+	213	204	9	9	0.57	15
FcM_L5273_1156-2338-	597	559	38	29	0.57	57
FcM_L5273_132-999+	306	298	8	8	0.58	21
FcM_L5303_468-1328-	798	778	20	20	0.54	29
FcM_L5311_656-2099-	603	584	19	16	0.54	48

FcM_L5351_1236-2920-	225	210	15	12	0.61	23
FcM_L5373_730-2469-	1215	1170	45	37	0.6	79
FcM_L5396_1225-2210-	663	640	23	19	0.56	35
FcM_L5397_3109-3702-	582	566	16	12	0.54	19
FcM_L5427_2383-3017-	546	530	16	11	0.55	28
FcM_L543_206-1902+	1467	1431	36	33	0.55	60
FcM_L5453_1170-2226-	777	748	29	26	0.59	49
FcM_L5470_1-477+	387	374	13	10	0.6	17
FcM_L5501_1-1373+	417	405	12	10	0.59	30
FcM_L5508_1-854+	777	762	15	13	0.61	21
FcM_L5546_336-1921-	507	488	19	15	0.6	29
FcM_L5553_95-1785+	1308	1273	35	29	0.53	49
FcM_L5559_1-1361+	954	918	36	32	0.56	60
FcM_L5590_388-1586-	450	430	20	20	0.58	29
FcM_L5610_1-824+	201	200	1	0	0.54	13
FcM_L562_1-1462+	1155	1132	23	21	0.58	29
FcM_L5620_149-832+	645	629	16	13	0.57	26
FcM_L5683_634-1847-	1146	1127	19	16	0.57	26
FcM_L5720_1-1526+	318	305	13	10	0.54	21
FcM_L5767_174-1821+	852	811	41	36	0.55	58
FcM_L5775_468-1198+	444	426	18	18	0.63	35
FcM_L5803_2480-3432+	705	657	48	40	0.55	61
FcM_L5832_110-4137+	528	497	31	26	0.62	48
FcM_L5846_79-1214+	366	349	17	7	0.58	65
FcM_L5855_1-714+	573	555	18	15	0.57	30
FcM_L5862_713-1467-	639	619	20	16	0.56	32
FcM_L5895_604-1749-	243	236	7	6	0.61	15
FcM_L5898_1-1393+	981	932	49	40	0.58	75
FcM_L5916_355-966+	204	198	6	3	0.53	11
FcM_L5948_806-2052-	396	384	12	10	0.57	22
FcM_L595_341-1971+	1275	1223	52	50	0.58	78
FcM_L5952_179-1511+	558	539	19	18	0.61	40
FcM_L6005_605-1341-	720	692	28	26	0.59	40
FcM_L6037_1-1895+	300	293	7	6	0.6	14
FcM_L6042_302-2029-	843	801	42	37	0.57	71
FcM_L6061_454-1622-	435	415	20	19	0.62	35
FcM_L6073_1-955+	597	575	22	21	0.59	36
FcM_L6079_1-1530+	783	756	27	22	0.59	41
FcM_L6101_298-1006-	438	425	13	10	0.54	31
FcM_L6118_334-1771+	417	403	14	11	0.61	41
FcM_L6299_1-957+	228	219	9	9	0.62	19
FcM_L6303_244-3142+	1368	1305	63	57	0.59	94
FcM_L6332_137-2080+	741	707	34	29	0.57	67
FcM_L6340_408-1428-	315	311	4	3	0.53	24
FcM_L6358_698-1669-	837	800	37	33	0.56	62

FcM_L6362_1151-2649-	891	865	26	22	0.62	49
FcM_L6379_438-1559-	591	560	31	30	0.6	51
FcM_L6381_82-1349+	477	466	11	11	0.55	28
FcM_L6411_381-1226-	720	703	17	15	0.56	28
FcM_L6426_1-957+	393	379	14	11	0.53	26
FcM_L6445_412-2617+	276	265	11	9	0.62	20
FcM_L645_1421-3387-	1344	1280	64	61	0.57	74
FcM_L6454_131-1554+	816	790	26	23	0.54	41
FcM_L6456_197-1159+	681	646	35	26	0.62	59
FcM_L6527_1-1475+	879	849	30	26	0.59	54
FcM_L6537_714-1416-	576	557	19	14	0.55	26
FcM_L6567_370-819+	192	186	6	5	0.57	8
FcM_L6578_476-1263-	321	305	16	12	0.61	28
FcM_L6611_65-1185+	531	515	16	15	0.53	32
FcM_L662_1-987+	651	632	19	16	0.56	32
FcM_L6647_1-1084+	747	724	23	22	0.53	42
FcM_L6647_1186-2307-	861	840	21	19	0.53	35
FcM_L6656_23-1092+	822	768	54	42	0.57	96
FcM_L6678_93-1921+	1023	983	40	35	0.58	73
FcM_L6696_1002-2471-	756	731	25	24	0.6	42
FcM_L670_870-1588-	654	648	6	5	0.63	6
FcM_L6706_1-1725+	375	349	26	25	0.58	44
FcM_L6711_1-1046+	870	842	28	28	0.58	48
FcM_L6763_1-662+	441	428	13	11	0.54	28
FcM_L677_1-1280+	1086	1060	26	20	0.59	36
FcM_L6805_114-1657+	582	557	25	18	0.55	41
FcM_L6828_1705-3907-	357	351	6	6	0.59	20
FcM_L6828_311-1176+	192	184	8	7	0.55	14
FcM_L6838_3757-5296-	408	395	13	12	0.59	22
FcM_L6917_85-1487+	312	304	8	7	0.59	25
FcM_L6956_420-2171-	564	546	18	14	0.59	38
FcM_L6970_1-695+	519	507	12	10	0.6	25
FcM_L7_1694-2590+	708	689	19	16	0.58	27
FcM_L70_3561-4721-	906	885	21	21	0.54	27
FcM_L702_55-801+	603	594	9	8	0.56	27
FcM_L708_1-989+	777	760	17	17	0.58	18
FcM_L709_1-1155+	1032	992	40	28	0.57	57
FcM_L7211_1-2194+	795	766	29	21	0.55	59
FcM_L7254_44-2075+	411	401	10	9	0.6	20
FcM_L729_235-1859+	1368	1324	44	38	0.6	69
FcM_L730_1240-2398-	666	646	20	16	0.63	41
FcM_L7328_1-634+	504	487	17	13	0.61	49
FcM_L7365_1-711-	540	511	29	21	0.57	53
FcM_L7402_361-1925-	348	338	10	6	0.57	18
FcM_L741_375-2026+	1092	1070	22	15	0.6	36

FcM_L7410_1-1033+	291	285	6	5	0.6	15
FcM_L7433_225-1800+	921	878	43	34	0.55	68
FcM_L745_432-1378+	468	446	22	16	0.57	41
FcM_L7456_1-2834+	573	555	18	15	0.59	32
FcM_L748_158-2757+	813	760	53	45	0.55	77
FcM_L7507_1-2102+	1158	1070	88	71	0.54	125
FcM_L7610_181-1397+	633	609	24	22	0.59	50
FcM_L762_1-1280+	1203	1164	39	38	0.55	66
FcM_L7666_274-1271+	657	640	17	11	0.59	38
FcM_L7694_56-1068+	927	905	22	20	0.64	49
FcM_L7695_27-1423+	1026	970	56	48	0.62	88
FcM_L7704_104-1016-	219	211	8	5	0.58	13
FcM_L7720_759-1798-	333	318	15	14	0.63	19
FcM_L7741_94-1493+	732	697	35	28	0.62	45
FcM_L7746_203-1386-	1101	1053	48	42	0.56	55
FcM_L7749_101-838+	609	595	14	9	0.54	30
FcM_L78_2098-3338-	804	779	25	19	0.58	32
FcM_L780_1-1860+	216	201	15	15	0.56	24
FcM_L7815_102-661+	315	304	11	9	0.52	20
FcM_L7820_846-2478-	909	894	15	14	0.55	29
FcM_L7857_3531-4619-	306	297	9	7	0.58	21
FcM_L7878_1-1287+	615	584	31	27	0.61	46
FcM_L793_1331-3307-	936	897	39	33	0.57	53
FcM_L796_1191-1793-	552	531	21	18	0.55	27
FcM_L798_2808-5171+	777	757	20	13	0.59	28
FcM_L803_297-1513+	1131	1117	14	14	0.58	14
FcM_L8035_1-1273+	273	270	3	2	0.59	33
FcM_L804_879-1282-	327	318	9	8	0.53	15
FcM_L81_225-2610+	279	263	16	13	0.6	23
FcM_L810_1-1389+	501	483	18	16	0.59	34
FcM_L82_1-1536+	1350	1324	26	20	0.61	34
FcM_L8231_1-926+	723	693	30	30	0.55	46
FcM_L8234_1-940+	582	560	22	18	0.58	43
FcM_L825_2070-2913-	624	601	23	20	0.55	42
FcM_L825_276-1332+	351	335	16	16	0.63	28
FcM_L828_2124-3782-	885	861	24	19	0.6	33
FcM_L8315_1026-1688-	465	457	8	8	0.56	27
FcM_L8333_1-1147+	834	795	39	38	0.6	63
FcM_L8461_1-868-	369	357	12	12	0.58	12
FcM_L851_117-2042+	1008	974	34	32	0.6	53
FcM_L8536_333-1398+	213	205	8	6	0.63	20
FcM_L859_1-1745+	393	375	18	15	0.59	32
FcM_L8666_1-1158+	348	333	15	15	0.58	23
FcM_L8666_1706-2355-	201	193	8	7	0.61	12
FcM_L8718_111-782+	594	568	26	20	0.56	40

FcM_L88_67-877+	720	707	13	13	0.58	13
FcM_L887_237-4077+	681	670	11	10	0.57	23
FcM_L8932_2346-3399-	906	870	36	28	0.57	54
FcM_L8979_529-1835-	1176	1142	34	26	0.61	51
FcM_L8984_1-816+	675	648	27	24	0.57	45
FcM_L903_1618-4582-	216	212	4	4	0.57	9
FcM_L91_3537-6115-	666	614	52	49	0.59	61
FcM_L926_1-502+	267	258	9	8	0.63	13
FcM_L9485_1-1210+	756	737	19	18	0.57	44
FcM_L9594_35-628+	363	339	24	23	0.56	34
FcM_L96_1-308+	183	181	2	2	0.57	7
FcM_L966_323-2112+	963	935	28	21	0.59	46
FcM_L967_198-1696+	525	512	13	13	0.61	34
FcM_L972_1-1017+	780	741	39	35	0.61	56
FcM_L973_88-583+	318	313	5	5	0.59	5
FcM_L9865_81-995+	282	270	12	6	0.61	21
FcM_L997_74-2675+	867	847	20	18	0.61	47
FcM_L3336_1112-1862-	585	573	12	11	0.59	15
FcM_L714_1016-2154-	681	670	11	10	0.57	23
FcM_L2046_4310-4669-	900	872	28	25	0.6	49